NASA Contractor Report 3194

Interaction Between a Normal Shock Wave and a Turbulent Boundary Layer at High Transonic Speeds

T. C. Adamson, Jr., M. S. Liou,
and A. F. Messiter

GRANT NSG-1326
SEPTEMBER 1980

NASA

NASA Contractor Report 3194

Interaction Between a Normal Shock Wave and a Turbulent Boundary Layer at High Transonic Speeds

T. C. Adamson, Jr., M. S. Liou,
and A. F. Messiter
The University of Michigan
Ann Arbor, Michigan

Prepared for
Langley Research Center
under Grant NSG-1326

NASA
National Aeronautics
and Space Administration

**Scientific and Technical
Information Branch**

1980

CONTENTS

Summary

An asymptotic description is derived for the interaction between a shock wave and a turbulent boundary layer in transonic flow, for a particular limiting case. The dimensionless difference between the external-flow velocity and critical sound speed is taken to be much smaller than one, but large in comparison with the dimensionless friction velocity. The basic results are derived for a flat plate, and corrections for longitudinal wall curvature and for flow in a circular pipe are also shown. In Part I, solutions are given for the wall pressure distribution and the shape of the shock wave. In Part II, solutions for the wall shear stress are obtained, and a criterion for incipient separation is derived. Part III contains simplified solutions for both the wall pressure and skin-friction distributions in the interaction region; these results are presented in a form suitable for use in computer programs.

INTERACTION BETWEEN A NORMAL SHOCK WAVE AND A TURBULENT BOUNDARY LAYER AT HIGH TRANSONIC SPEEDS

Part I - Pressure Distribution

A. F. Messiter

1. Introduction

In several recent studies, asymptotic methods have been used successfully for the derivation of rational approximations which describe the interaction of a turbulent boundary layer and a weak, stationary, normal shock wave. It appears that correct limiting forms of the equations can be determined, that numerical or analytical solutions to these equations are obtained easily enough to be of practical interest, and that numerical accuracy may be adequate for important parameter ranges. In the limiting case to be considered here, still for an unseparated boundary layer, the shock wave extends close to the wall, the upstream influence is small, and analytical solutions can be obtained for most of the flow field. Pressure distributions are derived in Part I; the wall shear stress and the possibility of predicting separation will be discussed in Part II.

In many transonic flows of interest, there occurs a shock wave which, in an inviscid-flow approximation, is normal to a solid boundary, at values of the Reynolds number large enough that the boundary layer along the wall is fully turbulent. Since the strength of the shock wave must decrease to zero in the supersonic part of the boundary layer, there can be no discontinuity in the pressure at the wall. It is observed that the shock wave becomes slightly curved and is displaced slightly in the upstream direction. As the Mach number upstream is increased, still below the value required for separation, the shock wave extends further into the boundary layer; experimental results [1, 2] show an initially rapid rise

in the wall pressure, followed by a gradual decrease in the pressure gradient over a distance several times larger than the boundary layer thickness.

Asymptotic descriptions of these flows, in the limit of infinite Reynolds number, have been discussed in References [3] through [10]; in particular, Ref. [8] contains the first steps of the present work. In each of these studies, the representation of the undisturbed boundary layer in terms of a velocity-defect layer and a wall layer [11, 12, 13] is regarded as providing an asymptotic description as the Reynolds number tends to infinity [14-18]. The pressure gradient in the boundary layer is large near the shock wave, and consequently the forces resulting from changes in the Reynolds stresses are of higher order than terms retained, in most of the boundary layer. Thus, as for laminar flow [19, 20, 21] , an asymptotic description of the changes in the mean flow can be obtained with the use of inviscid-flow equations for most of the boundary layer.

The form of the velocity profile, however, implies two important differences from the laminar-flow case. First, for an unseparated turbulent boundary layer the wall layer is extremely thin, and the displacement effect resulting from deceleration of fluid close to the wall remains very small, even in a large pressure gradient. Thus, if the undisturbed velocity profile is known outside the wall layer, an approximation to the pressure can be found without knowledge of the flow details near the wall and therefore without any further assumption about the nature of the turbulent stresses. Second, for a slightly supersonic external flow the sonic line is

located at an arbitrary position (outside the wall layer) in the undisturbed boundary layer, depending on the relative sizes of the nondimensional friction velocity and the nondimensional difference between the fluid velocity and the critical sound speed in the external flow. As the Reynolds number tends to infinity, one can then study three cases, such that the ratio of these parameters tends to infinity, remains constant, or approaches zero.

Adamson and Feo [3] considered an incident oblique shock wave in a flow with velocity only slightly greater than the sound speed, such that the sonic line is located very close to the edge of the boundary layer. The corresponding asymptotic formulation was shown to lead to a local-interaction problem requiring solution of the transonic small-disturbance equations for the local perturbations in the external flow, expressed in appropriately scaled variables. The influence of the boundary layer is represented on this scale through an effective wall boundary condition specifying a linear relationship between the streamline slope and the pressure gradient. Melnik and Grossman [4] studied a normal shock wave having strength, as measured by the nondimensional pressure jump, of the same order as the friction velocity, so that in the limit the sonic line is at an arbitrary location in the boundary layer. Numerical solutions of the transonic small-disturbance equations were obtained for perturbations in the defect portion of the boundary layer and in the neighboring external flow. Changes in the wall layer were also discussed in each of these papers. Melnik and Grossman later [5, 6] obtained additional numerical solutions for axisymmetric pipe flow. At higher upstream speeds, which might be characterized as "high

transonic speeds," the shock wave is stronger but the boundary layer can remain unseparated. For this case, a first approximation for the flow perturbations outside the wall layer was given by Adamson and Messiter [8] . The shock-wave strength, although still small, was taken to be large in comparison with the nondimensional friction velocity, so that in the undisturbed boundary layer the distance from the sonic line to the wall is much smaller than the boundary-layer thickness. The corresponding problem has also been discussed for an incident oblique shock wave [7, 9] . A brief preliminary description of some of the present results was given in Ref. [10] ; a few details have since been modified.

In the present work, analytical solutions are derived which incorporate additional physical effects as higher-order terms for the case, first discussed rather briefly in Ref. [8] , when the sonic line is very close to the wall. The functional form used for the undisturbed velocity profile is described in Section 2, to indicate how various parameters will be calculated for later comparison with experiment. The basic solutions for the pressure distribution are derived in Section 3. In Section 4 corrections are added for flow along a wall having longitudinal curvature and for flow in a circular pipe, and comparisons with available experimental data are shown. The restriction to weak shock waves is removed in Appendix A, and it is verified there that the simpler solutions of Section 3 are adequate. Some additional results pertinent to the asymptotic matching of solutions in the region of most rapid pressure rise, near the beginning of the interaction, are derived in Appendix B.

2. Undisturbed Velocity Profile

Nondimensional rectangular coordinates X and Y are measured along and normal to the wall, respectively, with Y = 0 at the wall and X = 0 at some point on the shock wave, e.g., at the intersection of the shock wave with the edge of the boundary layer as defined below. The reference length is a geometric length such as the length of the boundary layer from a leading edge up to the shock wave. The nondimensional mean-velocity components U and V, referred to the critical sound speed in the external flow, are in the X and Y directions respectively, and the term $\overline{\rho' V'}/\rho$ has been included in V. Here primes denote fluctuations about the mean, and $\overline{\rho' V'}$ denotes an average value. The nondimensional mean pressure P, density ρ, temperature T, and viscosity coefficient μ are referred to the critical values of pressure, density, and temperature, and the corresponding viscosity coefficient, in the flow just outside the boundary layer and ahead of the shock wave. The sum of the nondimensional Reynolds stress and viscous stress, in the boundary-layer approximation, is denoted by τ, and has been made nondimensional with twice the dynamic pressure, in terms of the same reference quantities. For later convenience the friction velocity u_τ is made nondimensional using the external-flow density:

$$u_\tau^2 = \frac{\tau_w}{\rho_e} = \frac{1}{2} U_e^2 c_f, \qquad U_e = 1 + \epsilon \tag{2.1}$$

where the subscripts e and w indicate values in the external flow and at the wall, respectively, and c_f is the undisturbed value of the skin friction coefficient, referred as usual to the dynamic pressure in the external flow.

The nondimensional difference between the fluid velocity and the critical sound speed in the external flow is ϵ, and in the present case $u_\tau << \epsilon << 1$. For simplicity, an adiabatic wall is assumed and the total enthalpy is taken to be uniform. The ratio of specific heats is γ and is constant.

As in references cited above, it is assumed that the undisturbed boundary layer can be described asymptotically in terms of a velocity-defect layer and a wall layer. The defect layer occupies most of the boundary layer, and its thickness is taken equal to a boundary-layer thickness δ. The velocity differs from the external-flow velocity by an amount of order u_τ, the shear stress is $\tau = O(u_\tau^2)$, and the layer thickness is $\delta = O(u_\tau)$. The much thinner wall layer has thickness denoted by $\tilde{\delta}$, and the velocity there is small, of order u_τ. Coordinates measured in terms of these nondimensional thicknesses are defined by

$$y = \frac{Y}{\delta}, \qquad \delta = O(u_\tau) \tag{2.2}$$

$$\tilde{y} = \frac{Y}{\tilde{\delta}}, \qquad \tilde{\delta} = \frac{\mu_w}{\mu_e}\left(\frac{T_w}{T_e}\right)^{\frac{1}{2}} \frac{U_e}{u_\tau} \frac{1}{\mathrm{Re}} \tag{2.3}$$

where $\tilde{\delta} << \delta$, and $\tilde{\delta}$ has been set equal to the ratio of the nondimensional local kinematic viscosity and a friction velocity $u_\tau(T_w / T_e)^{1/2} = (\tau_w / \rho_w)^{1/2}$ based on the density at the wall. The Reynolds number Re is based on the geometric reference length, undisturbed external-flow velocity, and kinematic viscosity; all parameters are understood to be evaluated immediately upstream of the shock wave.

The velocity U_u in the undisturbed boundary layer just ahead of the shock wave is expressed in the defect layer in terms of y and in the wall layer in terms of $\tilde{y}$, as follows:

$$U_u \sim U_e + u_\tau u_{01}(y), \qquad y = O(1) \tag{2.4}$$

$$U_u \sim u_\tau (T_w/T_e)^{1/2} \tilde{u}_{01}(\tilde{y}), \qquad \tilde{y} = O(1) \tag{2.5}$$

The form of the profile is shown in Fig. 1 for $u_\tau \ll \epsilon \ll 1$. Equations (2.4) and (2.5) are [13], respectively, the "law of the wake" and the "law of the wall," written here for a compressible boundary layer, and are taken to be asymptotic representations valid as $u_\tau \to 0$, with y and $\tilde{y}$ held fixed respectively. Throughout most of the analysis also $\epsilon \to 0$ such that $u_\tau/\epsilon \to 0$. In the wall layer the Reynolds stress and the viscous stress are both of the same order as the wall shear stress $\tau_w = O(u_\tau^2)$. Since $Y = O(\tilde{\delta})$ is extremely small, the momentum equation gives $\tau \sim \tau_w$. As $\tilde{y} = Y/\tilde{\delta} \to \infty$, the viscous stress becomes extremely small, while τ remains equal to τ_w in the limit, provided that also $y = Y/\delta \to 0$. The mixing length approximation $\kappa^2 \rho (\tilde{y} dU_u/d\tilde{y})^2 = \tau_w + \ldots$ is introduced here for $y \ll 1$ and $\tilde{y} \gg 1$, where κ is the von Kármán constant, taken equal to 0.41. For a perfect gas with uniform total enthalpy, $\rho T = \rho_w T_w$ and $T = \frac{1}{2}(\gamma + 1) - \frac{1}{2}(\gamma - 1)U^2$. Integration gives, for $y \ll 1$ and $\tilde{y} \gg 1$,

$$U_u = \Gamma \sin\{\Gamma^{-1}(T_w/T_e)^{\frac{1}{2}} u_\tau(\kappa^{-1} \ln \tilde{y} + c)\} \tag{2.6}$$

where c = constant and $\Gamma = (\gamma + 1)^{1/2}/(\gamma - 1)^{1/2}$. This is van Driest's [22] result, with the added simplifying assumption of uniform total enthalpy.

Expansions of Eqn. (2.6) for $U_u \to 1 + \epsilon$ and for $U_u \to 0$ should agree, respectively, with expansions of the defect-layer velocity (2.4) as $y \to 0$ and of the wall-layer velocity (2.5) as $\tilde{y} \to \infty$. For $U_u \to 1 + \epsilon$ and $U_u \to 0$, respectively, Eqn. (2.6) gives

$$U_u \sim 1 + \epsilon + (u_\tau/\kappa)(\ln y - 2\Pi) \tag{2.7}$$

$$U_u \sim u_\tau (T_w/T_e)^{1/2}(\kappa^{-1} \ln \tilde{y} + c) \tag{2.8}$$

where Π is Coles' [13] profile parameter; $c \approx 5.0$ and, for zero pressure gradient, $\Pi \approx 0.5$ or perhaps a little larger. Since $\tilde{y} = (\delta/\tilde{\delta})y$, comparison of Eqns. (2.6) and (2.7) gives

$$u_\tau \kappa^{-1} \ln(\delta/\tilde{\delta}) = (T_e/T_w)^{1/2} U_i(\epsilon) - u_\tau(2\Pi\kappa^{-1} + c) \tag{2.9}$$

where $U_i(\epsilon) = \Gamma \sin^{-1}(\Gamma^{-1} U_e)$. The expansions (2.7) and (2.8) require, respectively, $y \to 0$ slowly and $\tilde{y} \to \infty$ slowly as $u_\tau \to 0$; since $u_\tau = O(1/\ln \mathrm{Re})$, from Eqn. (2.9), one might take, e.g., $y = O(u_\tau^m)$ and $\tilde{y} = O(u_\tau^{-n})$ as $u_\tau \to 0$, where $m > 0$ and $n > 0$. A difference from the incompressible case arises because Eqn. (2.8) with $\tilde{y} = (\delta/\tilde{\delta})y$ does not agree with Eqn. (2.7). That is, the expansion as $\tilde{y} \to \infty$ of the wall-layer solution does not agree with the expansion as $y \to 0$ of the defect-layer solution. Thus these solutions have no common domain of validity and cannot be matched. This type of problem has been discussed in detail by Lagerstrom and Casten [23], with a model example related to flow at low Reynolds number. In the present case, the density has different values for $y = O(1)$

and for $\tilde{y} = O(1)$, and the difficulty is resolved by use of the solution (2.6) for $\tilde{\delta} << Y << \delta$; this feature was also noted by Adamson and Feo [3] and by Melnik and Grossman [4] .

The defect layer, where $y = O(1)$, has nearly constant density and is described in a first approximation by incompressible-flow equations. The domain of validity of Eqn. (2.6) can be made to include $y = O(1)$ if $\kappa^{-1}(\ln y - 2\Pi)$ is replaced by $u_{01}(y)$, where $u_{01}(y)$ is the same function as for incompressible flow. Then

$$U_u = \Gamma \sin\{\sin^{-1}(\Gamma^{-1}U_e) + \Gamma^{-1}(T_w/T_e)^{1/2} u_\tau u_{01}(y)\} \qquad (2.10)$$

Expansion for $u_\tau \to 0$ gives Eqn. (2.4) if y is held fixed, Eqn. (2.7) if $y \to 0$ sufficiently slowly that also $u_\tau \ln y \to 0$, and Eqn. (2.6) if $y = (\delta/\tilde{\delta})\tilde{y} \to 0$ more rapidly, such that $u_\tau \ln \tilde{y}$ is held fixed. The use of Eqn. (2.10) was suggested by Maise and McDonald [24] , who showed that this assumed profile permits good correlation with experimental data for adiabatic flat-plate boundary layers. Their interpretation of Eqn. (2.10) notes that a transformed velocity $\Gamma \sin^{-1}(\Gamma^{-1}U_u)$ is predicted to have the incompressible form $U_i(\epsilon) + (T_w/T_e)^{1/2} u_\tau u_{01}(y)$ everywhere outside the wall layer.

A second relation between δ and u_τ for $\partial P/\partial X = 0$ can be found with the help of the von Kármán integral of the momentum equation, following a derivation similar to that for incompressible flow given, e.g., by Cebeci and Smith [25] . The result is, to second order in u_τ/U_e,

$$\frac{m_1}{8}\delta = \frac{u_\tau}{U_e} + \{\frac{2}{\kappa}\frac{U_e}{U_i}(\frac{T_w}{T_e})^{1/2} + \frac{4}{m_1}(3\frac{T_w}{T_e} - 1)\int_0^\infty u_{01}^2 dy\}\frac{u_\tau^2}{U_e^2} \qquad (2.11)$$

The positive constant m_1 is defined by

$$m_1 = -8\int_0^\infty u_{01}(y)dy \qquad (2.12)$$

and occurs in another context in the following section. For analytical purposes, the function $u_{01}(y)$ is represented in Coles' [13] form

$$u_{01}(y) = \kappa^{-1}\ln y - \Pi\kappa^{-1}(1 + \cos \pi y) \qquad (2.13)$$

for $0 < y < 1$, with $u_{01}(y) = 0$ for $y > 1$.

In the derivation which follows, the boundary-layer thickness is taken as one of two important characteristic lengths. The other length is the distance from the wall to the sonic line in the undisturbed boundary layer, denoted in nondimensional form by δ_*. Substituting Eqn. (2.13) in Eqn. (2.10), setting $y = \delta_*/\delta$, and expanding for $\delta_*/\delta \to 0$ gives

$$u_\tau\kappa^{-1}\ln(\delta/\delta_*) = (T_e/T_w)^{1/2}[U_i(\epsilon) - U_i(0)] - 2\Pi\kappa^{-1}u_\tau \qquad (2.14)$$

As $\epsilon \to 0$, $\ln(\delta/\delta_*) \sim \kappa u_\tau^{-1}\epsilon\,[1 - (\gamma - 1)\epsilon/4 + \ldots] - 2\Pi$; thus $\delta_*/\delta \to 0$ if $u_\tau/\epsilon \to 0$. An alternate form of the velocity profile (2.6) in terms of a coordinate $y^* = Y/\delta_*$, is

$$U_u = \Gamma\sin\{\sin^{-1}(\Gamma^{-1}) + \Gamma^{-1}(T_w/T_e)^{1/2}\kappa^{-1}u_\tau\ln y^*\} \qquad (2.15)$$

for $y \to 0$ and $\tilde{y} \to \infty$.

3. Interaction Along a Plane Wall

As $u_T \to 0$, the orders of magnitude of the mean pressure gradient and fluid acceleration near the shock wave are larger than in the undisturbed boundary layer. The Reynolds-stress transport equations can be used to show that in most of the boundary layer the contributions to the mean forces resulting from changes in the turbulent stresses are sufficiently small, in comparison with the pressure and inertia terms, that they may be neglected as $u_T \to 0$, not only in a first approximation but also in the calculation of some higher-order terms. Correct asymptotic representations of the mean velocity and pressure perturbations can therefore be derived using inviscid-flow equations. Also, as noted at the end of this section, displacement effects resulting from flow changes very close to the wall are extremely small, and so the largest terms in the solution for V should approach zero as the distance from the wall decreases.

In the equations which follow, all laminar and turbulent stresses are neglected, as are the entropy changes across the shock wave; order-of-magnitude estimates given at the end of this section show that the neglected terms are in fact of higher order than any of the terms retained. The equations describing the fluid motion can then be written in the following form:

$$a^2 \operatorname{div} \vec{q} = \vec{q} \cdot \nabla \frac{q^2}{2} \tag{3.1}$$

$$a^2 = \frac{1}{2}(\gamma + 1) - \frac{1}{2}(\gamma - 1) q^2 \tag{3.2}$$

$$\rho \vec{q} \cdot \nabla \vec{q} = -\gamma^{-1} \nabla P \tag{3.3}$$

Here $\vec{q}$, q, and $a = (P/\rho)^{1/2}$ are, respectively, the velocity vector, the magnitude of the velocity, and the sound speed, all nondimensional with the critical sound speed in the external flow just ahead of the shock wave. The gradient and divergence operators imply differentiation with respect to the nondimensional variables X and Y. Crocco's theorem, simplified by the assumption of uniform total enthalpy, is

$$\vec{\Omega} \times \vec{q} = \gamma^{-1} T \nabla s \tag{3.4}$$

where $\vec{\Omega} = \text{curl } \vec{q}$, and the specific entropy s has been made nondimensional with the gas constant R. Since the upstream value of V contributes terms of higher order than those to be retained here, the shock-polar equation becomes

$$V_d^2 = (U_u - U_d)^2 \frac{U_u U_d - 1}{2U_u^2/(\gamma+1) - (U_u U_d - 1)} \tag{3.5}$$

where the subscripts u and d here denote, respectively, values immediately upstream and downstream of the shock wave. Since the jump in the velocity vector across a shock wave is in a direction normal to the shock, the shock-wave slope is

$$\frac{dX_s}{dY} = \frac{V_d}{U_u - U_d} \tag{3.6}$$

where the shock-wave location is denoted by $X = X_s(Y)$.

If the nondimensional friction velocity u_τ is small in comparison with the nondimensional shock-wave strength ϵ, the sonic line in the undisturbed boundary layer is very close to the wall, as can be seen from Eqn. (2.14) and Fig. 1. That is, if $u_\tau \to 0$ and $u_\tau/\epsilon \to 0$, then also $\delta_*/\delta \to 0$. A complete description of the local pressure changes would require both an "outer" solution, obtained by taking a limit of the equations with coordinates Y/δ and X/Δ held fixed, and an "inner" solution, obtained with Y/δ_* and X/Δ_* fixed, for suitable choices of Δ and Δ_*. The shock wave can extend nearly to the wall, as shown in Fig. 2, and so the upstream influence described by the inner solution is very small; it is shown later that $\Delta_* = O(u_\tau^{1/2}\delta_*)$, where $\delta_*/\delta = O(\exp(-\kappa\,\epsilon/u_\tau))$ from Eqn. (2.14). For the outer solution, therefore, U_u can be taken equal to the undisturbed velocity (2.10) or (2.4). The inner solution describes perturbations about the undisturbed boundary-layer flow, while the outer solution describes perturbations about a different boundary-layer flow, downstream of the shock wave; the two solutions should match in a proper asymptotic sense.

For $Y = O(\delta)$ the length scale Δ in the downstream direction is found from Eqn. (3.1) and the vorticity equation to be $\Delta = O(b_o\delta)$, where $b_o^2(\epsilon) = 1 - M_o^2$ and M_o is the Mach number in the external flow behind a normal shock wave. Coordinates x and y are defined by

$$x = \frac{X}{b_o\delta} \qquad y = \frac{Y}{\delta} \tag{3.7}$$

where

$$b_o = (\gamma+1)^{1/2}\epsilon^{1/2}\{1 - \tfrac{1}{4}(2\gamma+1)\epsilon + \ldots\} \tag{3.8}$$

Since the shock wave is nearly normal, the shock-polar equation (3.5) gives $U_d = (1+\epsilon)^{-1} + O(u_\tau)$. This result suggests that throughout the flow downstream of the shock wave U should be represented as a constant value $1 - \epsilon + \ldots$ plus small perturbations of order u_τ. It is convenient to separate the rotational part, which can be calculated from Crocco's theorem (3.4), and the irrotational part, which is to be found from the solution of Eqn. (3.1) satisfying the appropriate boundary conditions. In the limit as $u_\tau \to 0$ with x and y held fixed, the velocity components are then expressed in the form

$$U = (1+\epsilon)^{-1} + u_\tau u_1^{(r)}(x, y;\epsilon) + u_\tau^2 u_2^{(r)}(x, y;\epsilon) + \ldots$$

$$+ u_\tau \phi_{1x}(x, y;\epsilon) + u_\tau^2 \phi_{2x}(x, y;\epsilon) + \ldots \qquad (3.9)$$

$$V/b_o(\epsilon) = u_\tau \phi_{1y}(x, y;\epsilon) + u_\tau^2 \phi_{2y}(x, y;\epsilon) + \ldots \qquad (3.10)$$

where the functions of ϵ shown will be expanded below for $\epsilon \to 0$.

The entropy s is nearly constant along a streamline, and the equation of state gives $P = \rho T$, since changes in $\overline{\rho' T'}$ are of higher order than terms to be retained here. It follows that along a streamline $P\, T^{-\gamma/(\gamma-1)} \sim P_e T_u^{-\gamma/(\gamma-1)}$ to the order required here. Substitution of $T = a^2$ from Eqn. (3.2) then gives the pressure as

$$P/P_e = 1 - \gamma(U-U_u) - \gamma^2(U_u - 1)(U-U_u) + \ldots \qquad (3.11)$$

Also, Crocco's theorem gives $\Omega \sim \gamma^{-1} P\, ds/d\psi$, where $\psi_Y = \rho U$, $\psi_X = -\rho V$, and $\Omega = V_X - U_Y$, and so $\Omega/P \sim \Omega_u/P_e$ along a streamline. Substitution in the expression for Ω allows calculation of terms in the rotational part of U:

$$u_1^{(r)} = (1 + 2\gamma\epsilon + \ldots)u_{01}(y) \tag{3.12}$$

$$u_2^{(r)} = -\frac{\gamma - 1}{4} u_{01}^2(y) + \gamma \int_y^\infty u'_{01}(y)\phi_{1x}(x, y)dy + \ldots \tag{3.13}$$

Substitution of the representations (3.9) and (3.10) into Eqn. (3.1) leads to differential equations for ϕ_1 and ϕ_2:

$$\phi_{1xx} + \phi_{1yy} = 0 \tag{3.14}$$

$$\phi_{2xx} + \phi_{2yy} = -u_{2x}^{(r)} + (1+\epsilon)(M_o/b_o)^2(2 + (\gamma - 1)M_o^2)(u_1^{(r)} + \phi_{1x})\phi_{1xx} + (1+\epsilon)M_o^2\phi_{1y}(u_{1y}^{(r)} + 2\phi_{1xy}) \tag{3.15}$$

Expansion of the shock-wave slope (3.6) gives, after integration, the shock-wave location $x = x_s(y; u_\tau, \epsilon)$ as

$$x_s = u_\tau x_{s1}(y;\epsilon) + \ldots = \frac{u_\tau}{2\epsilon}(1 + \frac{1}{2}\epsilon + \ldots)\{\phi_1(0, y;\epsilon) - \phi_1(0, 1;\epsilon)\} + \ldots \tag{3.16}$$

where the origin of coordinates has been chosen so that $x_s = 0$ at $y = 1$. Thus the shock wave is located at $x = 0$ in a first approximation, as implied in Fig. 2, and the flow properties are to be studied in the quarter-plane $x > 0$, $y > 0$. Boundary conditions at $x = 0$ are found from the shock-polar equation (3.5), expanded in Taylor series about $x = 0$:

$$\phi_{1x}(0, y) = -2\{1 + (\gamma - 1)\epsilon + \ldots\}u_{01}(y) \tag{3.17}$$

$$\phi_{2x}(0, y) = -x_{s1}(y)\phi_{1xx}(0, y) + \frac{1}{2\epsilon}\{1 - (\gamma - \frac{3}{2})\epsilon\}\phi_{1y}^2(0, y) - \frac{\gamma - 1}{2} u_{01}^2(y) + \ldots \tag{3.18}$$

It is also required that $\phi_{1y}(x, 0) = \phi_{2y}(x, 0) = 0$ and that all disturbances approach zero as $x^2 + y^2 \to \infty$.

The limiting form of ϕ_1 as $\epsilon \to 0$ was first given in Ref. [8]; here a term proportional to ϵ is included. The solution is expressed in terms of a distribution of sources along the y-axis:

$$\phi_1(x, y) = -\frac{2}{\pi}\{1 + (\gamma - 1)\epsilon + \ldots\} \int_{-\infty}^{\infty} u_{01}(\eta) \ln\{x^2 + (y-\eta)^2\}^{1/2} d\eta \tag{3.19}$$

The extended definition $u_{01}(-y) = u_{01}(y)$ gives a potential for $-\infty < y < \infty$ which is symmetric about $y = 0$ and thus satisfies the boundary condition there. As $x^2 + y^2 \to 0$, the contribution to the complex velocity is

$$u_\tau(\phi_{1x} - i\phi_{1y}) = -2u_\tau\{1 + (\gamma - 1)\epsilon + \ldots\}\kappa^{-1}(\ln z - 2\Pi) + \ldots \tag{3.20}$$

where $z = x + iy$. The pressure P_w at the wall found from evaluation of Eqn. (3.11) as $y \to 0$ is

$$\frac{P_w - P_f}{P_e} = 2\gamma\, u_\tau\{1 + (2\gamma - 1)\epsilon + \ldots\} \frac{2x}{\pi} \int_0^{\infty} \frac{u_{01}(\eta) d\eta}{x^2 + \eta^2} + \ldots \tag{3.21}$$

where $P_f/P_e = 1 + \gamma\{2\epsilon + (2\gamma - 1)\epsilon^2 + \ldots\}$ is the pressure ratio across a normal shock wave when the upstream speed is $U_e = 1 + \epsilon$. At larger distances, as $x^2 + y^2 \to \infty$,

$$u_\tau(\phi_{1x} - i\phi_{1y}) = u_\tau\{1 + (\gamma - 1)\epsilon + \ldots\}\{\frac{m_1}{2\pi z} + \ldots\} \tag{3.22}$$

where m_1 is defined by Eqn. (2.12); substitution of the approximate analytical form (2.13) gives $m_1 = 8(1 + \Pi)/\kappa$. That is, the integrated effect is that of a concentrated source having nondimensional volume strength per unit length equal to $\{1 + \ldots\}m_1 u_\tau \delta$. One-fourth of this fluid appears to be added to the external flow in the quadrant $x > 0$, $y > 0$. Since

$d(\rho U) \sim (1 - M_o^2)dU$ along a streamline downstream of the shock wave, and $1 - M_o^2 \sim (\gamma+1)\epsilon$, the local increase in the boundary-layer displacement thickness is $\frac{1}{4}(\gamma+1)\epsilon\ m_1 u_\tau \delta + \ldots$, as can also be found by direct calculation. An equivalent observation was made for $\epsilon = O(u_\tau)$ by Melnik and Grossman [5, 6]. Perturbations in turbulent stresses contribute only a higher-order change locally; the present result does not include the further displacement effect which occurs on a larger length scale as a new equilibrium velocity profile is approached. Finally, the shock-wave shape found from Eqn. (3.16) is, for $y \to 0$,

$$x_s(y) - x_s(0) = \frac{u_\tau}{2\epsilon}\{1 + (\gamma - \tfrac{1}{2})\epsilon + \ldots\}\{\frac{\pi}{\kappa} y + \ldots\} \tag{3.23}$$

and, for $y \to \infty$,

$$x_s(y) - x_s(0) = \frac{u_\tau}{2\epsilon}\{1 + (\gamma - \tfrac{1}{2})\epsilon + \ldots\}\{\frac{m_1}{2\pi} \ln y + \frac{4}{\pi}\int_0^\infty u_{01}(\eta)\ln\eta\, d\eta + \ldots\}. \tag{3.24}$$

For $y = Y/\delta \to \infty$, the shock-wave displacement continues to increase, and should be matched with a suitable perturbed external-flow solution evaluated as $Y \to 0$.

The solution for ϕ_2 can be found in two parts. A particular solution of the differential equation (3.15) can be made to satisfy homogeneous boundary conditions $\phi_{2x}(0, y) = \phi_{2y}(x, 0) = 0$ if sources are distributed over the entire x, y plane with the source strength chosen to be an even function of both x and y. The boundary condition (3.18) at $x = 0$ is then satisfied by a distribution of sources along the y-axis, with strength taken

to be an even function of y so that ϕ_{2y} remains zero at y = 0, as in the solution for ϕ_1. Of special interest is the total source strength found by carrying out the integrations as $x^2 + y^2 \to \infty$, with the help of integrations by parts and Eqns. (3.14) and (3.17). The pressure, correct to order $u_\tau^2(x^2 + y^2)^{-1/2}$ as $x^2 + y^2 \to \infty$, and the second-order source strength m_2 are found to be

$$\frac{P - P_f}{P_e} = -\gamma \{u_\tau[1 + (2\gamma - 1)\epsilon + \ldots] m_1 + u_\tau^2(1 + \ldots) m_2 + \ldots\} \cdot \frac{1}{2\pi} \frac{x}{x^2+y^2} \tag{3.25}$$

$$m_2 = 2(5\gamma + 9)\int_0^\infty u_{01}^2(y)dy - 2(\gamma + 1)\int_0^\infty \phi_{1y}^2(x, 0)dy \tag{3.26}$$

For a constant value of y such that $y \gg 1$, P initially decreases as x increases from zero, reaches a minimum at x = y, and then increases again. However, there is a small error at the shock wave $x = x_s(y) = O(\epsilon^{-1} u_\tau \ln y)$, because the largest term in Eqn. (3.25) is $O(\epsilon^{-1} u_\tau^2 \ln y/y^2)$, whereas the correct first approximation is found from the shock-polar equation as $-\frac{1}{2}\gamma\, \epsilon^{-1} u_\tau^2 m_1^2/(2\pi y)^2$. If it is desired, the accuracy of Eqn. (3.25) can be improved near $x = x_s$ by addition of a term $-\gamma\, u_\tau^2 y^2 \phi_{2x}(0, y)/(x^2 + y^2)$ with $y^2\phi_{2x}(0, y)$ approximated by its leading terms O(ln y) and O(1) as $y \to \infty$; away from $x = x_s$ the added term is smaller than the second-order term originally shown.

As $x^2 + y^2 \to 0$, the perturbation velocity becomes large, and it is again clear that an inner solution is required. For the choice of origin

shown in Eqn. (3.16) and in Fig. 2, $x_s(0) \neq 0$ and so the singularity in Eqn. (3.20) is displaced from its correct location through a distance $-x_s(0) = O(u_\tau/\epsilon)$. The domain of validity near $x = 0$ can be extended slightly by addition of a term $-2u_\tau \kappa^{-1}(1 + \ldots)\ln(1 - x_s(0)/z)$ in Eqn. (3.20) for $u_\tau(\phi_{1x} - i\phi_{1y})$. This is accomplished formally by taking a limit as $x \to 0$ with $\epsilon x/u_\tau$ held fixed and then constructing a composite solution. The correction is local, and introduces only a smaller change of order $\epsilon^{-1}u_\tau^2/|z|$ when $|z/x_s(0)| \gg 1$. The modification is, however, necessary for matching with the inner solution. A discussion of the inner solution given in Ref. [8] is briefly reviewed here, in a slightly modified form. For $Y = O(\delta_*)$, the undisturbed velocity is $U_u = 1 + O(u_\tau)$, and the differential equations show that changes in U along a streamline are also $O(u_\tau)$ in a distance $\Delta X = O(u_\tau^{1/2}\delta_*)$. Inner variables x* and y* and disturbance velocities u* and v* are defined by

$$x^* = \frac{(\kappa\, T_e^{1/2})^{1/2}[\, X - b_o \delta x_s(0)]}{(\gamma+1)^{1/2} u_\tau^{1/2} \delta_*}, \qquad y^* = \frac{Y}{\delta_*} \tag{3.27}$$

$$u^* = \frac{\kappa\, T_e^{1/2}}{u_\tau}(U - 1), \qquad v^* = \frac{(\kappa\, T_e^{1/2})^{3/2} V}{(\gamma+1)^{1/2} u_\tau^{3/2}} \tag{3.28}$$

where factors $(\kappa\, T_e^{1/2})^{1/2}$ have been included for convenience. Equation (3.1) and the vorticity equation are then approximated by the transonic small-disturbance equations with prescribed vorticity:

$$u^* \partial u^*/\partial x^* - \partial v^*/\partial y^* + \ldots = 0 \tag{3.29}$$

$$\partial v^*/\partial x^* - \partial u^*/\partial y^* = -1/y^* + \ldots \tag{3.30}$$

The shock-wave relations (3.5) and (3.6) become

$$v_d^{*2} = \frac{1}{2}(u_u^* - u_d^*)^2(u_d^* + u_u^*) + \ldots \tag{3.31}$$

$$\frac{dx_s^*}{dy^*} = \frac{v_d^*}{u_u^* - u_d^*} \tag{3.32}$$

where the subscripts u and d again refer to quantities immediately upstream and downstream of the shock wave and the shock-wave location is given by $x^* = x_s^*(y^*)$. As $x^* \to -\infty$, u^* approaches the undisturbed form $u^* \sim \ln y^*$; the boundary condition at the wall is $v^*(x^*, 0) = 0$; and as $x^* \to \infty$, $y^* \to \infty$ the solution should agree with the outer solution evaluated for $x - x_s(0) \to 0$, $y \to 0$.

Although complete solutions for u^* and v^* can only be obtained numerically, the asymptotic behavior is found relatively easily upstream as $x^* \to -\infty$ and downstream as $x^* \to \infty$, $y^* \to \infty$. As $x^* \to -\infty$, the solution has the form

$$u^* \sim \ln y^* + e^{kx^*} f(y^*), \qquad v^* \sim k^{-1} e^{kx^*} f'(y^*) \tag{3.33}$$

where $f'' - (\ln y^*)k^2 f = 0$ subject to the conditions that $f'(0) = 0$ and that incoming disturbances be absent as $y^* \to \infty$; the latter implies $f' \sim -(\ln y^*)^{1/2} k f$ as $y^* \to \infty$. Numerical integration gives $k = 0.59$. Downstream a suitable class of intermediate limits should be studied. As $y^* \to \infty$, a shock wave is present and must approach the nearly normal shock wave described by the outer solution. Thus, for $y^* \to \infty$, since

$u_u^* \sim \ln y^*$, Eqns. (3.31) and (3.32) give $u^*(0, y^*) \sim -\ln y^*$. If an intermediate variable $y_\eta = y^*/\eta(u_\tau, \epsilon)$ is introduced, with $1 \ll \eta(u_\tau, \epsilon) \ll \delta/\delta^*$, then $\ln y^* \sim \ln \eta + \ln y_\eta$, where the first term is large and constant whereas the second term is O(1) and variable. In each of the differential equations (3.29) and (3.30) the two largest terms remain of the same order if $x^* = O(\eta\sqrt{\ln \eta})$ and $v^* = O(\sqrt{\ln \eta})$; then x^* and $y^*(\ln y^*)^{1/2}$ are of the same order. In the limit as $x^* \to \infty$ and $y^* \to \infty$ with $x^*/(y^*\sqrt{\ln y^*})$ held fixed, $\ln y^* \sim \ln x^*$ and so also $x^*/(y^*\sqrt{\ln y^*}) \sim x^*/(y^*\sqrt{\ln x^*})$. For the derivation of higher-order terms, not to be shown here, it is convenient to make this replacement. In this limit, then, the largest terms in $u^* + \ln y^*$ and $(\ln x^*)^{-1/2} v^*$ can be written as functions of $x^*/(y^*\sqrt{\ln x^*})$. The solutions are easily obtained and the results for U and V finally can be rewritten as

$$U \sim 1 + (\kappa T_e^{1/2})^{-1} u_\tau \ln y^* - (\kappa T_e^{1/2})^{-1} u_\tau \ln\{x^{*2}(\ln x^*)^{-1} + y^{*2}\} \qquad (3.34)$$

$$V \sim \{(\gamma+1)(\kappa T_e^{1/2})^{-1} u_\tau \ln x^*\}^{1/2} 2(\kappa T_e^{1/2})^{-1} u_\tau \tan^{-1}\{y^*(\ln x^*)^{1/2}/x^*\} \qquad (3.35)$$

Factors $(1 - M^2)^{1/2} \sim \{(\gamma+1)(\kappa T_e^{1/2})^{-1} u_\tau \ln x^*\}^{1/2}$, where M is the local Mach number, appear in the locations expected for solutions of the Prandtl-Glauert equation. The flow is represented by superposition of a known rotational flow and an initially unknown irrotational flow, described in terms of perturbation velocities U - 1 and $(1 - M^2)^{-1/2} V$ which are linear in $(\kappa T_e^{1/2})^{-1} u_\tau$ and are functions of variables $(1-M^2)^{-1/2}[X - b_o \delta x_s(0)]/\delta_*$ and Y/δ_*. For a limit such that $[x - x_s(0)]^2 + y^2 \to 0$ sufficiently slowly,

with $(1 - M^2)^{1/2}\, y/[x-x_s(0)]$ held fixed, the largest terms obtained if Eqns. (3.34) and (3.35) are rewritten in the outer variables x and y are identical to the largest terms found from Eqns. (3.9) and (3.10), with the help of Eqn. (3.12) and a modified Eqn. (3.20) in which z is replaced by $x - x_s(0) + iy$. Introduction of the inner solution thus removes the logarithmic singularity which appears in the outer solutions for the velocity and the pressure as $x, y \to 0$.

In the derivation of these results, terms $\partial(\rho \overline{U' U'})/\partial X$, $\partial(\rho \overline{U' V'})/\partial Y$, etc., were omitted from the momentum equation, and therefore a corresponding set of terms was omitted in Eqn. (3.1) and in the calculation of the changes in vorticity. Expressions for these quantities, and therefore also order-of-magnitude error estimates for the solutions given above, can be obtained from the Reynolds-stress transport equations [25] . The equation for $\partial(\rho \overline{U' U'})/\partial X$ contains, in particular, terms proportional to $\rho \overline{U' U'}\ \partial U/\partial X$. Ahead of the shock wave $\rho \overline{U' U'}$ is expected to be of the same order as $\rho \overline{U' V'}$, of order u_T^2. Relative changes at the shock wave have been estimated [26] to be proportional to the shock wave strength and are therefore small. Thus, $\rho \overline{U' U'} = O(u_T^2)$ downstream of the shock also; since $\partial U/\partial X =)(\epsilon^{-1/2})$ for $X = O(\epsilon^{1/2} u_T)$, the product is $O(u_T^2 \epsilon^{-1/2})$. Other terms involving velocity correlations are likewise at most $O(u_T^2 \epsilon^{-1/2})$. Neglected terms in the expansion of Eqn. (3.1) and the vorticity equation are also of this order, and can easily be shown to be small in comparison with any of the terms retained. Similarly, the derivative of the entropy along a mean streamline contains terms proportional to

$\rho \overline{U' V'} \partial U/\partial Y$, etc., and therefore is small enough to be neglected in the derivations above. At the shock wave the entropy jump for $Y = O(\delta)$ contains a constant term of order ϵ^3 and functions of y which are of order $\epsilon^2 u_\tau$, ϵu_τ^2, ... It can then be shown that these changes are also sufficiently small that Ω/P and $PT^{-\gamma/(\gamma-1)}$ remain constant along a mean streamline to the order considered here. Finally, the changes in Reynolds stresses become important in a sublayer where the perturbation in τ_Y is no longer negligible in comparison with the perturbation in ρUU_X. For $X = O(\epsilon^{1/2} u_\tau)$, since $\tau = O(u_\tau^2)$ and $U_X = O(\epsilon^{-1/2})$, the sublayer is defined by $Y = O(u_\tau^2 \epsilon^{1/2})$. As will be shown in detail in Part II, the relative change in τ is $O(\epsilon)$, and the new term in U which contributes to a displacement effect is $O(\epsilon\, u_\tau)$. From the continuity equation it follows that the corresponding term in V is $O(\epsilon^2 u_\tau^2)$. Thus, as $y \to 0$, the largest term in the outer solution for V which satisfies a nonzero boundary condition is $O(\epsilon^2 u_\tau^2)$, smaller than any of the terms retained above. All of the neglected terms arising from these effects are smaller than the terms retained by at least a factor of order ϵ.

4. Geometric Effects and Comparison with Experiment

The theory of the preceding section leads to a limiting form for the pressure distribution as $u_T \to 0$ and $u_T/\epsilon \to 0$, for unseparated flow. In the flow past an airfoil at supercritical speed, with a shock wave terminating a region of supersonic flow, the additional effect of surface curvature can also be important in changing the pressure distribution and delaying separation, as discussed below and in Part II. The boundary layer might remain attached for M_e up to about 1.25, depending on the profile shape; Re may be about 5×10^7 or perhaps as high as 10^8; and the flow ahead of the shock wave experiences a favorable pressure gradient, with magnitude which depends on the airfoil shape, so that the profile parameter Π is smaller than 0.5 (e.g., Ref. [30]). For a combination of parameters which is favorable with regard to requirements of the present theory, with $M_e = 1.26$, $Re = 10^8$, and $\Pi = 0$, the relative position of the sonic line is given by $\delta_* / \delta = 0.10$. This value would increase as M_e or Re decreases or as Π increases, as seen from Eqn. (2.14). Experimental results, however, are not yet available with detailed local pressure measurements for values of the parameters which correspond to such airfoil flows and which meet the requirements of the theory. For all available data, either the flow is separated or the values of the parameters are such that the sonic line is not close to the wall. Nonetheless, a comparison with data from Refs. [1] and [2] has been carried out, and the agreement seems favorable provided that corrections for geometric effects are included.

A wall having convex longitudinal curvature is described locally by $Y \sim -\frac{1}{2}KX^2$, where $K \ll 1$ if the radius of curvature is large in comparison with the reference length used in the definitions of X and Y. A local solution for the inviscid external flow near the foot of a normal shock wave shows a discontinuity in streamline curvature [27, 28] . Ahead of the shock wave $P_Y > 0$ to provide the required acceleration toward the wall; if the flow is irrotational, it follows that $U_Y < 0$. The shock-wave relations give $U_Y > 0$ and $P_Y < 0$ downstream; therefore also $V_X > 0$, whereas the tangency condition at the wall requires $V_X < 0$ as $Y \to 0$. The term in the complex velocity which satisfies the required conditions as $X, Y \to 0$ has the derivative

$$b_o U_X^{(c)} - iV_X^{(c)} \sim -(4/\pi)K \ln Z + iK + O(K) \qquad (4.1)$$

for $0 \leq \arg Z \leq \frac{1}{2}\pi$, where $Z = b_o^{-1}X + iY$ and, as before, $b_o^2(\epsilon) \sim (\gamma+1)\epsilon$. The largest omitted term is of order K and is real; the value depends on the flow description for $Z = O(1)$, and is known for symmetric two-dimensional or axisymmetric nozzle flows [29] .

Terms $U^{(c)}$ and $V^{(c)}$, of order $K\epsilon^{-1/2}u_\tau \ln u_\tau$ and Ku_τ, respectively when $Z = O(u_\tau)$, are now added to the expansions of U and V given by Eqns. (3.9) and (3.10). The rotational part of U is unchanged, and reformulation of the boundary-value problem for the perturbation potential shows that ϕ_1 is unchanged, whereas now ϕ_2 depends on K, through nonlinear terms in the potential equation; that is, $\phi_2 = \phi_2(x, y; \epsilon, K)$. The new terms in ϕ_2 contribute a change in U which is $O(Ku_\tau^2)$, smaller than terms retained previously provided that $K = 9(1)$. Thus, to the order considered here, for

$u_\tau/\epsilon \to 0$, a curvature correction is simply added to the earlier results. The new term in the pressure, written in terms of x and y, is

$$P^{(c)} = \frac{2\gamma K\delta}{\pi}\{2x \ln \delta + x \ln(x^2 + y^2) + \frac{\pi}{2} y - 2y \tan^{-1}\frac{y}{x} + Ax\} \quad (4.2)$$

where the constant A is determined only if a solution is known for the external flow at larger distances.

An early careful and comprehensive experimental study was carried out by Ackeret, Feldmann, and Rott [1] . In Figs. 3 and 4, predicted pressures are compared with their experimental results for $M_e = 1.32$, corresponding to $\epsilon = 0.247$, and $Re = 9.6 \times 10^5$, based on distance to the shock wave. Eqns. (2.9), (2.11) and (2.14) are used for approximate evaluation of other parameters. One more experimental value is needed; δ_* is chosen since it is easily read from the measured velocity profile and since only $\ln \delta_*$ enters the equations, so that an error has small effects on other quantities. For $\delta_* = 0.0055$, the calculations give $u_\tau = 0.051$, $\delta = 0.021$, and $\Pi = 0.28$. This value of Π seems plausible (e. g., Ref. [30]) because of the observed small favorable pressure gradient ahead of the shock wave. An adverse gradient of about the same magnitude is evident downstream, and is estimated here by $P_t^{-1}\partial P/\partial X \approx 0.12$, where P_t is the upstream stagnation pressure. A corresponding term is added to Eqn. (4.2) and the term proportional to $K\delta Ax$ is neglected. The local curvature of the plate can be inferred from measured pressures immediately behind the shock wave. It is estimated that $P_t^{-1}\partial P/\partial Y \approx 0.15$; since $P_Y \sim -\gamma V_X$, it follows that $K \approx 0.2$. With the kind assistance of Prof. Z. Plaskowski of the Institüt für Aerodynamik,

ETH Zürich, the author was able to measure ordinates of the plate actually used in the experiments; values in an appropriate neighborhood confirm the estimate $K \approx 0.2$. The origin $x = 0$ is chosen at the estimated position of the shock wave at the edge of the boundary layer, found using measured pressures outside the boundary layer together with Eqn. (3.24).

The comparison in Figs. 3 and 4 shows that the curvature effect is comparable in importance with the boundary-layer displacement effect; addition of the curvature term leads to a more pronounced "shoulder" in the predicted wall pressure distribution. The longitudinal pressure gradient due to tunnel divergence is also seen to be important. At the plate for typical values of x, say $4 < x < 14$, the prediction gives about 75 percent of the pressure drop below the value for a one-dimensional flow; outside the boundary layer, at $Y/\delta \approx 3.6$, the agreement is somewhat better. It is found that the velocity in Eqn. (3.21) is closely approximated by (const.)/x for $x \gtrsim 2$, so that Eqn. (3.25) for the pressure is adequate here, with the correction (4.2). Modest changes in the assumed values of the parameters do not have a major effect on the comparison; for example, at a given X, m_1/x does not depend strongly on Π because δ increases if Π decreases. The upstream exponential decay predicted by Eqn. (3.33) is also shown in Fig. 3, in the form $\Delta P/P_t \sim u_T \exp\{k(x^* - x_o^*)\}$, with x_o^* taken equal to -14 for approximate agreement with experiment. A major difficulty with this comparison is that the upstream sonic line lies at about $y = \delta_*/\delta = 0.26$, and the shock wave ends at a still larger distance from the wall, so that the inner region for $x^* = O(1)$, $y^* = O(1)$ is not negligibly small. At a higher

Reynolds number and therefore a lower u_τ, the shock wave would extend closer to the wall, and the size of the region in Fig. 3 where no prediction is given would be smaller. A second serious difficulty arises because the flow probably was separated. The authors of Ref. [1] stated that reversed flow would not be ascertained at any point; however, the velocity profiles shown seem inconclusive, since measurements were not possible very close to the wall. Calculations based on the theory of Part II of the present paper, for the parameter values given in Ref. [1], indicate that the flow was in fact separated, with a very thin separation bubble having length equal to a few boundary-layer thicknesses. The effect of such a bubble would give a more gradual pressure rise in the region of greatest disagreement in Fig. 3. Finally, a slight unsteadiness in the shock wave position would also contribute to a decrease in the measured pressure gradient.

A correction for flow in a circular pipe can be derived in terms of cylindrical coordinates x^+ and r^+ defined by

$$x^+ = \frac{X}{b_o(\epsilon)R} = \frac{\delta}{R}x, \qquad r^+ = 1 - \frac{Y}{R} = 1 - \frac{\delta}{R}y \tag{4.3}$$

where R is the ratio of the local pipe radius to the reference length, and Y is measured inward from the wall, so that $r^+ = 0$ at the axis. Solutions are to be found for $\epsilon \to 0$, $u_\tau/\epsilon \to 0$ with x^+, r^+ fixed. The wall shape is given by $r^+ = 1 + \epsilon^2 f(X/R)$ with $f = 0$ at $X/R = 0$. Velocity components U^+, V^+ in the x^+, r^+ directions can be written with the local curvature and boundary-layer effects shown separately:

$$U^+ = U^{(0)}(X/R, r^+; \epsilon) + KU^{(1)}(x^+, r^+) + \frac{1}{2} m_1 u_\tau \frac{\delta}{R} + u_\tau \frac{\delta}{R} U^{(2)}(x^+, r^+)$$

$$+ \ldots \qquad (4.4)$$

$$V^+ = V^{(0)}(X/R, r^+; \epsilon) + K b_o(\epsilon) V^{(1)}(x^+, r^+) + u_\tau \frac{\delta}{R} b_o(\epsilon) V^{(2)}(x^+, r^+) + \ldots \qquad (4.5)$$

where now $K = \epsilon^2 f''(0)$ is the wall curvature at the foot of the shock wave, made nondimensional with the reciprocal of the pipe radius. The terms $U^{(0)}$ and $V^{(0)}$ are the terms which would be present if the effects of the shock wave were ignored [29] . Terms proportional to K contain the local curvature effect, and terms proportional to $u_\tau \delta / R$ contain the local boundary-layer displacement effect. The latter is described in terms of a ring source of radius $r^+ = 1$ located at $x^+ = 0$ and having volume strength per unit length equal to $m_1 u_\tau \delta + \ldots$; numerical solutions for $u_\tau/\epsilon = O(1)$ given by Melnik and Grossman [6] also include this effect. For $x^+ \to \infty$, the fluid added at the source gives an increase of $\frac{1}{2} m_1 u_\tau \delta / R$ in U^+, shown explicitly in Eqn. (4.4).

The local solutions for $X/R = O(\epsilon^{1/2})$ are found in terms of a stream function defined by $\partial \psi^{(i)} / \partial r^+ = r^+ U^{(i)}$, $\psi^{(i)} / \partial x^+ = - r^+ V^{(i)}$, where i=1, 2. The largest terms in Eqn. (3.1), combined with the irrotationality condition, lead finally to

$$\psi^{(i)}(x^+, r^+) = \sum_{n=1}^{\infty} a_n^{(i)} e^{-\lambda_n x^+} r^+ J_1(\lambda_n r^+) \qquad (4.6)$$

where $J_1(\lambda_n) = 0$ for n=1, 2, 3, . . . , so that the wall boundary condition $\psi^{(i)}(x^+, 1) = 0$ is satisfied; also $\psi^{(i)} \to 0$ as $x^+ \to \infty$, and boundary values are to be specified at $x^+ = 0$. To the order required, the shock-polar equation reduces to the Prandtl relation, and so $\psi^{(1)} = r^{+2}(1 - r^{+2})/4$ at $x^+ = 0$. The condition that the ring source gives no term of order $u_\tau \delta/R$ in U^+ at $x^+ = 0$ implies $\psi^{(2)} = - m_1 r^{+2}/4$ at $x^+ = 0$. Comparison with the wall boundary condition shows that $\psi^{(2)}$ is discontinuous at the foot of the shock wave $x^+ = 0$, $r^+ = 1$; the value obtained as $x^+ \to 0$, $r^+ \to 1$ depends on the direction of approach. The coefficients $a_n^{(1)}$ can be found from the solutions of Messiter and Adamson [29] or by direct calculation, and the coefficients $a_n^{(2)}$ are found directly:

$$a_n^{(1)} = - \frac{4}{\lambda_n^3 J_o(\lambda_n)} \qquad a_n^{(2)} = \frac{m_1}{2\lambda_n J_o(\lambda_n)} \tag{4.7}$$

for n=1, 2, 3, ...

For calculation of the pressure distribution and the shock-wave shape, it is convenient to introduce the corresponding velocity potential $\phi^{(2)}$, which satisfies $\partial \phi^{(2)}/\partial x^+ = U^{(2)}$ and $\partial \phi^{(2)}/\partial r^+ = V^{(2)}$, and which has a logarithmic singularity at $x^+ = 0$, $r^+ = 1$. With the help of the asymptotic form for $J_o(\lambda_n r^+)$, one can show the singular part explicitly:

$$\phi^{(2)}(x^+, r^+) = -\frac{m_1}{2} \sum_{n=1}^{\infty} \{ \frac{1}{\lambda_n} \frac{J_o(\lambda_n r^+)}{J_o(\lambda_n)} e^{-\lambda_n x^+}$$

$$- \frac{(-1)^n}{\pi (n+\frac{1}{4})(r^+)^{1/2}} e^{-\pi (n+\frac{1}{4})x^+} \cos[\pi (n+\frac{1}{4})r^+ - \frac{\pi}{4}] \}$$

$$- \frac{m_1}{2\pi (r^+)^{1/2}} \mathcal{R} \{ \ln \frac{1+\zeta}{1-\zeta} + 2 \tan^{-1}\zeta - 4\zeta \} \qquad (4.8)$$

where $\ln \zeta = -(\pi/4)\{x^+ + i(1 - r^+)\}$, and $\mathcal{R}$ indicates that the real part is to be taken. As $x^+ \to 0$ and $r^+ \to 1$, the largest term in the complex velocity $U^{(2)} - iV^{(2)}$ is due to a two-dimensional source of strength m_1, in agreement with Eqn. (3.22). The change in the boundary-layer displacement effect is then found by subtracting the source term from $U^{(2)} - iV^{(2)}$ and adding the constant term which remains as $x^+ \to \infty$. If the numerically small contribution of the infinite series is omitted, the corresponding correction to the wall pressure is

$$\frac{\Delta P_w}{P_e} = -\gamma u_\tau \frac{\delta}{R} \frac{m_1}{2} \left(1 + \frac{e^{-5\pi x^+/4}}{1 - e^{-\pi x^+}} - \frac{1}{\pi x^+} \right) \qquad (4.9)$$

As $x^+ = X/(b_o R) \to 0$, $\Delta P_w/P_e$ approaches a constant value $-\frac{1}{8}\gamma m_1 u_\tau \delta/R$, which implies an additional second-order correction to the boundary-layer solution found in Section 3 for $X = O(b_o \delta)$. The shock-wave shape is found directly from the potential; in particular, as $r^+ \to 1$ the displacement of

the shock from its intersection with the axis is found by adding the perturbation potential from Section 3 to that found here, and subtracting the common term proportional to ln Y. The result is

$$\Delta X_S = -(4\pi\epsilon)^{-1}(\gamma+1)^{1/2}\epsilon^{1/2} m_1 u_\tau \delta \ln(R/\delta) + O(u_\tau \delta \epsilon^{-1/2}) \qquad (4.10)$$

In Fig. 5 a comparison is made with pressures measured in a circular pipe by Gadd [2], for $M_e = 1.12$ and $\epsilon = 0.097$. The length of an equivalent flat-plate boundary layer is not a given quantity; instead, Gadd's estimated value for boundary-layer thickness is used here, along with the estimate $\delta_*/\delta = 0.45$ found from the measured velocity profile. The sonic line is therefore still further from the wall than in the Ackeret experiment. Other approximate values are calculated as $u_\tau = 0.04$, $\delta = 0.02$, and $\Pi = 0.1$; the Reynolds number corresponding to these values is Re = 6×10^6. A pressure gradient due to small divergence of the test section is estimated downstream by $P_t^{-1} \partial P/\partial X = 0.06$. The effect of finite pipe radius is seen to be about as large as the boundary-layer displacement effect. The upstream exponential decay is also shown, with x_o^* again taken equal to -14. Again there is a relatively large region where no prediction is made and where numerical solution of the transonic small-disturbance equations is required. Such a solution was obtained by Melnik and Grossman [4] for this case and is also shown in Fig. 5. For large x the analytical and numerical solutions differ by an amount about equal to the correction for the change in pipe cross-section area.

5. Concluding Remarks

The interaction of a turbulent boundary layer with a weak normal shock wave has been described here and elsewhere [3, 4, 8] in terms of a rational approximation based on systematic asymptotic expansion procedures. The interaction is characterized by two small parameters, a nondimensional friction velocity u_τ and a nondimensional shock-wave strength ϵ, and limiting forms of the local solutions can be studied as $u_\tau \to 0$ and $\epsilon \to 0$. For the case $u_\tau/\epsilon \to \infty$ [3] , analytical solutions indicated that separation does not occur; solutions for u_τ/ϵ held fixed [4] , with the first approximation described by the transonic small-disturbance equations, gave the same result. If, finally, $u_\tau/\epsilon \to 0$, it appeared that analytical solutions would be possible and that perhaps the onset of separation could be discussed. Solutions for the pressure have been obtained here and will be used in Part II for the calculation of wall shear stress and a discussion of incipient separation.

The largest terms in the pressure, of order u_τ, are derived quite easily, and a number of higher-order effects have been added. Corrections of order ϵu_τ give, e.g., a 35% change if $M_e = 1.25$. A partial solution for terms of order u_τ^2 shows that these terms likewise are significant, typically giving changes of 25% to 50% for $Re = 10^6$ or 10^7. Corrections of order κu_τ and $u_\tau \delta/R$, obtained in analytical form for a wall with longitudinal curvature and for a circular pipe respectively, are found to be numerically important for the tests of Refs. [1] and [2] .

In the solutions for these higher-order terms, the dependence on the parameters is of course shown explicitly, and the relative importance of different effects is therefore apparent. It is not, however, possible to obtain analytical solutions in the asymptotically small inner region which accounts for the upstream influence. For values of the parameters corresponding to actual transonic flight conditions, it is possible for this region to be relatively small. Experimental results, however, are not available in this parameter range; for existing data, either the flow is separated or the sonic line is not close to the wall. Nonetheless, some comparisons with such data were attempted, and the agreement seems fairly good downstream from the inner region. The predicted pressures remain somewhat higher than the experimental values, and the correction terms calculated thus far are large enough to suggest that additional higher-order terms would be likely to give still further improvement.

An essential feature of the asymptotic flow description in terms of u_τ and ϵ is the two-layer structure of the undisturbed profile, expressed by the law of the wake and the law of the wall. It is this property which permits the calculation of interaction pressures without knowledge of changes in shear stresses close to the wall. In other studies [31, 32] which were not based on use of this profile, derivation of a sublayer solution was necessary before the calculation of the pressure could be completed; these studies also introduced a linearized formulation for the main part of the boundary layer. In the present asymptotic description for $u_\tau/\epsilon \to 0$, sublayer effects do not

appear even among the second-order terms in the pressure. Linear equations appear naturally as a consequence of the limiting case considered, and the procedure for adding higher-order terms is clear. In the formulation for u_τ/ϵ held fixed [4] , again the flow details near the wall do not influence the pressure. The differential equations obtained in the limit are, however, nonlinear and numerical solution is required. For $u_\tau/\epsilon \to \infty$ [3] , the pressure once more is found without knowledge of changes in the wall shear stress.

A complete asymptotic description for $0 < u_\tau/\epsilon < \infty$ is therefore now available, with numerical solutions obtained as $u_\tau \to 0$ and $\epsilon \to 0$ if u_τ/ϵ is fixed and analytical solutions if $u_\tau/\epsilon \to \infty$ or $u_\tau/\epsilon \to 0$. For accurate calculations in parameter ranges of practical interest, some further extensions appear to be needed. In the present case, as $u_\tau/\epsilon \to 0$, the necessary condition that the sonic line be close to the wall is met for a relatively narrow range of the parameters. The solutions for wall pressure would be more useful if a simple curve fit was introduced for the inner region, say by means of a straight line tangent to the source solution downstream and to the exponential solution upstream. The choice $x_o^* \approx -14$ in the exponential term was made for agreement with experiment in Fig. 3; the results shown in Fig. 5 suggest that the magnitude is too large and that perhaps a more suitable tentative value would be $x_o^* = -10$. The present solutions also suggest that terms of higher order than those retained in Ref. [4] are likely to be important for $u_\tau/\epsilon = O(1)$. In this case the curvature correction would no longer have a simple form, but would have to be incorporated in the numerical

solution through the use of modified boundary conditions. Moreover, it appears that certain terms of order u_τ^2, and possibly still other higher-order corrections, will also be essential for numerical accuracy, in the wall shear (Part II) as well as in the pressure. Finally, the local interaction influences the potential flow at larger distances; the manner of introducing corrections in the external flow deserves further study.

Appendix A: Interaction at Supersonic Speeds

Solutions as $u_\tau \to 0$ with ϵ fixed, such that the restriction to weak shocks is removed and the flow is considered supersonic rather than transonic, permit estimation of previously neglected higher-order terms in ϵ. It is found that an outer solution obtained for X/δ and Y/δ fixed can no longer be matched with the inner solution derived for x^* and y^* held fixed. Instead, it appears that a set of intermediate limits should also be considered, such that $u_\tau \ln y^*$ is held fixed, e.g., such that $y = (\delta_*/\delta)y^* = O(\delta_*^n/\delta^n)$ for $0 < n < 1$.

For each value of $u_\tau \ln y^*$ such that $0 < u_\tau \ln y^* < u_\tau \ln (\delta/\delta_*)$, the velocity profile (2.15) gives a value for U_u in the range $1 < U_u < 1 + \epsilon$. The flow downstream of the shock wave is then described in terms of small perturbations about a uniform flow with properties found from the jump conditions for a normal shock wave, and indicated by a subscript o, as follows:

$$U_o = \frac{1}{U_u} \tag{A.1}$$

$$\frac{P_o}{P_e} - 1 = 2\gamma \frac{1 - U_o^2}{(\gamma+1)U_o^2 - (\gamma - 1)} \tag{A.2}$$

$$\frac{\rho_o}{\rho_u} = \frac{1}{U_o^2} \tag{A.3}$$

$$B_o^2 = 1 - M_o^2 = \frac{1 - U_o^2}{1 - \frac{\gamma-1}{\gamma+1} U_o^2} \tag{A.4}$$

The perturbation quantities can be expressed in terms of variables $X/(B_o Y)$ and either $u_\tau \ln y^*$ or $u_\tau \ln x^*$; the latter is more convenient. Variables σ and λ are defined by

$$\sigma = u_\tau \kappa^{-1} \ln \frac{X}{B_o \delta_*}, \qquad \lambda = \frac{X}{B_o Y} \tag{A.5}$$

Here $\sigma = O(1)$ and $\lambda = O(1)$, $B_o = B_o(\sigma)$, and $0 < \sigma < \sigma_\delta$, where σ_δ will be defined in Eqn. (A.8) such that $U_o(\sigma_\delta) = (1+\epsilon)^{-1}$. If $\sigma \to 0$, then $B_o^2 \sim (\gamma+1)(\kappa T_e^{1/2})^{-1} u_\tau \ln x^*$, as noted following Eqn. (3.35), and λ is proportional to $x^*/(y^* \sqrt{\ln x^*})$, the similarity variable suggested for the derivation of Eqns. (3.34) and (3.35). The relation $\kappa^{-1} u_\tau \ln (Y/\delta_*) = \sigma - \kappa^{-1} u_\tau \ln \lambda$ implies the equivalence of $u_\tau \ln y^*$ and $u_\tau \ln x^*$ already noted. At the shock wave $\lambda = \lambda_s(\sigma)$, any quantity f has the form

$$f(\kappa^{-1} u_\tau \ln y^*) \sim f(\sigma) - \kappa^{-1} u_\tau f'(\sigma) \ln \lambda_s \tag{A.6}$$

where f may be, e.g., U_u, U_d, P_d or ρ_d. In particular, U_u at the shock wave is evaluated by replacing $\kappa^{-1} u_\tau \ln y^*$ with σ in Eqn. (2.15) and then setting $f = U_u$ in Eqn. (A.6); therefore $U_o(\sigma)$ is defined by

$$1/U_o(\sigma) = \Gamma \sin \{\sin^{-1}(\Gamma^{-1}) + \Gamma^{-1}(T_w/T_e)^{1/2}\sigma\} \tag{A.7}$$

where $\Gamma = (\gamma+1)^{1/2}/(\gamma-1)^{1/2}$ as before. For $U_o(\sigma_\delta) = (1+\epsilon)^{-1}$, σ_δ is defined by

$$\sigma_\delta = \kappa^{-1} u_\tau \ln(\delta/\delta_*) + 2\Pi \kappa^{-1} u_\tau. \tag{A.8}$$

and can be calculated with the help of Eqn. (2.14). It also follows that $U_o'(\sigma_\delta) = -(1+\epsilon)^{-2}$.

For the region downstream of the shock wave, Eqns. (3.1), (3.3), (3.5) and (3.6) suggest expansions of the flow quantities in the form

$$U = U_o(\sigma) + \kappa^{-1} u_\tau U_1(\lambda, \sigma) + \ldots \tag{A.9}$$

$$V = B_o(\sigma)\kappa^{-1} u_\tau V_1(\lambda, \sigma) + \ldots \tag{A.10}$$

$$P = P_o(\sigma) + \kappa^{-1} u_\tau P_1(\lambda, \sigma) + \ldots \tag{A.11}$$

$$\rho = \rho_o(\sigma) + \ldots \tag{A.12}$$

The differential equations (3.1) and (3.3) lead to the system

$$U_{1_\lambda} - \lambda V_{1_\lambda} = -\lambda^{-1} U_o' \tag{A.13}$$

$$\gamma\rho_o U_o U_{1_\lambda} + P_{1_\lambda} = -\gamma\rho_o U_o \lambda^{-1} U_o' - \lambda^{-1} P_o' \tag{A.14}$$

$$\gamma\rho_o U_o V_{1_\lambda} - \lambda P_{1_\lambda} = 0 \tag{A.15}$$

The vorticity $\Omega = V_X - U_Y$, referred to later, is found from these equations as

$$\Omega = -\frac{u_\tau}{\kappa Y}\left(U_o' + \frac{P_o'}{\gamma\rho_o U_o} \right) \tag{A.16}$$

The solutions for U_1 and P_1 must satisfy boundary conditions at the shock wave $\lambda = \lambda_s$, and it is required that $V_1 \to 0$ as $\lambda \to \infty$. The results are

$$U_1 = -U_o' \ln \lambda - \frac{P_o'}{2\gamma\rho_o U_o} \ln (\lambda^2 + 1) \tag{A.17}$$

$$V_1 = \frac{P_o'}{\gamma\rho_o U_o}\left(\frac{\pi}{2} - \tan^{-1}\lambda\right) \tag{A.18}$$

$$P_1 = -\frac{1}{2} P_o' \ln \frac{\lambda^2}{\lambda^2 + 1} \tag{A.19}$$

As $\lambda \to 0$, U_1 and P_1 have a logarithmic form consistent with the second

term in the expansion (A. 6). Equation (3. 6) for the shock-wave shape gives

$$X_s \sim \kappa^{-1} u_\tau \frac{\pi B_o P'_o}{2\gamma \rho_o (1-U_o^2)} Y \qquad \text{(A. 20)}$$

for $0 < \sigma < \sigma_\delta$; thus $\lambda_s = O(u_\tau)$. The slope dX_s/dY is $O\{u_\tau^{1/2}/(\ln x^*)^{1/2}\}$ or $O(u_\tau)$ as $\sigma \to 0$ or $\sigma \to \sigma_\delta$, respectively. Since $P_1 \to 0$ as $\lambda \to \infty$, the wall pressure is found from Eqn. (A. 2), for $0 < \sigma < \sigma_\delta$, as

$$\frac{P_w}{P_e} - 1 = 2\gamma \frac{1 - U_o^2}{(\gamma+1)U_o^2 - (\gamma-1)} + o(u_\tau) \qquad \text{(A. 21)}$$

For $X = O(\delta)$ and $Y = O(\delta)$, variables x and y are defined by

$$x = \frac{X}{B_o(\sigma_\delta)\delta} \qquad y = \frac{Y}{\delta} \qquad \text{(A. 22)}$$

where $B_o(\sigma_\delta)$ is the value given by Eqn. (A. 4) with $U_o(\sigma_\delta) = (1 + \epsilon)^{-1}$. The differential equations give $\Omega \sim - U_Y - (\gamma\rho U)^{-1} P_Y$, and ahead of the shock wave $\Omega \sim - (u_\tau/\delta) u'_{01}(y)$. Relative changes in Ω along a streamline are small except at the shock wave, and so the first approximation for Ω remains a function of Y, which can be calculated from the shock-wave relations, in a form which agrees with Eqn. (A. 16) as $y \to 0$. The flow is then described as a uniform flow at speed $U_o(\sigma_\delta)$ with superimposed small perturbations, the rotational part being shown explicitly:

$$U \sim \frac{1}{1+\epsilon} + u_\tau \{ U'_o(\sigma_\delta) + \frac{P'_o(\sigma_\delta)}{\gamma \rho_o(\sigma_\delta) U_o(\sigma_\delta)} \} u_{01}(y) + u_\tau \phi_x(x, y) \qquad \text{(A. 23)}$$

$$V \sim u_\tau B_o(\sigma_\delta) \phi_y(x, y) \qquad \text{(A. 24)}$$

For $u_\tau \to 0$, it follows from Eqn. (3.1) that ϕ must satisfy Laplace's equation. The shock-wave relation $U_d U_u \sim 1$ gives the boundary values for $\phi_x(0, y)$, the shock-wave location being taken as $x \sim 0$ in a first approximation; also $\phi_y(x, 0) = 0$ and $\nabla\phi \to 0$ as $x^2 + y^2 \to \infty$. The solution is

$$\phi(x, y) = -\frac{P_o'(\sigma_\delta)}{\pi\gamma\rho_o(\sigma_\delta)U_o(\sigma_\delta)} \int_{-\infty}^{\infty} u_{01}(\eta)\ln\{x^2 + (y-\eta)^2\}^{1/2} d\eta \qquad (A.25)$$

This result has the same form as the solution (3.19), which is recovered if the coefficient $P_o'/(\rho_o U_o)$ is expanded for $\epsilon \to 0$. As $x^2 + y^2 \to \infty$, the complex velocity and shock-wave shape have the same form as in Eqns. (3.22) and (3.24), respectively, but the source strength is now $u_\tau \delta m_1 P_o'/(2\gamma\rho_o U_o)$, evaluated at $\sigma = \sigma_\delta$. Since $P_x \sim -\gamma\rho_o(\sigma_\delta)U_o(\sigma_\delta)U_x$, the wall pressure is

$$P_w \sim P_o(\sigma_\delta) + \frac{2}{\pi} P_o'(\sigma_\delta) u_\tau \, x \int_0^{\infty} \frac{u_{01}(\eta)}{x^2+\eta^2} d\eta \qquad (A.26)$$

The expansion as $x^* \to \infty$ of an inner solution derived for $x^* = O(1)$ gives $P_w/P_e \sim 1 + 2\gamma(\kappa T_e^{1/2})^{-1} u_\tau \ln x^*$, which does not agree with the expansion of Eqn. (A.26) as $x \to 0$. Instead, the two results are the leading terms of Eqn. (A.21) expanded for $\sigma \to 0$ and $\sigma \to \sigma_\delta$ respectively. Thus one can construct inner and outer limit-process solutions, but they cannot be matched in the usual way, and the expansions (A.9) through (A.12) are not limit-process expansions. This asymptotic structure is closely analogous to, and is a direct consequence of, that for the velocity in the undisturbed boundary layer. A solution for P_w which is valid for $0 < \sigma \leq \sigma_\delta$ can be written in a form analogous to Eqn. (2.10), by use of a suitable correction

to the argument of the function P_o:

$$P_w \sim P_o\left(\sigma_\delta + \frac{2}{\pi} u_\tau x \int_0^\infty \frac{u_{01}(\eta)d\eta}{x^2 + \eta^2}\right) \qquad \text{(A. 27)}$$

If $u_\tau \to 0$ with x held fixed, the first two terms in the expansion of Eqn. (A. 27) are the terms shown in Eqn. (A. 26). If $u_\tau \to 0$ and $x \to 0$ with $u_\tau \ln x^*$ held fixed, Eqn. (A. 21) is recovered. The result (A. 27) would replace Eqn. (3. 21) if ϵ were not small. However, $0 < \epsilon < 0.3$ if $1 < M_e < 1.4$, and even at $\epsilon = 0.3$ these two results differ only slightly; e.g., $P_o(\sigma_\delta)$ differs from its three-term representation as $\epsilon \to 0$ by less than three percent at $M_e = 1.4$. Corrections for $\epsilon = O(1)$ are therefore of far less importance than the higher-order effects described in Sections 3 and 4.

Appendix B: Intermediate Solutions

For $u_\tau \ll \epsilon \ll 1$, intermediate solutions can be derived for $\delta_* \ll Y \ll \delta$ and $u_\tau^{1/2} \delta_* \ll X \ll \epsilon^{1/2} \delta$. In applications where u_τ/ϵ is a much smaller number than in the examples of Section 4, these solutions can be used to give higher-order terms in the region of the steepest gradient in wall pressure. From a theoretical viewpoint, the solutions can be used to show details of the higher-order matching of terms in the outer and inner solutions. The first-order inner solution for the wall pressure as $x^* \to \infty$ is $P_w/P_e \sim 1 + O(u_\tau \ln x^*)$, whereas the outer solution as $x \to 0$ gives $P_w/P_e \sim P_f/P_e + O(u_\tau \ln x)$, where $P_f/P_e \sim 1 + O(\epsilon)$. That is, the inner and outer solutions for P_w describe small perturbations from different constant values. Matching of the solutions is nonetheless possible provided that $\epsilon \to 0$; if, however, $\epsilon = O(1)$, the solutions no longer can be matched, as explained in Appendix A. Derivation of some higher-order terms for $\epsilon \to 0$ helps to verify that the matching procedure can be carried out to higher order.

A shock wave in the external flow can extend into the boundary layer almost to the sonic line, which is located close to the wall in the present case for $u_\tau \ll \epsilon$. Near the sonic line the beginning of the pressure rise implies outgoing compression waves, in a weakly rotational mean flow described by the velocity-defect profile, which will coalesce to form an outgoing shock wave with very small downstream inclination from the normal to the wall. For $Y = O(\delta_*)$, the undisturbed profile is $U_u = 1 + O(u_\tau)$, and an "inner" solution, discussed briefly in Section 3, describes changes in U which are also $O(u_\tau)$ along a streamline. In the limit as $u_\tau \to 0$, nontrivial equations

are obtained for describing this initial change if $X = O(u_\tau^{1/2}\,\delta_*)$ and $V = O(u_\tau^{3/2})$. These are the transonic small-disturbance equations, with prescribed vorticity. For the second approximations, to be discussed below, an additional term must be retained in the expansion of Eqn. (3.1), and a correction to the vorticity is needed. To second order in u_τ, for $Y = O(\delta_*)$, the entropy s is unchanged across the shock wave, and also $\rho u = 1 + O(u_\tau)$, so that the streamlines are approximately lines Y = constant. The first terms in equation (3.4) give $\Omega U \sim \gamma^{-1} T\,ds/dY$, where $\Omega = \partial V/\partial X - \partial U/\partial Y$, and changes along a streamline are related by $\Omega^{-1}\,\Delta\Omega \sim T^{-1}\,\Delta T - U^{-1}\,\Delta U$. Since $U \sim 1$ and $T \sim 1$, and since Eqn. (3.2) with $T = a^2$ gives $\Delta T \sim -(\gamma - 1)\,\Delta U$, the change in vorticity becomes $\Delta\Omega \sim -\gamma\Omega\,\Delta U$. The total vorticity is then

$$\frac{\partial V}{\partial X} - \frac{\partial U}{\partial Y} = -\frac{dU_u}{dY} + \gamma\,(U - U_u)\,\frac{dU_u}{dY} + \cdots \qquad (B.1)$$

where U_u is found from Eqn. (2.15). A somewhat longer calculation based on expansion of the differential equation for the vorticity shows that this change in vorticity contains two contributions, one from the change in density and one from the torque which acts on a fluid element because the pressure gradient and density gradient vectors are in different directions.

Coordinates x^*, y^* and perturbation velocity components u^*, v^* are defined in Eqns. (3.27) and (3.28). The inner region $Y = O(\delta_*)$, $X = O(u_\tau^{1/2}\,\delta_*)$ sketched in Fig. 2 is to be understood as vanishingly small in the limit as $u_\tau/\epsilon \to 0$. To the order needed in the derivations which follow, Eqn. (3.1) and the vorticity equation become

$$u^* u^*_{x^*} - v^*_{y^*} = -(\gamma - \tfrac{1}{2})\,\alpha^*\,u_\tau\,u^{*2}\,u^*_{x^*} + \cdots \qquad (B.2)$$

$$v^*_{x^*} - u^*_{y^*} = -\frac{du^*_u}{dy^*} + \gamma\alpha^* u_\tau (u^* - u^*_u)\frac{du^*_u}{dy^*} + \cdots \qquad (B.3)$$

where u^*_u refers to u^* in the undisturbed boundary layer, found from Eqn. (2.15), and α^* is a constant defined by $\alpha^* = (\kappa T_e^{1/2})^{-1}$. Changes in the slopes of the characteristics $dx^*/dy^* = u^{*-1/2}$ are O(1) in the region where x^* and y^* are O(1), and so the outgoing compression waves presumably will first coalesce to form a shock wave at a finite value of y^*. The shock-wave shape will be described in the new variables by $x^* = x^*_s(y^*)$. The shock-wave relations (3.5) and (3.6) become

$$v^{*2}_d = \frac{1}{2}(u^*_u - u^*_d)^2 (u^*_d + u^*_u - u_\tau \alpha^* u^{*2}_u + \cdots) \qquad (B.4)$$

$$\frac{dx^*_s}{dy^*} = -\frac{v^*_d}{u^*_d - u^*_u} \qquad (B.5)$$

where the subscripts u and d again indicate values immediately upstream and downstream of the shock wave. In obtaining Eqn. (B.4) use has been made of the anticipated result that $u^*_d \sim -u^*_u$, since the shock wave is nearly normal. The value of u^*_u can depend on the solution, since for $y^* = O(1)$ the pressure disturbance extends ahead of the shock wave. But the outgoing compression waves which originate here, within a distance $X = O(u_\tau^{1/2}\,\delta_*)$ upstream, are overtaken by the shock wave when $Y \gg \delta_*$, and so the upstream flow is the undisturbed boundary-layer flow when $Y \gg \delta_*$. Henceforth the subscript u will refer to conditions in the undisturbed boundary layer.

The discussion preceding Eqn. (3.34) suggests the use of variables t and λ defined by

$$t = \ln x^* \tag{B.6}$$

$$\lambda = \frac{x^*}{y^* (\ln x^*)^{1/2}} = \frac{X}{Y (\gamma+1)^{1/2} (\alpha^* u_\tau \ln x^*)^{1/2}} \tag{B.7}$$

This definition of λ is equivalent to that given in Eqn. (A.5) if $u_\tau \ln x^*$ is small. Solutions are now sought for $u_\tau \to 0$ and $t \to \infty$, such that $u_\tau t \to 0$ and λ is held fixed. If u^* and v^* are now regarded as functions of the new variables t and λ, the differential equations become

$$\frac{1}{t^{1/2}} u^* \left(\frac{1}{\lambda} u_t^* + \left(1 - \frac{1}{2t}\right) u_\lambda^*\right) + \lambda v_\lambda^*$$
$$= -\left(\gamma - \frac{1}{2}\right) \alpha^* u_\tau \frac{1}{t^{1/2}} u^{*2} \left(u_\lambda^* + \frac{1}{\lambda} u_t^* + \cdots\right) + \cdots \tag{B.8}$$

$$\frac{1}{t^{1/2}} \left(\frac{1}{\lambda} v_t^* + \left(1 - \frac{1}{2t}\right) v_\lambda^*\right) + \lambda u_\lambda^*$$
$$= -1 + \alpha^* u_\tau \left(\gamma u^* - \frac{\gamma+1}{2} t + \cdots\right) + \cdots \tag{B.9}$$

The forms for the first terms in an expansion for u^* should correspond to the terms required at the shock wave, found from $u_d^* \sim -\ln y^*$ with $y^* = x^*/(\lambda t^{1/2})$, and the forms for additional terms in u^* and v^* are found using equations (B.4), (B.8), and (B.9). It is then assumed that

$$u^* \sim \{t u_0(\lambda) + (\ln t)\bar{u}_1(\lambda) + u_1(\lambda) + (t^{-1} \ln t)\bar{u}_2(\lambda)$$
$$+ t^{-1} u_2(\lambda) + \cdots\} + \alpha^* u_\tau \{t^2 u_0^{(1)}(\lambda) + (t \ln t)\bar{u}_1^{(1)}(\lambda)$$
$$+ t u_1^{(1)}(\lambda) + \cdots\} + \cdots \tag{B.10}$$

$$v^* \sim \{t^{1/2} v_1(\lambda) + (t^{-1/2} \ln t)\bar{v}_2(\lambda) + t^{-1/2} v_2(\lambda) + \cdots\}$$
$$+ \alpha^* u_\tau \{t^{3/2} v_1^{(1)}(\lambda) + \cdots\} + \cdots \tag{B.11}$$

It will be seen that these assumed forms are sufficient to provide the first few terms of a self-consistent set of solutions to the inviscid-flow equations.

When the assumed expansions (B.10) and (B.11) for $t \to \infty$ and $u_\tau t \to 0$ are substituted into the differential equations (B.8) and (B.9), it is easily seen that the largest terms u_0 and $u_0^{(1)}$ are constants, the values of which are to be determined from the shock-wave conditions. In the new variables the shock-wave shape can be written as $\lambda = \lambda_s(t)$. Substitution in the shock-polar equation (B.4), with u_u^* found from Eqn. (2.15), gives

$$t^{1/2} v_1(\lambda_s) + \cdots = 2^{-1/2} \{t - t u_0(\lambda_s) + \cdots\} \{t - \frac{1}{2} \ln t - \ln \lambda_s - \frac{\gamma - 1}{4} \alpha^* u_\tau t^2 + \cdots + t u_0(\lambda_s) + (\ln t) \bar{u}_1(\lambda_s) + u_1(\lambda_s) + \cdots + \alpha^* u_\tau t^2 u_0^{(1)}(\lambda_s) + \cdots - \alpha^* u_\tau t^2 + \cdots\}^{1/2} \tag{B.12}$$

Equation (B.5) gives the shock-wave shape in the form

$$\frac{dx_s^*}{dy^*} = \frac{t^{1/2} v_1(\lambda_s) + \cdots}{t - t u_0(\lambda_s) + \cdots} = O\left(\frac{1}{(\ln x^*)^{1/2}}\right) \tag{B.13}$$

Integration then gives $x_s^* = O(y^*/(\ln x^*)^{1/2})$ and so $\lambda_s = O(t^{-1})$. Thus the functions of λ_s in Eqns. (B.12) and (B.13) can all be written as series expansions about $\lambda_s = 0$, with $\ln \lambda_s \sim - \ln t$. The largest term in the square root in Eqn. (B.12) must be $O(t^{-1/2})$, and so the first several terms inside the brackets must add to zero. In particular, it follows that

$$u_0(\lambda) = -1 \quad , \quad u_0^{(1)}(\lambda) = \frac{3 + \gamma}{4} \tag{B.14}$$

The differential equations for $\bar{u}_1$, u_1, and v_1 are

$$\bar{u}_1' = 0 \quad , \quad u_1' - \lambda v_1' = \frac{1}{\lambda} \quad , \quad \lambda u_1' + v_1' = -1 \tag{B.15}$$

and it is also required that $v_1 \to 0$ as $\lambda \to \infty$. As $\lambda \to 0$, it is found from the solution for u_1 that $u_1 \sim \ln\lambda + \text{const}$. The shock-polar equation (B.12) then given $\bar{u}_1(\lambda_s) = 1/2$ and $u_1(\lambda) - \ln\lambda \to 0$ as $\lambda \to 0$. The solutions are

$$\bar{u}_1(\lambda) = \frac{1}{2} \quad , \quad u_1(\lambda) = \ln \frac{\lambda}{\lambda^2 + 1} \quad , \quad v_1(\lambda) = 2\tan^{-1}\left(\frac{1}{\lambda}\right) \tag{B.16}$$

The largest terms in $u^* + \ln y^*$ and in $(\ln x^*)^{-1/2} v^*$, i.e., $u_1 + \ln\lambda$ and v_1, respectively, are functions of the variable $\lambda = (x^*/y^*)(\ln x^*)^{-1/2}$ and so have a self-similar form. Furthermore, if M is the local Mach number, $(1 - M^2) \sim (\gamma + 1)(1 - U)$ and so, using $\ln y^* \sim \ln x^*$ for $\lambda = O(1)$,

$$1 - M^2 \sim (\gamma + 1)\, \alpha^* u_\tau \ln x^* \tag{B.17}$$

$$\lambda \sim (1 - M^2)^{-1/2} X/Y \tag{B.18}$$

That is, the Prandtl-Glauert factor $(1 - M^2)^{1/2}$ appears in a familiar position in the variable λ, and also appears in the velocity component V, which can be written $V \sim (1 - M^2)^{1/2} \alpha^* u_\tau v_1(\lambda)$. Also, the solutions for u_0, $\bar{u}_1$, and $u_0^{(1)}$ are consistent with the result $u_d^* \sim -\ln y^* + \frac{3+\gamma}{4} \alpha^* u_\tau \ln^2 y^*$ which would be found if the shock wave were exactly normal. The expansions (B.10) and (B.11) for u^* and v^* then describe small perturbations about a parallel flow with $U \sim 1 - \alpha^* u_\tau \ln y^* + \frac{3+\gamma}{4} (\alpha^* u_\tau \ln y^*)^2$, and the largest terms satisfy equations which are essentially the Prandtl-Glauert equations, but with specified non-zero vorticity, and written in a self-similar form. These terms are given in Eqns. (3.34) and (3.35).

The pressure is then found from equation (3.11), and for $\lambda \to \infty$

$$P_w/P_e \sim 1 + 2\gamma\alpha^* u_\tau \ln x^* \tag{B.19}$$

where $P_e \sim 1 - \gamma\epsilon + \cdots$. The result (B.19) was given by Adamson and Messiter [8], and, with the replacement $\ln y^* \sim \ln x^*$, the first-order solutions (3.34) and (3.35) also are easily shown to be equivalent to their results for the velocity components. In addition, the first-order shock-wave shape, for $\delta^* \ll Y \ll \delta$, follows from equation (3.6) as

$$\begin{aligned} X_s(Y) &\sim \frac{1}{2}\pi\,(\ln x^*)^{-1}(\gamma+1)^{1/2}\,(\alpha^* u_\tau \ln x^*)^{1/2}\,Y \\ \lambda_s(t) &\sim \frac{1}{2}\frac{\pi}{t} \end{aligned} \tag{B.20}$$

An attempt at using the term $\frac{1}{4}(3+\gamma)\,\alpha^* u_\tau t^2$ in u^* to obtain a correction in the wall pressure P_w leads to a difficulty because the second-order term in the pressure formula (3.11) contains a factor $\ln y^*$, whereas a result for $\lambda \to \infty$ is required which depends only on x^*. If the replacement $\ln y^* \sim \ln x^* + \ln\lambda$ is made in this expression, it might be anticipated that a higher-order term in u^* would permit cancellation of the term in P which contains the factor $\ln\lambda$. With this assumption the improved approximation for P_w is found to be

$$P_w/P_e \sim 1 + 2\gamma\alpha^* u_\tau \ln x^* + \frac{1}{2}\gamma(3\gamma - 1)(\alpha^* u_\tau \ln x^*)^2 + \cdots \tag{B.21}$$

The calculation of higher-order terms below shows that the cancellation does actually occur, and so the assumed result (B.21) is in fact obtained for P_w.

Solutions are next derived for $\bar{u}_2$, u_2, $\bar{u}_1^{(1)}$, and $u_1^{(1)}$. The differential equations (B.8) and (B.9) give $\bar{u}_1^{(1)\prime} = 0$ and

$$\bar{u}_2' - \lambda \bar{v}_2' = \frac{1}{2}\left(u_1' - \frac{1}{\lambda}\right) \qquad \lambda \bar{u}_2' + v_2' = 0$$

$$u_2' - \lambda v_2' = \left(\frac{1}{2} + u_1\right)\left(u_1' - \frac{1}{\lambda}\right) \qquad \lambda u_2' + v_2' = \frac{1}{2}\left(v_1' - \frac{1}{\lambda} v_1\right) \quad \text{(B.22)}$$

$$u_1^{(1)'} - \lambda v_1^{(1)'} = \frac{1}{4}(5\gamma+1)u_1' - \frac{7}{4}(\gamma+1)\frac{1}{\lambda} \qquad \lambda u_1^{(1)'} + v_1^{(1)'} = -\frac{1}{2}(3\gamma+1)$$

The shock-polar equation (B.12), after substitution of the solutions (B.16), and with the additional terms now needed, is

$$\begin{aligned}\pi t^{1/2} + \cdots + \alpha^* u_\tau t^{3/2} v_1^{(1)}(\lambda_s) + \cdots \\ = 2^{-1/2}\{2t + \cdots\}\{&\frac{\gamma-1}{4}\alpha^* u_\tau t \ln t + \frac{\gamma-1}{2}\alpha^* u_\tau t \ln \lambda_s + \cdots \\ &+ (t^{-1}\ln t)\bar{u}_2(\lambda_s) + t^{-1}u_2(\lambda_s) + \alpha^* u_\tau (t\ln t)\bar{u}_1^{(1)}(\lambda_s) \\ &+ \alpha^* u_\tau t u_1^{(1)}(\lambda_s) + \cdots + \alpha^* u_\tau t(\ln t + 2\ln\lambda_s) + \cdots\}^{1/2}\end{aligned} \quad \text{(B.23)}$$

where the functions of λ_s are to be expanded about the result (B.20) $\lambda_s \sim \frac{1}{2}\pi t^{-1}$, for $t \to \infty$. Since the differential equations give $\bar{u}_1^{(1)} = \text{constant}$ and $u_1^{(1)} \sim -\frac{1}{2}(\gamma+3)\ln\lambda$ as $\lambda \to 0$, it follows from the shock-polar equation (B.23) that $\bar{u}_1^{(1)}(\lambda) = -(\gamma+3)/4$ and

$$\bar{u}_2(0) = u_2(0) - \frac{1}{2}\pi^2 = \left[u_1^{(1)}(\lambda) + \frac{\gamma+3}{2}\ln\lambda\right]_{\lambda=\lambda_s} = 0 \quad \text{(B.24)}$$

In addition it is required that $\bar{v}_2$, v_2, $v_2^{(1)} \to 0$ as $\lambda \to \infty$. The solutions are

$$\bar{u}_2(\lambda) = -\frac{\lambda^2}{2(\lambda^2+1)} \qquad \bar{v}_2(\lambda) = \frac{1}{2}\left(\tan^{-1}\lambda - \frac{\pi}{2} - \frac{\lambda}{1+\lambda^2}\right)$$

$$u_2(\lambda) = \frac{1}{\lambda^2+1}\ln\frac{\lambda^2}{\lambda^2+1} - \frac{1}{2}\ln\frac{\lambda}{\lambda^2+1} + \frac{1}{2}\left(\frac{\pi}{2} - \tan^{-1}\lambda\right)^2 + \frac{3\pi^2}{8}$$

$$v_2(\lambda) = -\frac{\lambda}{\lambda^2+1}\ln\frac{\lambda}{\lambda^2+1} + \frac{1}{2}\left(\tan^{-1}\lambda - \frac{\pi}{2}\right)\ln\frac{\lambda^2}{\lambda^2+1} + \frac{1}{2}\int_\lambda^\infty \frac{\ln(\lambda^2+1)}{\lambda^2+1}\,d\lambda$$

$$\bar{u}_1^{(1)} = -\frac{1}{4}(\gamma+3) \quad \text{(B.25)}$$

$$u_1^{(1)}(\lambda) = -\frac{1}{2}(\gamma-1)\ln(\lambda^2+1) - \frac{1}{2}(\gamma+3)\ln\lambda - \frac{1}{4}(5\gamma+1)\frac{\lambda^2}{\lambda^2+1}$$

$$v_1^{(1)}(\lambda) = \frac{1}{4}(\gamma+5)\left(\tan^{-1}\lambda - \frac{\pi}{2}\right) - \frac{1}{4}(5\gamma+1)\frac{\lambda}{\lambda^2+1}$$

The improved solution for the wall pressure is, in terms of $t \equiv \ln x^*$,

$$P_w/P_u \sim 1 + \gamma\alpha^* u_\tau \{2t - \ln t + \frac{1}{2} t^{-1} \ln t - \frac{3\pi^2}{8} t^{-1} + \cdots\}$$
$$+ \gamma(\alpha^* u_\tau)^2 \{\frac{1}{2}(3\gamma - 1)t^2 - \frac{1}{2}(3\gamma - 1)t \ln t + \frac{1}{4}(5\gamma + 1)t + \cdots\} + \cdots \quad (B.26)$$

The solution for $u^*(x^*, y^*)$ as $x^* \to \infty$ can be compared with the expansion as $x \to 0$ of the result derived for $x = O(1)$. Retaining only the terms which increase in size, one finds for the velocity

$$U - 1 \sim -\alpha^* u_\tau \ln x^* + \frac{1}{2}\alpha^* u_\tau \ln \ln x^* + \alpha^* u_\tau \ln \lambda - \alpha^* u_\tau \ln(1 + \lambda^2)$$
$$+ \frac{\gamma + 3}{4}(\alpha^* u_\tau)^2 \ln^2 x^* - \frac{\gamma + 3}{4}(\alpha^* u_\tau)^2 \ln x^* \ln \ln x^*$$
$$+ (\alpha^* u_\tau)^2 \left\{-\frac{\gamma - 1}{2}\ln(\lambda^2 + 1) - \frac{3 + \gamma}{2}\ln\lambda - \frac{5\gamma + 1}{4}\frac{\lambda^2}{\lambda^2 + 1}\right\} \ln x^* + \cdots \quad (B.27)$$

As $x^* \to 0$, the largest terms in Eqn. (B.27) agree with the largest terms in the expansion of Eqn. (3.9) as $x \to \infty$, found with the help of Eqns. (3.12) and (3.20). For another comparison, the expansion of Eqn. (A.27) for the pressure as $\epsilon \to 0$ and $x \to 0$ is equivalent to the three terms shown in Eqn. (B.21).

The order of magnitude of V as $\lambda \to \infty$ can be found from consideration of the region for $\lambda >> 1$ in which changes in τ can no longer be neglected in the X-momentum equation. For intermediate limits such that $\lambda \to \infty$ slowly, the inertia and pressure terms are still dominant, whereas for intermediate limits such that $y \to \infty$ slowly, the equation remains $\tau_Y \sim 0$. There must then be a special limit for which all these terms are retained. It is found rather easily that this balance of terms occurs for $Y/X = O(u_\tau)$. Solutions in this limit are

obtained in Refs. [3] and [4] and in Part II of the present work, for the cases $\epsilon << u_T$, $\epsilon = O(u_T)$, and $\epsilon >> u_T$, respectively. For the present case (Part II), a term of order $u_T^2 \ln x^*$ in U, when substituted in an expansion of Eqn. (3.1), leads to the result that $V = O(u_T^3 \ln x^*)$, smaller than any of the terms in V retained above. It is this argument which implies the boundary condition $V \to 0$ as the distance from the wall decreases, to all orders of magnitude considered in this and subsequent sections.

The result (B.26) does include the correction term anticipated in Eqn. (B.21) and also shows a number of additional terms. In one of the smaller terms a factor $\ln y^*$ has been replaced by $\ln x^*$ in anticipation, as before, that the omitted part $\ln \lambda$ would be cancelled in the next approximation. This minor difficulty appears to arise because a different approximation is needed if $y^* = O(1)$ and therefore $\ln \lambda = O(t)$. Here u^* is not correctly approximated by $-\ln y^*$ because the gas in this region has not passed through a shock wave, but instead has undergone changes described by the transonic small-disturbance equations in a region where $x^* = O(1)$. However, P_Y is extremely small if $y^* = O(1)$ and $x^* >> 1$, and so P_w is obtained from the above solution in the limit as $\lambda \to \infty$. If the expansion had been carried out instead in terms of $\ln y^*$ rather than $\ln x^*$, it would evidently have been necessary to derive additional "inner" solutions for $y^* = O(1)$, because in this formulation P is expanded for $\ln y^* \to \infty$ and does not approach a function of x^* as the corresponding similarity variable becomes large.

References

[1] J. Ackeret, F. Feldmann, and N. Rott, Untersuchungen an Verdichtungsstössen und Grenzschichten in schnell bewegten Gasen. Mitteilungen aus dem Inst. für Aerodyn., ETH Zürich, Nr. 10 (1946). Translated as NACA TM 1113 (1947).

[2] G. E. Gadd, Interactions between Normal Shock Waves and Turbulent Boundary Layers. A.R.C. 22559, R. & M. 3262 (1961).

[3] T. C. Adamson, Jr., and A. Feo, Interaction between a Shock Wave and a Turbulent Boundary Layer in Transonic Flow. SIAM J. Appl. Math. 29, 121-145 (1975).

[4] R. E. Melnik and B. Grossman, Analysis of the Interaction of a Weak Normal Shock Wave with a Turbulent Boundary Layer. AIAA Paper No. 74-598 (1974).

[5] R. E. Melnik and B. Grossman, Further Developments in an Analysis of the Interaction of a Weak Normal Shock Wave with a Turbulent Boundary Layer. Symposium Transsonicum II, K. Oswatitsch and D. Rues, eds., Springer-Verlag (1976), pp. 262-272.

[6] R. E. Melnik and B. Grossman, Interactions of Normal Shock Waves with Turbulent Boundary Layers at Transonic Speeds. Transonic Flow Problems in Turbomachinery, T. C. Adamson, Jr., and M. F. Platzer, eds., Hemisphere Publ. Co. (1977), pp. 415-433.

[7] T. C. Adamson, Jr ., The Structure of Shock Wave-Boundary Layer Interactions in Transonic Flow. Symposium Transsonicum II, K. Oswatitsch and D. Rues, eds., Springer-Verlag (1976), pp. 244-251.

[8] T. C. Adamson, Jr., and A. F. Messiter, Normal Shock Wave-Turbulent Boundary Layer Interactions in Transonic Flow near Separation. Transonic Flow Problems in Turbomachinery, T. C. Adamson, Jr., and M. F. Platzer, eds., Hemisphere Publ. Co. (1977), pp. 392-414.

[9] T. C. Adamson, Jr., and A. F. Messiter, Shock Wave-Turbulent Boundary Layer Interactions in Transonic Flow. Advances in Engineering Science, NASA CP-2001 (1976), pp. 1425-1435.

[10] A. F. Messiter and T. C. Adamson, Jr., A Study of the Interaction of a Normal Shock Wave with a Turbulent Boundary Layer at Transonic Speeds, Advanced Technology Airfoil Research, NASA CP 2045 (1978), vol. I, pp. 271-279.

[11] T. von Kármán, Theorie des Reibungswiderstandes. Konferenz über Hydromechanische Probleme des Schiffsantriebs, Hamburg, 1932. Reprinted in Collected Works of Theodore von Kármán, Butterworths (1956), vol. II, pp. 394-414.

[12] C. B. Millikan, A Critical Discussion of Turbulent Flows in Channels and Circular Tubes, Proc. 5th Int. Cong. Appl. Mech. (1938), pp. 386-392.

[13] D. E. Coles, The Law of the Wake in the Turbulent Boundary Layer. J. Fluid Mech. 1, 191-226 (1956).

[14] H. Tennekes, Outline of a Second-Order Theory of Turbulent Pipe Flow. AIAA J. 6, 1735-1740 (1968).

[15] K. S. Yajnik, Asymptotic Theory of Turbulent Shear Flows. J. Fluid Mech. 42, 411-427 (1970).

[16] G. L. Mellor, The Large Reynolds Number Asymptotic Theory of Turbulent Boundary Layers. Int. J. Eng. Sci. 10, 851-873.

[17] W. B. Bush and F. E. Fendell, Asymptotic Analysis of Turbulent Channel and Boundary-Layer Flow. J. Fluid Mech. 56, 657-681 (1972).

[18] N. Afzal, A Higher Order Theory for Compressible Turbulent Boundary Layers at Moderately Large Reynolds Number. J. Fluid Mech. 57, 1-25 (1973).

[19] K. Stewartson and P. G. Williams, Self-Induced Separation. Proc. Roy. Soc. A 312, 181-206 (1969).

[20] A. F. Messiter, A. Feo and R. E. Melnik, Shock-Wave Strength for Separation of a Laminar Boundary Layer at Transonic Speeds. AIAA J. 9, 1197-1198 (1971).

[21] H. M. Brilliant and T. C. Adamson, Jr., Shock Wave Boundary Layer Interactions in Laminar Transonic Flow. AIAA J. 12, 323-329 (1974).

[22] E. R. van Driest, Turbulent Boundary Layer in Compressible Fluids. J. Aero. Sci. 18, 145-160 (1951).

[23] P. A. Lagerstrom and R. G. Casten, Basic Concepts Underlying Singular Perturbation Techniques. SIAM Review 14, 63-120 (1972).

[24] G. Maise and H. McDonald, Mixing Length and Kinematic Eddy Viscosity in a Compressible Boundary Layer. AIAA J. 6, 73-80 (1968).

[25] T. Cebeci and A. M. O. Smith, Analysis of Turbulent Boundary Layers. Academic Press, 1974.

[26] H. S. Ribner, Shock-Turbulence Interaction and the Generation of Noise. NACA TN 3255 (1954).

[27] G. E. Gadd, The Possibility of Normal Shock Waves on a Body with Convex Surfaces in Inviscid Transonic Flow, Z. Angew. Math. Phys. 11, 51-58 (1960).

[28] K. Oswatitsch and J. Zierep, Das Problem des senkrechten Stosses an einer gekrümmten Wand, Z. Angew. Math. Mech. 40, 143-144 (1960).

[29] A. F. Messiter and T. C. Adamson, Jr., On the Flow near a Weak Shock Wave Downstream of a Nozzle Throat. J. Fluid Mech. 69, 97-108 (1975).

[30] J. E. Lewis, R. L. Gran, and T. Kubota, An Experiment on the Adiabatic Compressible Turbulent Boundary Layer in Adverse and Favorable Pressure Gradients, J. Fluid Mech. 51, 657-672 (1972).

[31] R. Bohning and J. Zierep, Der senkrechte Verdichtungsstoss an der gekrümmten Wand unter Berücksichtigung der Reibung, Z. Angew. Math. Phys. 27, 225-240 (1976).

[32] G. R. Inger and W. H. Mason, Analytical Theory of Transonic Normal Shock-Turbulent Boundary-Layer Interactions, AIAA J. 14, 1266-1272 (1976).

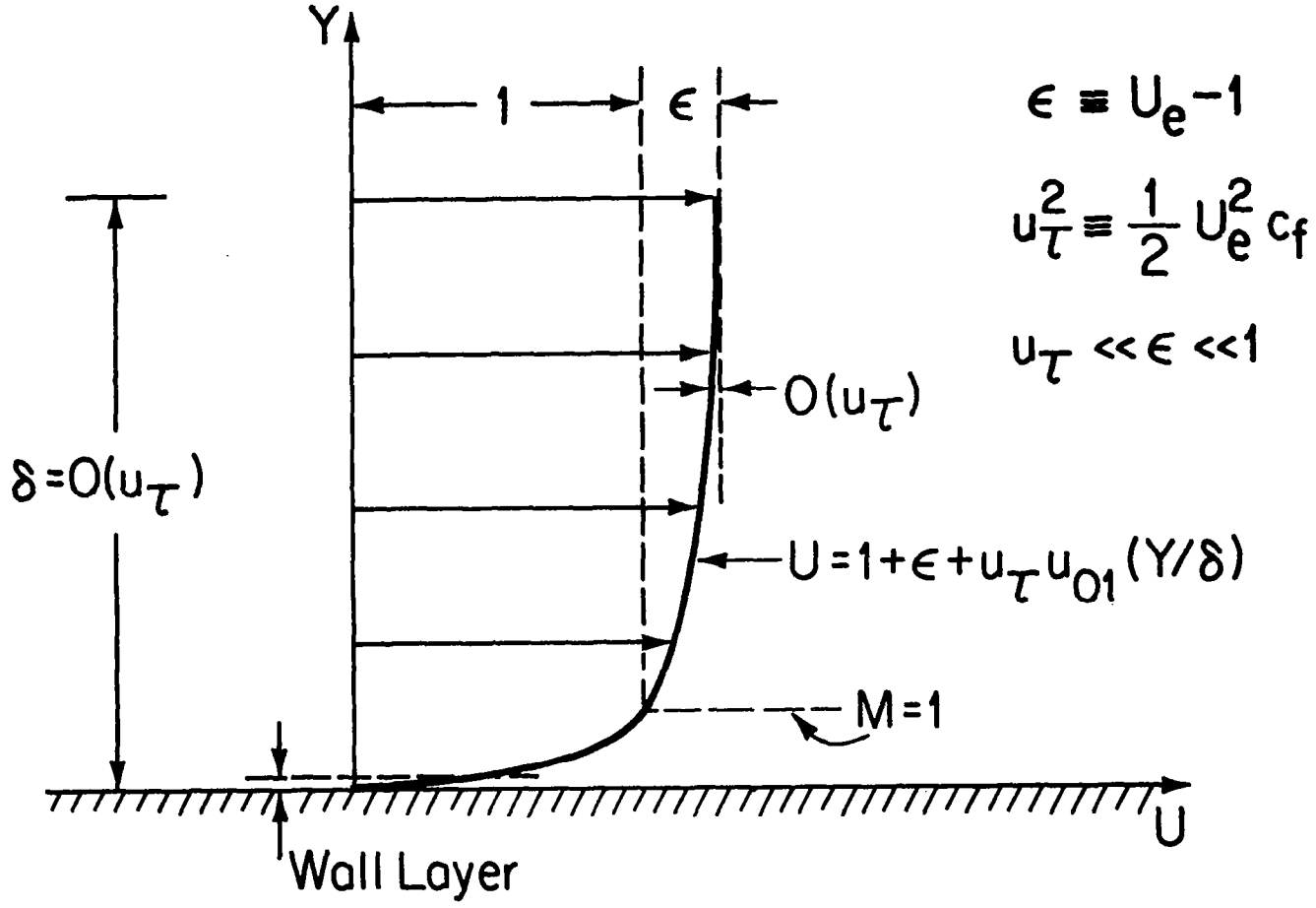

Figure 1. Undisturbed velocity profile.

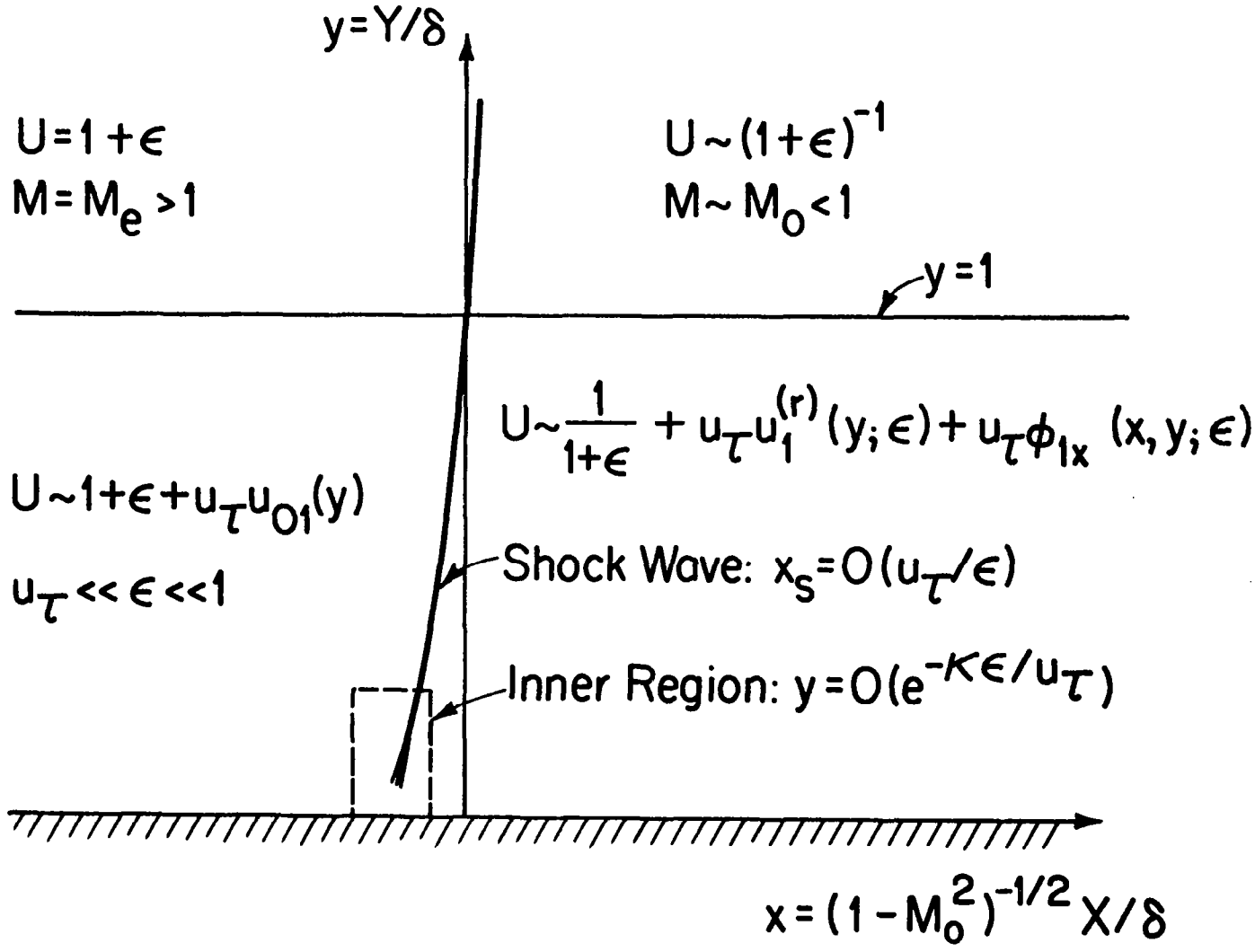

Figure 2. Asymptotic representation of "outer" flow.

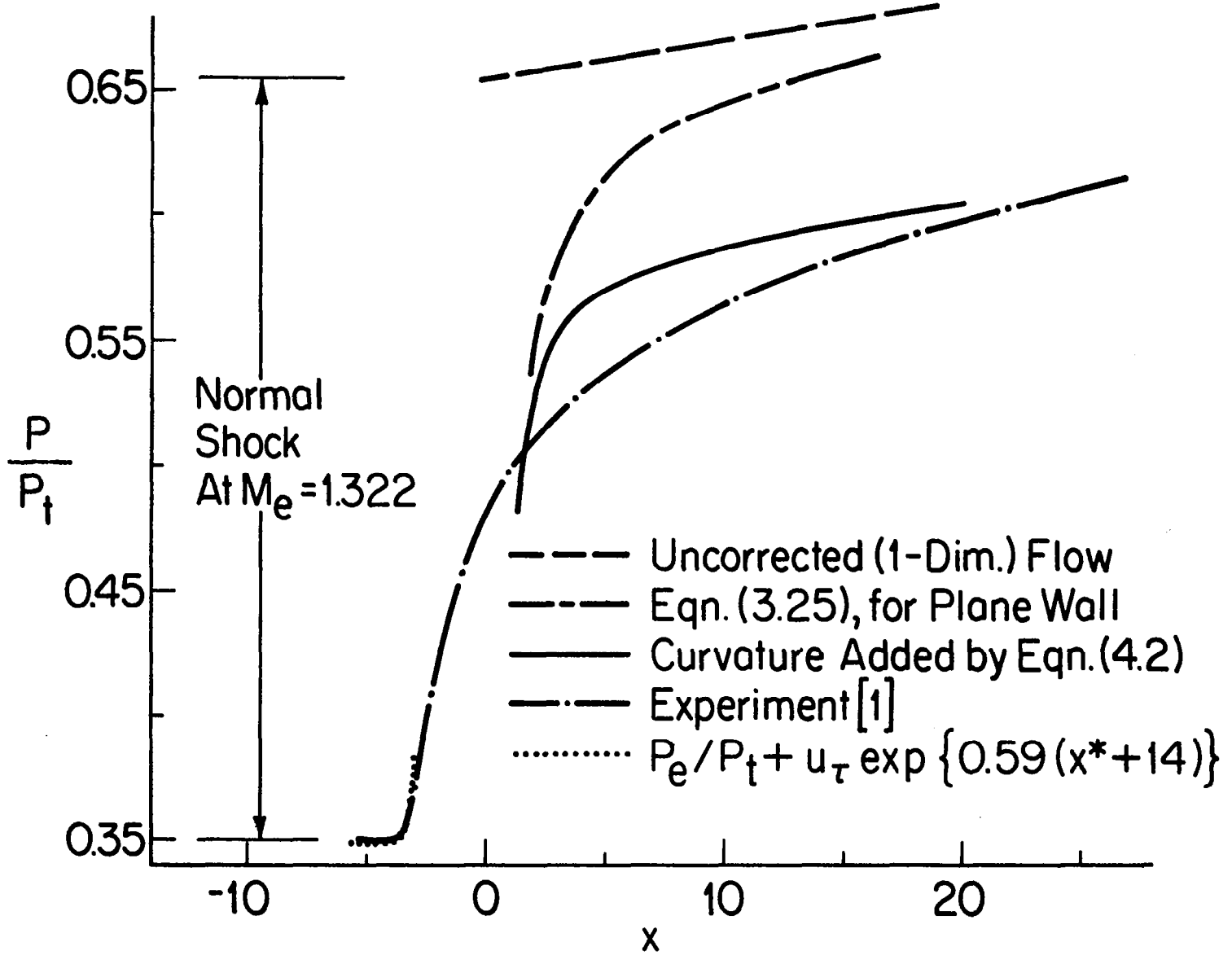

Figure 3. Pressure at wall with longitudinal curvature: M_e = 1.322, Re = 9.6 x 10^5, K ≈ 0.2.

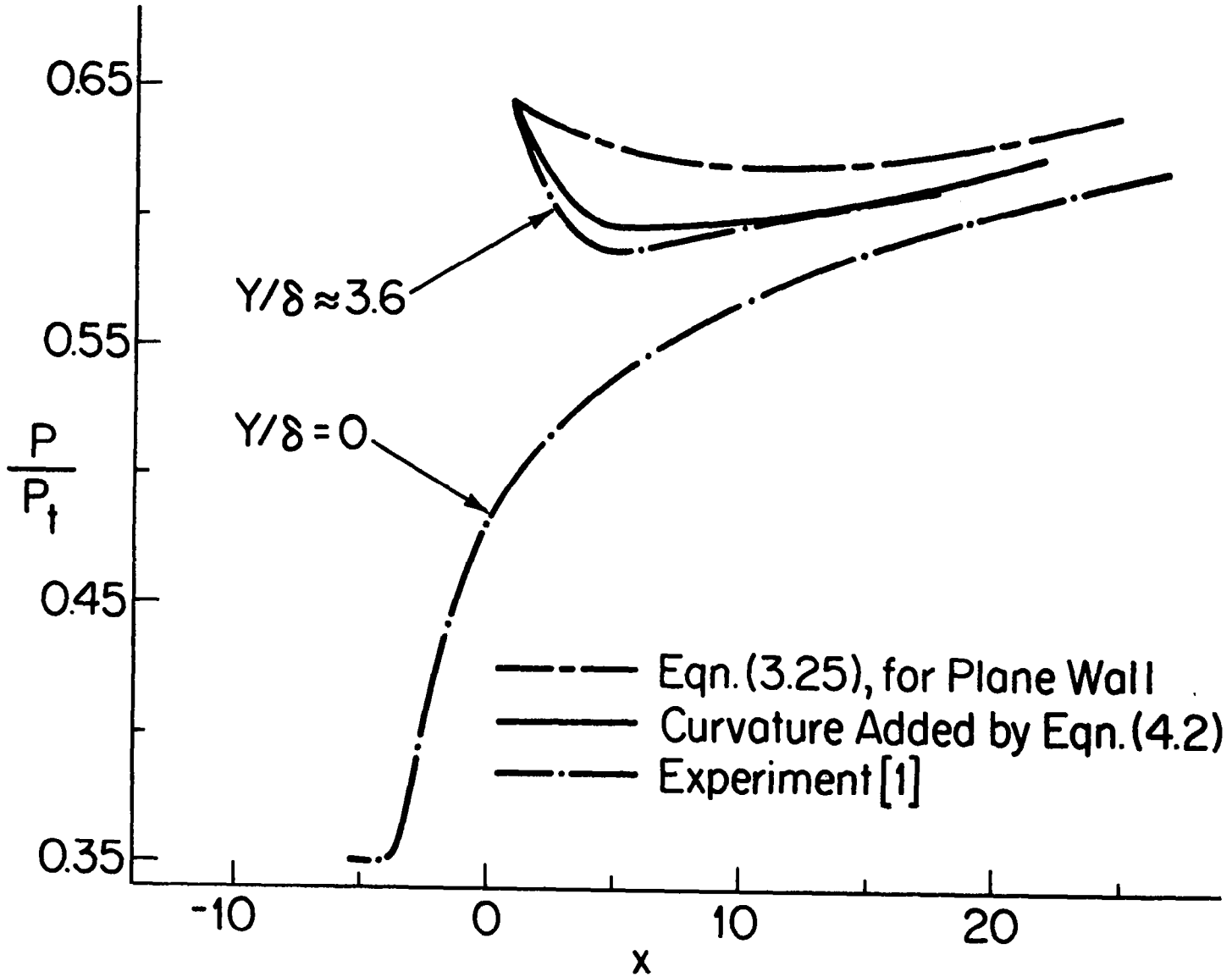

Figure 4. Pressure outside boundary layer, at $Y/\delta \approx 3.6$, for curved wall: $M_e = 1.322$, $Re = 9.6 \times 10^5$, $K \approx 0.2$.

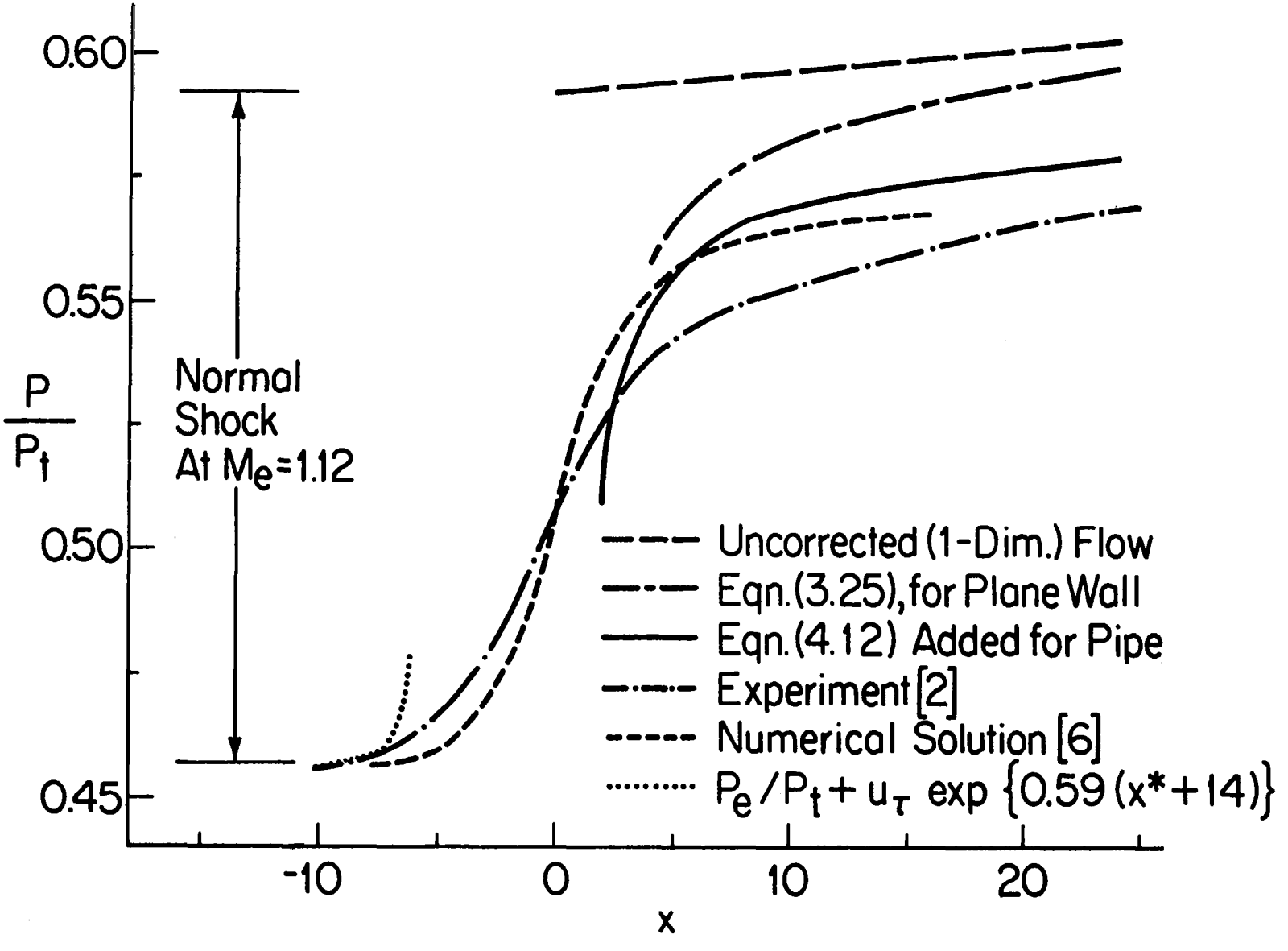

Figure 5. Pressure at wall of circular pipe: $M_e = 1.12$, $Re \approx 6 \times 10^6$, $\delta/R \approx 0.055$.

INTERACTION BETWEEN A NORMAL SHOCK WAVE AND A TURBULENT BOUNDARY LAYER AT HIGH TRANSONIC SPEEDS

Part II - Wall Shear Stress

M. S. Liou* and T. C. Adamson, Jr.

*Present address: Flight Sciences Department, McDonnell Douglas Research Laboratories, Box 516, St. Louis, Missouri 63166, U.S.A.

1. Introduction

When a shock wave impinges upon a wall, it penetrates the boundary layer along the surface and both the shock wave and the boundary layer are changed from their undisturbed states. If the boundary layer remains unseparated, these mutually induced changes take place in a small interaction region. For a turbulent boundary layer, it has been established [1-8] that an asymptotic description of the interaction region requires a three layer structure. In the outermost layer, comprising most of the boundary layer, pressure forces are much larger than forces resulting from Reynolds or viscous stresses so the governing equations are those for an inviscid flow. For the limit process to be considered, the solutions for this inviscid flow region are those given in Part I of this paper [9] , hereafter referred to as (I). Immediately adjacent to the wall is the wall layer, in which viscous and Reynolds stresses dominate to lowest order. Between these two layers is the Reynolds stress sublayer [1] (referred to as the blending layer in reference [2]) in which momentum transfer toward the wall is carried out by turbulent means (Reynolds stresses); the dominant terms in the equation of motion are the Reynolds stress, pressure gradient, and inertia terms.

This paper is concerned with the analysis of the flow in the two inner layers, the Reynolds stress sublayer and the wall layer, the goal being the calculation of the shear stress at the wall in the interaction region. As indicated above, the limit processes considered are those used

in (I). Thus, if ϵ is equal to the nondimensional difference between the velocity and the critical sound speed in the flow external to the boundary layer, and u_τ is the nondimensional friction velocity, we consider limit processes such that $u_\tau << \epsilon << 1$. In previous analyses for $\epsilon << u_\tau$ (Reference [1]) and $\epsilon = O(u_\tau)$ (Reference [2]) it was found that it was not possible to formulate an asymptotic criterion for shock induced separation. Here, it will be shown that even for $\epsilon >> u_\tau$ there is no apparent asymptotic separation criterion. However, example calculations will be used to show that the equation derived for the wall shear stress may be used to predict conditions for incipient separation with reasonable accuracy.

It is worthwhile reiterating the fact pointed out in (I) that for an unseparated boundary layer the solutions in the inviscid and inner layers are uncoupled. Because the inner layers are so thin, the change in pressure across them is negligible to the order retained and so the solution for the pressure found in the inviscid layer in the limit as the wall is approached is indeed the wall pressure. With this pressure distribution known, then, solutions in the inner layers may be found, leading to a relation for the wall shear stress. Thus, the unseparated flow case is a weak interaction problem. This is not the case for a laminar boundary layer and occurs for the turbulent boundary layer because the wall layer is so thin that the upstream influence of the interaction causes negligible lifting of the fluid from the wall; that is, to the order retained the V component of the velocity is zero, in the

inviscid layer, as the wall is approached. This point will be discussed again later.

In order to complete the formulation of the problem in the inner layers, it is necessary to specify a closure condition. Here, we use a mixing length model, including the van Driest damping factor, to write an eddy viscosity [10]. Such a closure model appears to give satisfactory results as long as the flow is unseparated [11] and has the virtue of simplicity; when the flow is separated, use of such a model gives results which have the correct trends but which do not agree well with experiment.

2. Solutions in the Inner Layers

As in (I), transonic flow over a flat plate with a turbulent boundary layer is considered, with a normal shock wave intersecting the boundary layer; an adiabatic wall is assumed as are conditions such that the total enthalpy may be taken to be uniform throughout the flowfield. Nondimensional Cartesian coordinates X and Y are measured parallel and perpendicular to the wall respectively, with the origin at the point where the normal shock wave intersects the boundary layer. Lengths are made dimensionless with respect to the distance from the leading edge of the flat plate to the shock impingement point, $\bar{L}$, and Cartesian velocity components U and V with respect to the critical sound speed in the flow upstream of the shock wave and external to the boundary layer (hereafter referred to as the external flow), $\bar{a}^*_e$. The

overbars indicate dimensional quantities. The mean temperature, T, density, ρ, pressure, P, and viscosity coefficient, μ, are referred to their critical values in the external flow, e.g., $\bar{T}^*_e$, $\bar{P}^*_e$, etc. We write the Reynolds number, Re, in the usual fashion and for convenience define a Reynolds number parameter, Re^*, as follows

$$Re = \left(\frac{\bar{\rho}\,\bar{U}\,\bar{L}}{\bar{\mu}}\right)_e \tag{1a}$$

$$Re^* = \left(\frac{\bar{\rho}^*\,\bar{a}^*\,\bar{L}}{\bar{\mu}^*}\right)_e \tag{1b}$$

The term $\langle \rho' V' \rangle / \rho$ is included in V, where the primes denote fluctuating quantities and the bracket denotes the average value. The friction velocity, u_τ, is made dimensionless with respect to $\bar{a}^*_e$, and is defined in terms of the external flow density as follows

$$u_\tau^2 = \frac{1}{\bar{a}^{*2}_e}\,\frac{\bar{\tau}_{wu}}{\bar{\rho}_e} = \frac{\tau_{wu}}{\rho_e} = \frac{1}{2}\,U_e^2\,c_{fu} \tag{2}$$

where $\bar{\tau}_{wu}$ is the shear stress at the wall in the undisturbed flow at $\bar{X} = \bar{L}$, and where c_{fu} is the corresponding skin friction coefficient defined as shown. Finally, the external flow velocity and Mach number are written in terms of a parameter, ϵ, as

$$U_e = 1 + \epsilon \tag{3a}$$

$$M_e^2 = \frac{U_e^2}{1 - \left(\frac{\gamma-1}{2}\right)(U_e^2 - 1)} \tag{3b}$$

where for transonic flow, $\epsilon << 1$. As in (I), the problem considered here is one for which $u_T << \epsilon << 1$.

In both inner layers to be considered here, the characteristic thickness of the region is small compared to its characteristic length. As a result, normal Reynolds and viscous stress terms may be neglected compared to the corresponding shear stress terms and the transverse pressure gradient is negligible, to the order retained in the analysis. The solutions to which these inner layer solutions must match in a direction normal to the wall are those solutions found in (I), expanded in the limit as $y = Y/\delta \to 0$, where $\delta = \bar{\delta}/\bar{L}$ is of the order of the boundary layer thickness. In the limit as $x = X/\Delta \to -\infty$, where $\Delta = \bar{\Delta}/\bar{L}$ is of the order of the extent of the interaction region, the solutions must match with the corresponding relations in the undisturbed boundary layer. It is seen, then, that the flow problem in the inner layers of the interaction region is formulated as a boundary layer problem with a known pressure gradient. This also helps explain why an additional layer (Reynolds stress sublayer) is necessary in the turbulent boundary layer case. That is, in either the laminar or turbulent interaction, there is an outer layer in the interaction region where pressure forces dominate over shear forces, and inviscid flow equations hold to lower orders. Obviously, then, solutions in the outer layer do not satisfy the no-slip condition at the wall and a new boundary layer must be considered at the wall. In laminar flow, a boundary layer is described asymptotically by a single layer and so only one

so called viscous sublayer is needed in the laminar interaction. However, a turbulent boundary layer has a two layer asymptotic structure; as a result, two inner layers are needed to describe this boundary layer in the interaction region. The Reynolds stress sublayer is the equivalent of the velocity defect layer, as will be seen.

With the above remarks in mind, it is possible to write a simplified set of governing equations in which only those terms needed in either of the two layers considered here are retained. They are as follows:

$$\frac{\partial(\rho U)}{\partial X} + \frac{\partial(\rho V)}{\partial Y} = 0 \tag{4a}$$

$$\rho U \frac{\partial U}{\partial X} + \rho V \frac{\partial U}{\partial Y} = -\frac{1}{\gamma}\frac{\partial P}{\partial X} + \frac{\partial}{\partial Y}\left(\rho \kappa^2 D Y^2 \left|\frac{\partial U}{\partial Y}\right| \frac{\partial U}{\partial Y} + \frac{\mu}{Re^*}\frac{\partial U}{\partial Y}\right) \tag{4b}$$

$$\frac{\partial P}{\partial Y} = 0 \tag{4c}$$

$$T + \left(\frac{\gamma-1}{2}\right)U^2 = \frac{\gamma+1}{2} \tag{4d}$$

$$P = \rho T = P(X) \tag{4e}$$

$$D = \left\{1 - \exp\left(-\frac{Y Re^* u_\tau}{26}\right)\right\}^2 \tag{4f}$$

where γ is the ratio of specific heats, D is the damping factor, and $\kappa = 0.41$ is the von Kármán constant. Since terms of order u_τ^2 will be retained in the solutions, it should be pointed out that terms such as $\langle \rho' U' \rangle / \rho$ in the continuity equation (4a), and $\langle \rho' T' \rangle$ in the

equation of state, (4e), which are of order u_τ^2, are not included because perturbations from the undisturbed flow values of each of these terms would be of higher than second order. Since the undisturbed flow solutions are considered known to second order, and we are interested only in the perturbations from the undisturbed flow, it is not necessary to include the terms in question. As mentioned previously, it is assumed that the wall is adiabatic, and turbulent and laminar Prandtl numbers are unity, so that the stagnation enthalpy is constant, as in equation (4d).

As shown in (I), for the case $\epsilon/u_\tau >> 1$ the distance from the wall to the sonic line is exponentially small compared to the thickness of the boundary layer. Since the extent of the upstream influence of the interaction region is ordered by the thickness of the subsonic region, the upstream influence is confined to a region, hereafter referred to as the inner region, which is exponentially small in the x direction compared to the main part of the interaction region, hereafter referred to as the outer region. That is, in the x direction, the interaction region actually consists of two regions, one thin compared to the other; in the y direction, each of these regions is subdivided into the three layers mentioned previously. Following the procedure employed in (I), the solutions in the outer region will be shown here in some detail. Because the upstream influence is confined to the inner region, the flow entering the shock wave in the outer region is simply the undisturbed flow at the point in question. Inner region solutions,

which are found using precisely the same methods employed in the outer region, are given in reference [12] .

Reynolds Stress Sublayer

In the Reynolds stress sublayer, which is intermediate to the outer inviscid flow layer and the wall layer, inertia terms are balanced by both the pressure gradient and Reynolds stress terms in the equation of motion in the flow direction. The extent of the outer interaction region is $X = O(\Delta)$, where, as shown in (I),

$$\Delta = b_o \delta \qquad \delta = O(u_\tau) \qquad (5a, b)$$

$$b_o = (\gamma+1)^{1/2} \epsilon^{1/2} (1 - (2\gamma+1)\epsilon/4 + \ldots) \qquad (5c)$$

If the dimensionless (referred to $\bar{L}$) thickness of the layer is taken to be $Y = O(\hat{\delta})$, say, then since the Reynolds stress $= O(u_\tau^2)$ and from (I), $\partial P/\partial X = O(u_\tau/\Delta)$, the fact that the pressure gradient and Reynolds stress terms in Eqn. (4b) must be of the same order indicates that $\hat{\delta} = O(u_\tau \Delta)$. Here, for convenience, we define $\hat{\delta}$, $\hat{y}$ and x as follows:

$$\hat{\delta} = u_\tau \Delta \qquad (6a)$$

$$Y = \hat{\delta}\,\hat{y} \qquad X = \Delta x \qquad (6b, c)$$

The solutions to which those in the Reynolds stress sublayer must match as $\hat{y} \to \infty$ are those in the outer inviscid flow layer, written in the limit as $Y/\delta = y \to 0$. The equations for the U component of velocity and the pressure, (Eqns. (3.9), (3.12), (3.19), (3. 21) and (4. 2) of (I) are summarized here for convenience. Thus,

$$U(x,0) = (1+\epsilon)^{-1} + u_\tau [(1+2\gamma\epsilon + \ldots)u_{01}(y) + (1 + (\gamma-1)\epsilon + \ldots)u_1(x)] + \ldots - K\delta \frac{4x}{\pi} \ln(C_o \delta x) + \ldots \quad (7a)$$

$$\frac{P_w(x)}{P_e} = \frac{P(x,0)}{P_e} = 1 + \gamma(2\epsilon + (2\gamma-1)\epsilon^2 + \ldots) - u_\tau \gamma (1 + (2\gamma-1)\epsilon + \ldots)u_1(x) + \ldots + K\delta \frac{4\gamma x}{\pi} \ln(C_o \delta x) + \ldots \quad (7b)$$

$$u_1(x) = -\frac{4x}{\pi} \int_0^\infty \frac{u_{01}(\eta)d\eta}{(x^2 + \eta^2)} \quad (7c)$$

where $P_e = 1 - \gamma\epsilon + O(\epsilon^3)$ is the dimensionless pressure in the external flow. The function $u_{01}(y)$ describes the variation of the velocity from its value in the external flow in the velocity defect layer in the undisturbed flow. That is, if U_u represents this velocity component, it may be expanded as

$$U_u = U_e + u_\tau u_{01}(y) \quad (8)$$

and $u_{01}(y)$ is the variable part of the velocity distribution in the velocity defect layer in the corresponding incompressible boundary layer [13] . The form given by Coles [14] is used here

$$u_{01}(y) = \kappa^{-1}[\ln y - \Pi (1 + \cos \pi y)] \qquad 0 < y \leq 1$$
$$= 0 \qquad y > 1 \quad (9)$$

where Π is Coles' profile parameter. The last terms in Eqns. (7a) and (7b) are due to the curvature of the wall, i.e., for a wall with convex curvature described locally by

$$Y = -\frac{1}{2} K X^2 + \ldots \tag{10}$$

where $K \ll 1$ and $K \to 0$ as $u_\tau \to 0$ and $\epsilon \to 0$ such that $K/\epsilon \to 0$. The value of the constant C_o is found from the solution for the flow field external to the boundary layer.

If Eqn. (7a) is written in terms of the Reynolds stress sublayer variable, $\hat{y}$, the result is

$$\begin{aligned} U(x,0) = (1+\epsilon)^{-1} + u_\tau[&(1 + 2\gamma\epsilon + \ldots)(\frac{1}{\kappa} \ln \frac{\hat{\delta}}{\delta} + \hat{u}_{01}(\hat{y}) + \ldots) \\ &+ (1 + (\gamma - 1)\epsilon + \ldots)u_1(x)] + \ldots \\ &- K\delta \frac{4x}{\pi} \ln (C_o \delta x) + \ldots \end{aligned} \tag{11}$$

where

$$\hat{u}_{01}(\hat{y}) = \kappa^{-1}(\ln \hat{y} - 2\Pi) \tag{12}$$

Thus, equation (11) is the equation to which $U(x, \hat{y})$ must match as $\hat{y} \to \infty$. As mentioned previously, $\partial P/\partial Y = 0$ to the order retained here. This is easily derived from the equation of motion in the Y direction (e.g., see reference [12]). Hence, the pressure as written in equation (7b) holds throughout both the Reynolds stress sublayer and the thinner wall layer.

In view of the form of equations (11) and (12), the general expansions for U and V are written as follows

$$U(x,\hat{y}) = (1+\epsilon)^{-1} + u_\tau\left[\frac{1}{\kappa}\ln\frac{\hat{\delta}}{\delta} + \hat{u}_{01}(\hat{y}) + \hat{u}_1(x,\hat{y})\right]$$

$$+ \epsilon u_\tau \frac{1}{\kappa}\ln\left(\frac{\hat{\delta}}{\delta}\right)\hat{u}_{1\ell}(x,\hat{y}) + \epsilon u_\tau \hat{u}_{11}(x,\hat{y}) + \ldots$$

$$+ K\delta\,\hat{u}_{1c}(x,\hat{y};\delta) + \ldots \qquad (13a)$$

$$V(x,\hat{y}) = \hat{\nu}_1 v_1(x,\hat{y}) + \ldots \qquad (13b)$$

The corresponding expressions for the temperature, $T(x,\hat{y})$, and density, $\rho(x,\hat{y})$, are found by substituting equation (13a) in the energy equation, (4d) and substituting the resulting expression for the temperature and equation (7b) in the equation of state, Eqn. (4e). If the expansions for U, V, P, and ρ and stretched variables x and y are substituted into Equation (4b), the governing equations for $\hat{u}_1$, $\hat{u}_{1e}$, and $\hat{u}_{11}$ are found. Thus,

$$\frac{\partial \hat{u}_1}{\partial x} = -\frac{1}{\gamma}\frac{\partial \hat{P}_1}{\partial x} + \frac{\partial}{\partial \hat{y}}\left[(1+\kappa\hat{y}\frac{\partial \hat{u}_1}{\partial \hat{y}})^2\right] \qquad (14a)$$

$$\frac{\partial \hat{u}_{1\ell}}{\partial x} = \frac{\partial}{\partial \hat{y}}(2\kappa\hat{y}\frac{\partial \hat{u}_{1\ell}}{\partial \hat{y}}) \qquad (14b)$$

$$\frac{\partial \hat{u}_{11}}{\partial x} + \gamma\frac{\partial \hat{u}_1}{\partial x} = -\frac{1}{\gamma}\frac{\partial \hat{P}_{11}}{\partial x} + \frac{\partial}{\partial y}(2\kappa\hat{y}\frac{\partial \hat{u}_{11}}{\partial \hat{y}}) \qquad (14c)$$

$$\frac{\partial \hat{u}_{1c}}{\partial x} = -\frac{1}{\gamma}\frac{\partial \hat{P}_{1c}}{\partial x} + \frac{\partial}{\partial \hat{y}}(2\kappa\hat{y}\frac{\partial \hat{u}_{1c}}{\partial \hat{y}}) \qquad (14d)$$

where from Eqn. (7b), $\hat{P}_1$, $\hat{P}_{11}$, and $\hat{P}_{1c}$ are defined as follows

$$\hat{P}_1(x) = -\gamma u_1(x) \qquad (15a)$$

$$\hat{P}_{11}(x) = -\gamma(2\gamma-1)u_1(x) \qquad (15b)$$

$$\hat{P}_{1c}(x;\delta) = \frac{4\gamma x}{\pi} \ln (C_o \delta x) \tag{15c}$$

It should be noted that both $\hat{u}_{1c}$ and $\hat{P}_{1c}$ really denote two terms, one of order $\ln \delta$ and one of order 1. They are written as one here for convenience. Also, it is found [12] that $\hat{v}_1 = O(\epsilon\, u_\tau^2)$, thus confirming the result used in Part I that, to the order considered here, $V(x, 0) = 0$ in the outer inviscid flow layer.

Insofar as $\hat{u}_1(x, \hat{y})$ is concerned, it is seen from Equation (11) that $\hat{u}_1 \to u_1(x)$ as $\hat{y} \to \infty$. It will be shown later that the same functional dependence must hold as $\hat{y} \to 0$. Since $P_1 = P_1(x)$, the solution which satisfies both matching conditions and the governing equation, (14a), is

$$\hat{u}_1 = \hat{u}_1(x) = -\frac{\hat{P}_1(x)}{\gamma} = u_1(x) \tag{16}$$

This result has been used in deriving equations (14b) and (14c). It is easily shown [1, 12] that the solutions to equations (14b)-(14d) may be written as follows

$$\hat{u}_{1\ell} = 2\gamma + \int_0^x \frac{B_{1\ell}(\xi)}{(x-\xi)} \exp\left\{-\frac{\hat{y}}{2\kappa(x-\xi)}\right\} d\xi \tag{17a}$$

$$\hat{u}_{11} = -\gamma \hat{u}_1 - \frac{1}{\gamma}\hat{P}_{11} + 2\gamma \hat{u}_{01} + \int_0^x \frac{B_{11}(\xi)}{(x-\xi)} \exp\left\{-\frac{\hat{y}}{2\kappa(x-\xi)}\right\} d\xi \tag{17b}$$

$$\hat{u}_{1c} = -\frac{\hat{P}_{1c}}{\gamma} + \int_0^x \frac{(B_{\ell c}(\xi) \ln \delta + B_{1c}(\xi))}{(x-\xi)} \exp\left\{-\frac{\hat{y}}{2\kappa(x-\xi)}\right\} d\xi \tag{17c}$$

where the $B_i(\xi)$ are functions to be found by matching. As $\hat{y} \to \infty$, the integral terms in each of equations (17) go to zero exponentially and it is seen

that the remaining terms match with their counterparts in equation (11). As $x \to 0$, for $\hat{y}$ = constant, the solutions satisfy the shock wave jump conditions to the relevant order, as they should. As $\hat{y} \to 0$, one finds [1] the following asymptotic behavior for the integrals

$$\int_0^x \frac{B_i(\xi)}{(x-\xi)} \exp\{ - \frac{\hat{y}}{2\kappa(x-\xi)} \} d\xi \sim - B_i(x) \ln(\frac{\hat{y}}{2\kappa}) + g_i(x) + \ldots \qquad (18a)$$

$$g_i(x) = \lim_{b \to 0} [\int_0^{x-b} \frac{B_i(\xi)}{(x-\xi)} d\xi + B_i(x) \ln b] - \gamma_e B_i(x) \qquad (18b)$$

where γ_e = Euler's constant = 0.57721.

The solutions for U may thus be found from equation (13a), (16), and (17). Since, as mentioned previously, one can find the density and temperature in terms of the velocity, using the energy equation and the equations of state, it is seen that a complete analytical solution may be found for the Reynolds stress sublayer in the outer region, valid to terms of order ϵu_τ. It should be noted that the continuity equation could be used to find the term of order ν_1 in V; since it is not used anywhere in this analysis, the solution for V is not included. Finally, it is of interest to write the solution for U in the limit as $\hat{y} \to 0$ for later use in matching with the wall layer solution. Thus,

$$U = (1+\epsilon)^{-1} + u_\tau[\kappa^{-1}\ln\frac{\hat{\delta}}{\delta} + \hat{u}_{01}(\hat{y}) + u_1(x)]$$

$$+ \epsilon u_\tau \kappa^{-1}\ln(\frac{\hat{\delta}}{\delta})[2\gamma - B_{1\ell}(x)\ln(\frac{\hat{y}}{2\kappa}) + g_{1\ell}(x) + \ldots]$$

$$+ \epsilon u_\tau[(\gamma-1)u_1(x) + 2\gamma\hat{u}_{01}(\hat{y}) - B_{11}(x)\ln(\frac{\hat{y}}{2\kappa}) + g_{11}(x) + \ldots] + \ldots$$

$$+ K\delta[-\frac{4x}{\pi}\ln(C_o\delta x) - (B_{\ell c}(x)\ln\delta + B_{1c}(x)\ln(\frac{\hat{y}}{2\kappa}) + g_{\ell c}(x)\ln\delta$$

$$+ g_{1c}(x) + \ldots] + \ldots \qquad (19)$$

Wall Layer

At the wall, Reynolds stresses are zero and the skin friction is, of course, due entirely to viscous stress. Immediately adjacent to the wall, then, is a layer in which, as the wall is approached, momentum transfer is accomplished less and less by turbulent means and more and more by molecular mechanisms. In this layer, Reynolds and viscous stresses are of the same order. The flow entering the interaction region in this layer has a velocity $U = O(u_\tau)$ and this order holds in the interaction region as well. If the thickness of the layer is taken to be $Y = O(\tilde{\delta})$, then by equating the orders of the Reynolds and viscous stress terms in equation (4b), one can show that $\tilde{\delta} = O[(Re^* u_\tau)^{-1}]$. Here, in order to write $\tilde{\delta}$ in terms of familiar quantities, we set

$$\tilde{\delta} = A(Re^* u_\tau)^{-1} \qquad (20a)$$

$$A = \frac{\mu_w}{\mu_e}(\frac{T_w}{T_c})^{1/2} U_e \frac{Re^*}{Re} = O(1) \qquad (20b)$$

With these orders for Y and U, and since in the interaction region $X = O(\Delta)$ and $\partial P/\partial X = O(u_\tau/\Delta)$, it is seen that, even though a pressure gradient exists, the only terms in equation (4b) are the Reynolds and viscous stress terms, to the order retained. The resulting equation is easily integrated to give

$$\rho\, D(\tilde{y})(\kappa\, \tilde{y}\, \frac{\partial U}{\partial \tilde{y}})^2 + \frac{\mu\, u_\tau}{A}\, \frac{\partial U}{\partial \tilde{y}} = u_\tau^2\, \rho_e \tau_w \tag{21a}$$

$$\tau_w(x) = \bar{\tau}_w/\bar{\tau}_{wu} \tag{21b}$$

$$Y = \tilde{\delta}\tilde{y} \tag{21c}$$

where, as indicated in Eqn. (21 b), the shear stress at the wall, $\tau_w(x)$, is made dimensionless with its value in the undisturbed boundary layer at $\bar{X} = \bar{L}$, so that as $x = X/\Delta \to -\infty$, $\tau_w \to 1$. Equation (21a) is essentially the same equation used in references [1] and [2]; the only difference lies in the closure conditions used.

With the orders mentioned above for U, P, X, and Y, and for $\rho = O(1)$, it is easy to show [12] that $V = O(u_\tau \tilde{\delta}/\Delta)$ and to corroborate equation (4c) to the order retained. Since $U = O(u_\tau)$, then from the energy equation, (4d), it is seen that $T = T_w + O(u_\tau^2)$ and from the equation of state, equation (4e), then, that variations in ρ in the Y direction are also $O(u_\tau^2)$. Hence, to order u_τ^2, $\rho = \rho_w$ and as pointed out previously by Melnik and Grossman [2] and Adamson and Feo [1], the fact that $\rho_w \neq \rho_e$ leads to the result that limit process expansions in the wall layer do not match with corresponding expansions from the Reynolds stress sublayer; thus, this

difficulty arises only in compressible flow. The difficulty may be overcome by taking advantage of the range of validity of equation (21a). That is, in any intermediate limit $\tilde{\delta} << Y << \hat{\delta}$, equation (21a) is still the governing equation; it is necessary to retain additional terms only for $Y = O(\hat{\delta})$. Hence equation (21a) may be used to derive solutions which will match with those found using limit process expansions in either limit, $Y = O(\hat{\delta})$ or $Y = O(\tilde{\delta})$. Although the methods of solution used by Adamson and Feo and Melnik and Grossman are equivalent, the latter's method is more straightforward and will be used here.

It is clear both from physical arguments, and from consideration of equation (21a) that as Y increases such that $\tilde{y} >> 1$, the viscous terms become negligible compared to the Reynolds stress terms; this is borne out by using the solution to be derived to compare the two terms. Also, for $\tilde{y} >> 1$, the damping factor D is represented by unity plus exponentially small terms (eqn. 5). Finally, the density may be written in terms of the velocity and pressure, in general, by using equations (4e) and (4d). Since $P = P(x)$ to the order retained, equation (21a) may be integrated to give,

$$U(x, \tilde{y}) = \Gamma \sin \left\{ \frac{1}{\Gamma} \left(\frac{T_w}{T_e} \right)^{1/2} \left(\frac{\tau_w}{P_w/P_e} \right)^{1/2} u_\tau \left(\frac{1}{\kappa} \ln \tilde{y} + B(x) \right) \right\} \tag{22a}$$

$$\Gamma = \sqrt{\frac{\gamma+1}{\gamma-1}} \tag{22b}$$

where $T_w = (\gamma+1)/2$ is the temperature at the wall and T_w/T_e can be found in terms of U_e from the energy equation, (4d). B(x) is a function of integration which should be evaluated by matching equation (22a) with the

limit process expansion solution valid in the wall layer ($\tilde{y} = O(1)$); that is, it should be found as a result of integration from the wall to the $\tilde{y}$ value in question, using the boundary conditions at the wall. However, it is only necessary to evaluate B(x) to lowest order here, and this may be done by noting that if there were no shock wave, then B(x) = C, the constant from the undisturbed flow wall layer solution (eqn. (2.8), in (I)). Here, then, B(x) is written in terms of an asymptotic expansion

$$B(x) = C + \omega(u_\tau)\, B_1(x) + \ldots \tag{23}$$

where $\omega(u_\tau) \to 0$ as $u_\tau \to 0$.

Since equations (22a) must match with equation (19), in the limit as $\tilde{y} \to \infty$, $\hat{y} \to 0$, it is seen that τ_w must have an expansion of the following form

$$\tau_w(x) = 1 + a_1\epsilon + a_2\epsilon^2 + \ldots + u_\tau\, \tau_1(x) + \epsilon\, u_\tau \frac{1}{\kappa} \ln\left(\frac{\hat{\delta}}{\delta}\right)\tau_{1\ell}(x)$$

$$+ \epsilon\, u_\tau\, \tau_{11}(x) + \ldots + K\delta\, \tau_{1c}(x) + \ldots \tag{24}$$

That is, as $\tilde{y} \to \infty$, such that $u_\tau \kappa^{-1} \ln \tilde{y} = O(1)$,

$$u_\tau \ln \tilde{y} = u_\tau \ln \frac{\hat{\delta}}{\delta} + u_\tau \ln \frac{\delta}{\tilde{\delta}} + u_\tau \ln \hat{y} \tag{25}$$

where, as shown in (I) (equation (2.9))

$$\frac{u_\tau}{\kappa} \ln \frac{\delta}{\tilde{\delta}} = \left(\frac{T_e}{T_w}\right)^{1/2} \Gamma \sin^{-1}\{U_e/\Gamma\} - u_\tau\left(\frac{2\Pi}{\kappa} + C\right) \tag{26}$$

and the expansion for τ_w shown in equation (24) follows to insure the indicated matching. Thus, if equations (7b), (23), (24), (25), and (26) are substituted into equation (22a) and the resulting equation is compared with

equation (19) term by term, the unknown parameters and functions in equations (24) and (19) may be found. The resulting solution for τ_w, the shear stress at the wall in the outer interaction region, and the corresponding values for the B_i and g_i (calculated once the B_i are known using equation (18b)) in equation (19) are

$$\tau_w(x) = 1 + a_1\epsilon + \frac{a_1(a_1-1)}{2}\epsilon^2 + \ldots - u_\tau \frac{a_1}{2} u_1(x)$$

$$+ \epsilon\, u_\tau \kappa^{-1} \ln\left(\frac{\hat{\delta}}{\delta}\right)(2\gamma - a_1)\left(\gamma + \frac{1}{2} - \frac{a_1}{4}\right)$$

$$+ \epsilon\, u_\tau \left\{ u_1(x)\left[\frac{a_1}{4}\left(1 - 3\gamma - \frac{3a_1}{2}\right) + \gamma\left(\gamma + \frac{1}{2}\right)\right]\right.$$

$$- 2\Pi \kappa^{-1}(2\gamma - a_1)\left(\gamma + \frac{1}{2} - \frac{a_1}{4}\right)$$

$$\left. + \kappa^{-1}(2\gamma + 1 - \frac{a_1}{2})(\gamma - \frac{a_1}{2})(\ln x - \gamma_e + \ln 2\kappa)\right\} + \ldots$$

$$+ K\,\delta\, \frac{2a_1 x}{\Pi} \ln(C_o \delta x) + \ldots \qquad (27a)$$

$$a_1 = -4\sqrt{\frac{\gamma-1}{2}}\left(\sin^{-1}\frac{1}{\Gamma}\right)^{-1} + 2\gamma \qquad (27b)$$

$$B_{1\ell} = g_{1\ell} = 0 \qquad (27c)$$

$$B_{11} = \kappa^{-1}\left[2\gamma + 1 - \frac{a_1}{2}\right] \qquad (27d)$$

$$g_{11} = B_{11}(\ln x - \gamma_e) \qquad (27e)$$

where $u_1(x)$ is given in equation (7c). Equation (27a), then, is the solution for $\tau_w(x)$ in the interaction region, including the effects of curvature in the external flow field. It has, in most respects, the same form as the equation

derived by Melnik and Grossman [2], differing mainly in the order of the various terms, the inclusion of specific analytical solutions at each order of approximation, and the inclusion of the curvature terms.

The order to make numerical calculations for a given Reynolds number, Re, and external flow Mach number, $M_e = 1 + (\gamma+1)\epsilon/2 + \ldots$, it is necessary to provide relations for u_τ and δ in terms of Re and ϵ. One of the required equations is equation (26), with equations (20) for $\tilde{\delta}$; the other is given in (I), (eqn. (2.11), 2.12)). This equation, with the values of the integrals as given by Cebeci and Smith [10] is repeated here for completeness.

$$\delta = \frac{u_\tau}{U_e}\frac{\kappa}{(1+\Pi)} + \left(\frac{u_\tau}{U_e}\right)^2 \left\{ \frac{2}{(1+\Pi)\sin^{-1}\left(\frac{U_e}{\Gamma}\right)} \frac{U_e}{\Gamma}\left(1 - \frac{U_e^2}{\Gamma^2}\right)^{-1/2} \right.$$

$$\left. + \frac{1}{2}\left(\frac{1}{(1+\Pi)^2}\right) \frac{\left[2+(U_e/\Gamma)^2\right]}{\left[1-(U_e/\Gamma)^2\right]} \left(2 + 3.1787\Pi + \frac{3}{2}\Pi^2\right) \right\} \qquad (28)$$

where $T_e/T_w = 1 - (U_e/\Gamma)^2$ from the energy equation, (4d). Finally, it is necessary to write an equation for the viscosity, $\mu(T)$, to be used in equations (20). Here, $\mu = T^n$ was used, with calculations being performed for $n = 3/4$.

Finally, it should be noted that although the solutions presented here are found to orders of approximation such that pressure gradient and inertia terms were not retained in the equation of motion in the wall layer, higher order solutions involving these terms have been investigated [12]. It was found that the first terms to involve the pressure gradient were of order $\tilde{\delta}/\Delta$ in U and of order $\tilde{\delta}/u_\tau\Delta$ in τ_w. Thus, they give very small corrections to the solutions presented.

3. Numerical Calculations and Separation Criterion

The variation of τ_w with x for various values of external flow Mach number (and thus ϵ) and Reynolds numbers representative of modern aircraft are shown in figure 1. The numerical computations were carried out using equations (27a) for $\mu = T^{3/4}$, $\gamma = 1.4$, $\Pi = 1/2$, $C = 5$ and $K = 0$; these values seem to be suitable for flow over a flat plate. The curves show the general features found experimentally in the interaction region. That is, $\tau_w(x)$ goes through a minimum, say $(\tau_w)_{min}$; as M_e increases, $(\tau_w)_{min}$ decreases, while as Re increases $(\tau_w)_{min}$ increases. Thus, the effect of increasing M_e and therefore the strength of the shock wave is to decrease the value of τ_w everywhere in the interaction region and hence to force the flow toward separation; increasing Re gives the opposite effect. It should be noted that $\tau_w \to 1$ as $x \to 0$ because the solution shown in Eqn. (27a) is for the outer interaction region. A solution for τ_w valid in the inner region can be written in terms of the solutions for the pressure perturbations in the inner inviscid flow region [12]; The solution is found in precisely the same manner as that illustrated here for the outer region and results in a solution similar to that given in Eqn. (27a). Finally, a composite solution for τ_w could be written, using the solutions valid in the inner and outer regions. Because of the limit processes considered in this work ($\epsilon >> u_\tau$), this composite solution would show only a small variation in τ_w for $x < 0$. However, since analytical solutions cannot be obtained for the pressure in the inner region, no solution for τ_w in the inner region has been included here.

It is not possible to compare the solution for τ_w with experimental results

for a completely two dimensional unseparated flow because none are available. In those cases where the flow was apparently unseparated (e.g., references [15, 16]), τ_w was not measured, and in more recent work, where τ_w has been measured (e.g., references [17, 18, 19]) the flow is separated. In separated flow, the shock wave takes on a lambda configuration near the boundary layer and a relatively strong pressure gradient develops in the Y direction in the flow external to the boundary layer [18]; the flow picture is quite different from the unseparated flow case considered here.

Although experimental results for truly two dimensional flow are not available for comparison, there is one set of measurements in a tube in which the flow is approximately two dimensional [20]. Thus, if R is the dimensionless (with respect to $\bar{L}$) radius of the tube, $\delta/R \cong 0.04$ to 0.08; in addition, the changes in the core flow (external to the boundary layer) due to the rapid increase in the boundary layer displacement thickness through the interaction region give corrections which are asymptotically of higher order than those retained in Eqn. (27a). In presenting the tube data, Gadd fitted power law velocity profiles to the measured profiles and inferred values of $\bar{\delta}$ (dimensional boundary layer thickness) immediately upstream of the interaction. Using equations derived using power law profiles, he also gave Reynolds numbers associated with the tunnel stagnation pressure and Mach number for each test. Skin friction measurements were derived from Stanton tube measurements. In determining the flow parameters to be used in calculating τ_w for comparison with each of Gadd's experiments, it was decided to use Gadd's values of $\bar{\delta}$, Re, M_e, and stagnation pressure, $\bar{P}_{te}$ as being a self-

consistent set of data to calculate the necessary ϵ, u_τ, δ, and Π for use in τ_w. Thus, it is easy to show that if $\mu = T^n$,

$$\text{Re}\,\delta = \frac{\bar{P}_t}{\bar{P}_{at}} \frac{M_e}{[1 + \frac{\gamma-1}{2} M_e^2]^{\frac{\gamma}{\gamma-1}}} (1 - \frac{U_e^2}{\Gamma^2})^{-n-1/2} \frac{\bar{a}_w \bar{\delta}}{\bar{\nu}_w} \tag{29}$$

Here, $\bar{a}_w$ and $\bar{\nu}_w$ are the dimensional speed of sound and kinematic viscosity respectively, evaluated at the wall temperature (atmospheric temperature, taken to be 59°F.) and in the case of $\bar{\nu}_w$, at atmospheric sea level density; $\bar{P}_{at}$ refers to atmospheric pressure. Using the given values of M_e, $\bar{P}_t$, $\bar{\delta}$, and $\bar{\tau}_w$, Eqns. (3), (26), (with Eqn. (20) for $\bar{\delta}$), (28) and (29) were used to calculate the equivalent ϵ, u_τ, δ, and Π. From equation (2), then, the corresponding c_{fu} could be calculated. The ratio of the calculated C_{fu} to the value inferred from the standard tube measurements ranged from 1.05 to 1.29 in four cases reported by Gadd (Figures 25 to 28, reference [20]). For this reason and because of uncertainties in the calibration of the Stanton tube, it was decided to compare values of c_f/c_{fu}, which is equal to τ_w as given in equation (27a). The results of this comparison are shown in figure 2, for the case $M_e = 1.15$,, $\text{Re} = 7 \times 10^6$, (Figure 25, reference [20]). The remaining parameters are given under figure (2). The point $X'/\delta = 0$, defined by Gadd as the position at which $P_w/P_{te} = 0.528$, was found by using equation (7b). It is seen that the measured upstream influence is not small. That is, c_f/c_{fu} is not small for $X < -1$ say, as required for this theory, so that even if the solution for τ_w for $x < 0$ were available, it is not expected that it would give good agreement. In fact, using the above mentioned parameters,

$\delta_*/\delta = 0.5$, where δ_* is the dimensionless distance to the sonic line in the undisturbed boundary layer; evidently the values for Re, ϵ, and Π do not form a good combination for comparison with the theory. On the other hand, a slight unsteadiness in the position of the shock wave could have contributed to the slow variation of the measured c_f/c_{fu} upstream of and in the neighborhood of the minimum. Nevertheless, the value and the position of the minimum of c_f/c_{fu} are predicted quite accurately. Downstream of the minimum the comparison is fairly good; in this regard, however, it is interesting to note that the negative curvature seen on the calculated curve but not on this particular experimental curve, is a feature found in other experimental results which could not be used here because small separation bubbles existed.

It is of interest at this point to consider the problem of predicting conditions under which the interaction brings the flow to the point of incipient separation. First, it is seen from equation (27a) that there is no asymptotic condition for incipient separation; that is, unlike the laminar case, in which $\epsilon_s = O(Re^{-1/5})$ is the asymptotic criterion [21], there is no relation between ϵ and Re which holds in the limit as $Re \to \infty$ as a condition for separation. This is an important difference between the two flows, and it is of interest to investigate the reason for its occurrence. The effect of the interaction, through the induced adverse pressure gradient, is to slow the fluid. In the boundary layer, then, the stream tubes must become wider and, due to the constraint of the wall, the V velocity component increases at points away from the wall, causing the outer flow to lift away from the wall also. In the laminar case, the thickening of streamtubes is greatest in the viscous sublayer.

The resulting V component of velocity is large enough that the flow external to the boundary layer is affected to lowest order so that the external and boundary layer flows must be considered simultaneously, i.e., a strong interaction results [21, 22]. No matter how large Re becomes, this strong interaction occurs, with the thickness of the viscous sublayer and boundary layer decreasing as Re increases, according to their asymptotic dependence on Re. The sublayer momentum flux and viscous stresses decrease and the strength of the shock wave necessary to cause enough displacement of the fluid to result in separation decreases as Re increases. In the turbulent case, even for $\epsilon >> u_\tau$, the interaction is a weak interaction to lowest order because the wall layer is so thin. Thus, until separation occurs, the outward displacement of the fluid in the wall layer due to the interaction is too small to cause any effect in the lowest order solutions in the flow external to the boundary layer. A strong interaction does not occur until a separation bubble exists. Since there is no mechanism through which variations in the wall layer and external flows can interact, before a separation bubble is formed, it appears that no asymptotic criterion exists for incipient separation. However, it may be that such a criterion will result from an asymptotic solution for the separated flow problem in the limit as the size of the bubble shrinks to zero.

Although the solution for $\tau_w(x)$ does not give an asymptotic criterion for separation, there remains the possibility that conditions for incipient separation can be found simply by assuming that equation (27a) is an accurate solution for $\tau_w(x)$ at values of M_e and Re near separation. It is

clear from figures 1 and 2 that the solution shows the correct form with a minimum value, and it is possible to calculate the corresponding values of Re and M_e (i.e., ϵ) for which $(\tau_w)_{min} = 0$, the condition for incipient separation. It must be emphasized that equation (27a) is not being used in an asymptotic sense in such a calculation; thus in order for τ_w to go to zero, one or more terms in the expansion must become as large as the first term. Instead, we consider equation (27a) as being a good approximation to $\tau_w(x)$ in a numerical sense as long as ϵ^3 and u_τ^2 (the orders of the first terms neglected) are small compared to one.

To illustrate the use of equation (27a) for $\tau_w(x)$ to predict conditions for separation, we choose the remainder of Gadd's tubes flow experiments in which c_f was measured [20]. That is, Gadd presented four plots of c_f vs. X'/δ (Figures 25-28, reference [20]), the first of which is shown in figure 2. In each case he also performed oil-flow experiments, which indicated that in one case (used in figure 2) the flow was not separated, but that in the three other cases, separation did occur. Although the plotted values of c_f did not indicate the occurrence of separation in these three cases, it should be noted that the values of c_f were inferred from measurements from a Stanton tube aligned facing the flow; thus, accurate reverse flow measurements could not be made. Calculations of τ_w were made for each of these cases, using the same method for calculating the necessary parameters, as mentioned in the discussion of figure 2. The resulting values for $(\tau_w)_{min} = (c_f/c_{fu})_{min}$ for each case are as follows:

(1) $M_e = 1.27$ $\quad Re = 10^7$ $\quad (\tau_w)_{min} = -0.080$

(2) $M_e = 1.26$ $\quad Re = 1.27 \times 10^7$ $\quad (\tau_w)_{min} = -0.020$

(3) $M_e = 1.34$ $\quad Re = 1.93 \times 10^7$ $\quad (\tau_w)_{min} = -0.344$

Thus these calculated results indicate that in all three cases the flow is separated, in agreement with the oil-flow experiments. In case (2), the extent of the region where $\tau_w < 0$, i.e., the extent of the separation bubble, appears to be very small; the flow is barely separated.

If we denote by M_{es} the Mach number of the external flow at incipient separation, equation (27a) may be used, with the condition that $(\tau_w)_{min} = 0$, to find M_{es} as a function of Re. A typical result is shown in figure (3) for $K = 0$ and $\Pi = 1/2$, i.e., for conditions associated with flow along a flat plate. It is seen that according to this prediction, M_{es} increases as Re increases. This result is in agreement with measurements made by Roshko and Thomke [23] for supersonic flow at high Reynolds numbers. The magnitude of the increase in M_{es} over a large range of Re, however, is small enough that this result could help explain the conclusion that there was little or no variation with Re, reached by Settles, Bogdonoff, and Vas [24].

The effects of curvature on M_{es}, as predicted by equation (27a) can also be compared with experimental results. Evidently, the only data available are those presented in figure (37) of reference [20], reproduced here as figure 4. The value of the coordinate along the abscissa, t, is given as $t \cong 2.6\,\delta/R$ where R is the radius of curvature; in view of equation (10), then, one can write $t = 2.6\delta K$. Although there is no dependence on Reynolds number shown, it is assumed here that the range of Reynolds numbers is

10^6 to 10^7 and calculated results are given for both values. Finally, on an airfoil with supercritical flow, the flow is accelerating up to the shock wave; since Π depends on the pressure gradient in the undisturbed flow upstream of the interaction, the value of Π on an airfoil will be different for different curvatures. For zero pressure gradient $\Pi \cong 0.5$, whereas for highly accelerating flow Π is smaller and can become negative [25]. Therefore, at $t = 0$, $\Pi \tilde{=} 0.5$, ($K = 0$) and at $t = 0.015$, it was decided to use a value of Π for moderately accelerated flows, $\Pi = 0$. The values of M_{es} at $t = 0$ can be found from figure (3). Those at $t = 0.015$, for which $K = 0.021$ at $Re = 10^6$ and $K = 0.028$ at $Re = 10^7$, were calculated, again using equation (27a). The results are shown in figure (4). It is seen that at the conditions associated with flow over a flat plate (t=0) the calculated M_{es} compares very well with the value given by the line drawn through the experimental data. On the other hand, at higher curvature ($t = 0.015$) the calculated values are considerably less than those found experimentally. In reference [20] there was some discussion of the fact that criteria for separation might have been too stringent in the curved surface cases so that, for example, the point through which the drawn line passes at $M_{es} = 1.31$ perhaps should have been at $M_{es} = 1.29$. If this were the case and if negative values of Π were called for, the agreement at $t = 0.015$, would be much better.

The present results for criteria for shock induced incipient separation may be compared with theoretical predictions given by Bohning and Zierep [26], who postulated a two layer model for the interaction region and were able to calculate an equation for c_f. Two comparisons were made, both for

flat plates, at Re values of 10^6 and 5×10^6; these Re are in the range of results presented in reference [26]. At Re = 10^6, the predicted values of M_{es} are 1.24 and 1.18 and at Re = 5×10^6 they are 1.26 and 1.30, where the M_{es} calculated by the present method is the first, in each case. Thus, although the two solutions give the same M_{es} at some Re between 10^6 and 5×10^6, Bohning and Zierep's solution shows a much greater variation of M_{es} with Re than that shown here. However, the present results appear to be in closer agreement with experimental measurements [23, 24] for a related problem. The present theory could not be compared with very recent analytical results given by Inger [27], who also used a two layer model, since conditions for incipient separation were not presented.

Although there appears to be no asymptotic criterion for separation in the limit as Re $\to \infty$ ($u_\tau \to 0$) and $\epsilon \to 0$, there remains the possibility that there exists a criterion involving a large M_e as Re $\to \infty$. Thus, it is necessary to consider the behavior of τ_w for $\epsilon = O(1)$. Based on the present analysis, it is seen that for $\epsilon = O(1)$, $u_\tau \ll 1$, the solution for $\tau_w(x)$ would be of the following form in the outer interaction region:

$$\tau_w(x) = \tau_{w_d}(\epsilon) + u_\tau \tau_{w_1}(x;\epsilon) + \ldots \tag{30}$$

where $\tau_{w_d}(\epsilon)$ is the value which $\tau_w(x)$ approaches far downstream of the shock wave. Since the lowest order solutions for the velocities would be of the same form in each of the layers as for $\epsilon \ll 1$, it is seen that, from matching solutions in the limit $u_\tau \to 0$, one would obtain

$$\Gamma \sin\left\{\left(\frac{\tau_{w_d}}{P_d/P_e}\right)^{1/2} \sin^{-1}\left(\frac{U_e}{\Gamma}\right)\right\} = U_d \tag{31}$$

Here P_d and U_d are the values of P and U immediately downstream of the shock wave in the inviscid flow external to the boundary layer respectively, and are thus the values which P and U approach as $x \to \infty$ in the interaction region. If the jump conditions across a shock wave are used to write U_d and P_d/P_e in terms of U_e and these expressions are substituted into equation (31), one obtains an expression for τ_{w_d} in terms of U_e. Thus,

$$\tau_{w_d} = \left[\frac{1 + (\frac{\gamma+1}{2})(U_e^2 - 1)}{1 - (\frac{\gamma-1}{2})(U_e^2 - 1)}\right]\left[\frac{\sin^{-1}(\frac{1}{\Gamma U_e})}{\sin^{-1}(\frac{U_e}{\Gamma})}\right]^2 \tag{32}$$

If $U_e = 1 + \epsilon$ is substituted into equation (32) and the resulting equation expanded for $\epsilon \ll 1$, it is found that $\tau_{w_d} = 1 + a_1\epsilon + a_1(a_1-1)\epsilon^2/2 + \ldots$, in agreement with the first three terms of equation (27a).

It is clear from equation (32) that, since $1 \leq U_e < \Gamma$ for $1 \leq M_e < \infty$ (see eqn. (36)), $\tau_{w_d} \neq 0$ for any M_e; instead τ_{w_d} goes through a minimum value of 0.512 at $M_e = 2.55$, for $\gamma = 1.4$, and then begins to rise with increasing M_e. Hence, there is apparently no limiting value for M_{es} as $Re \to \infty$. Moreover, since $U_e \to \Gamma$ as $M_e \to \infty$, it is clear that $\tau_{w_d} \to \infty$. Recalling the definition of $\tau_w(x)$, one can see that this limit means that for high Mach number flow the shear stress far downstream of the interaction must be large compared to that of the undisturbed flow. This apparent anomaly can be explained by considering equation (21a). The density, in the first term, can be written as P/T through the equation of state. Now, in the wall layer, the temperature differs from the constant temperature of the wall by only higher order terms. On the other hand, since $\partial P/\partial Y = 0$

through the wall layer and Reynolds stress sublayer, P is the pressure from the inviscid flow layer and so varies from P_e to P_d. As $M_e \to \infty$, $P_d/P_e \to \infty$ and so from equation (21a), $\tau_{w_d} \to \infty$ also. In general, since the Reynolds shear stress, $-\rho < U' V' >$, includes the density, this result appears to be independent of the specific closure condition as long as $< U' V' >$ does not go to zero as $M_e \to \infty$, and is another significant departure from the laminar case. Experimental verification of the large values of τ_{w_d} at high Mach numbers is given in measurements by Marvin, et al. [28] .

4. Concluding Remarks

The use of asymptotic methods of analysis results in a relatively simple relation for the shear stress at the wall in the interaction region. This relation may be used to predict conditions for incipient separation. In order to obtain the proper variation of τ_w vs. x, which includes a minimum in τ_w, it is necessary to include terms of higher order than the first approximation; evidently this would be the case also if one were to calculate τ_w for the case $u_\tau = O(\epsilon)$ [2] .

Although the range of parameters in available experiments does not allow for exhaustive testing of the theory, comparisons which could be made are encouraging; more accurate results should be obtained at the high Reynolds

numbers associated with modern transonic aircraft.

Acknowledgment

The authors wish to thank Dr. R. Enlow, University of Otago, Dunedin, New Zealand, for his help in performing numerical calculations.

References

[1] T. C. Adamson, Jr. and A. Feo, "Interaction Between a Shock Wave and a Turbulent Boundary Layer in Transonic Flow," SIAM J. Appl. Math., 29, 121-145 (1975).

[2] R. E. Melnik and B. Grossman, "Analysis of the Interaction of a Weak Normal Shock Wave with a Turbulent Boundary Layer," AIAA Paper No. 74-598 (1974).

[3] R. E. Melnik and B. Grossman, "Further Developments in an Analysis of the Interaction of a Weak Normal Shock Wave with a Turbulent Boundary Layer," Symposium Transsonicum II, K. Oswatitsch and D. Rues, eds., Springer-Verlag, 262-272 (1976).

[4] T. C. Adamson, Jr., "The Structure of Shock Wave Boundary Layer Interactions in Transonic Flow," Symposium Transsonicum II, K. Oswatitsch and D. Rues, eds., Springer-Verlag 244-251 (1976).

[5] R. E. Melnik and B. Grossman, "Interaction of Normal Shock Waves with Turbulent Boundary Layers at Transonic Speeds," Transonic Flow Problems in Turbomachinery, T. C. Adamson, Jr. and M. F. Platzer, eds., Plenum Press, 415-433 (1977).

[6] T. C. Adamson, Jr. and A. F. Messiter, "Normal Shock Wave-Turbulent Boundary Layer Interactions in Transonic Flow Near Separation," Transonic Flow Problems in Turbomachinery, T. C. Adamson, Jr. and M. F. Platzer, eds., Plenum Press, 392-414 (1977).

[7] T. C. Adamson, Jr. and A. F. Messiter, "Shock Wave-Turbulent Boundary Layer Interactions in Transonic Flow, Advances in Engineering Science, NASA CP-2001, 1425-1435 (1976).

[8] A. F. Messiter and T. C. Adamson, Jr., "A Study of the Interaction of a Normal Shock Wave with a Turbulent Boundary Layer at Transonic Speeds," NASA Conference on Advanced Technology Airfoil Research, Vol. I, NASA Conf. Publ. 2045, 271-279 (1978).

[9] A. F. Messiter, "Interaction Between a Normal Shock Wave and a Turbulent Boundary Layer at High Transonic Speed, Part I; Pressure Distribution," NASA CR-3194, 1980. (See page 1 of this report.)

[10] T. Cebeci and A. M. O. Smith, "Analysis of Turbulent Boundary Layers," Academic Press (1974).

[11] J. R. Viegas and T. J. Coakley, "Numerical Investigation of Turbulence Models for Shock-Separated Boundary Layer Flows," AIAA J., 16, 293-294 (1978).

[12] M. S. Liou, "Asymptotic Analysis of Interaction between a Normal Shock Wave and a Turbulent Boundary Layer in Transonic Flow," Ph. D. Dissertation, The University of Michigan, Ann Arbor, Michigan (1977).

[13] G. Maise and H. McDonald, "Mixing Length and Kinematic Eddy Viscosity in a Compressible Boundary Layer," AIAA J., 6, 73-80, (1968).

[14] D. E. Coles, "The Law of the Wake in the Turbulent Boundary Layer," J. Fluid Mech., 1, 191-226 (1956).

[15] J. Ackeret, F. Feldmann and N. Rott, "Untersuchungen an Verdichtungsstössen und Grenzschichten in Schnell Bewegten Gasen," Mitteilungen aus dem Inst. für Aerodyn., ETH Zürich, Nr 10 (1946). Translated as NACA TM 1113 (1947).

[16] H. W. Liepmann, "Interaction Between Boundary Layers and Shock Waves in Transonic Flow," J. Aero. Sci., 13, 623-637 (1946).

[17] R. J. Vidal, C. E. Wittliff, P. A. Catlin and B. H. Sheen, "Reynolds Number Effects on the Shock Wave-Turbulent Boundary Layer Interaction at Transonic Speeds," AIAA Paper No. 73-661 (1973).

[18] J. W. Kooi, "Experiment on Transonic Shock-Wave Boundary-Layer Interaction," NLR MP 75002 U, National Aerospace Laboratory, The Netherlands (1975).

[19] G. G. Mateer, A. Brosh, and J. R. Viegas, "A Normal Shock-Wave Turbulent Boundary-Layer Interaction at Transonic Speeds," AIAA Paper No. 76-161 (1976).

[20] G. E. Gadd, "Interaction Between Normal Shock Waves and Turbulent Boundary Layers," A.R.C. 22559, R. and M. 3262 (1962).

[21] A. F. Messiter, A. Feo and R. E. Melnik, "Shock Wave Strength for Separation of a Laminar Boundary Layer at Transonic Speeds," AIAA J., 9, 1197-1198 (1971).

[22] H. M. Brilliant and T. C. Adamson, Jr., "Shock Wave Boundary Layer Interactions in Laminar Transonic Flow," AIAA J., 12, 323-329 (1974).

[23] A. Roshko and G. J. Thomke, "Supersonic Turbulent Boundary-Layer Interaction with a Compression Corner at Very High Reynolds Number," Proceedings of the 1969 Symposium, Viscous Interaction Phenomena in Supersonic and Hypersonic Flow, University of Dayton Press, 109-138 (1970).

[24] G. S. Settles, S. M. Bogdonoff and I. E. Vas, "Incipient Separation of a Supersonic Turbulent Boundary Layer at High Reynolds Numbers," AIAA J., 14, 50-56 (1976).

[25] J. E. Lewis, R. L. Gran and T. Kubota, "An Experiment on the Adiabatic Compressible Turbulent Boundary Layer in Adverse and Favorable Pressure Gradients," J. Fluid Mech., 51, 657-672 (1972).

[26] R. Bohning, and J. Zierep, "Bedingung Für Das Einsetzen Der Ablösung Der Turbulenten Grenzschicht an Der Gekrummten Wand Mit Senkrechtem Verdichtungsstoss," ZAMP, 29, 190-198 (1978).

[27] G. R. Inger, "Transonic Shock-Turbulent Boundary Layer Interaction with Suction and Blowing," AIAA Paper No. 79-0005 (1979).

[28] J. G. Marvin, C. C. Horstman, M. W. Rubesin, T. J. Coakley and M. I. Kussoy, "An Experimental and Numerical Investigation of Shock-Wave Induced Turbulent Boundary-Layer Separation at Hypersonic Speeds," Flow Separation, AGARD CP-168, 25-1 to 25-13, November (1975).

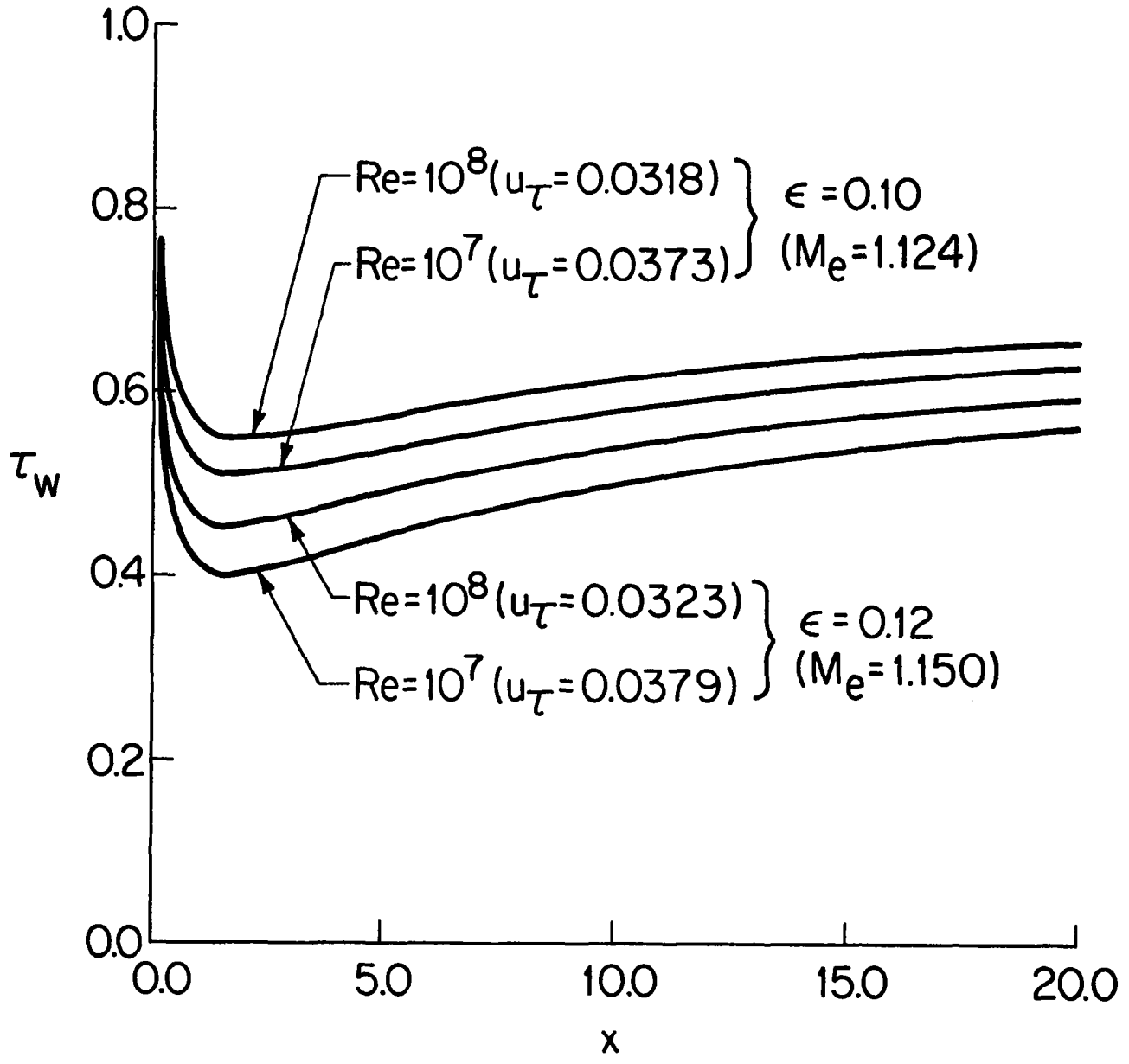

Figure 1. τ_w vs x for various values of Me and Re, for flow over a flat plate. (Eqn. (27a) with Π = 0.5, K = 0).

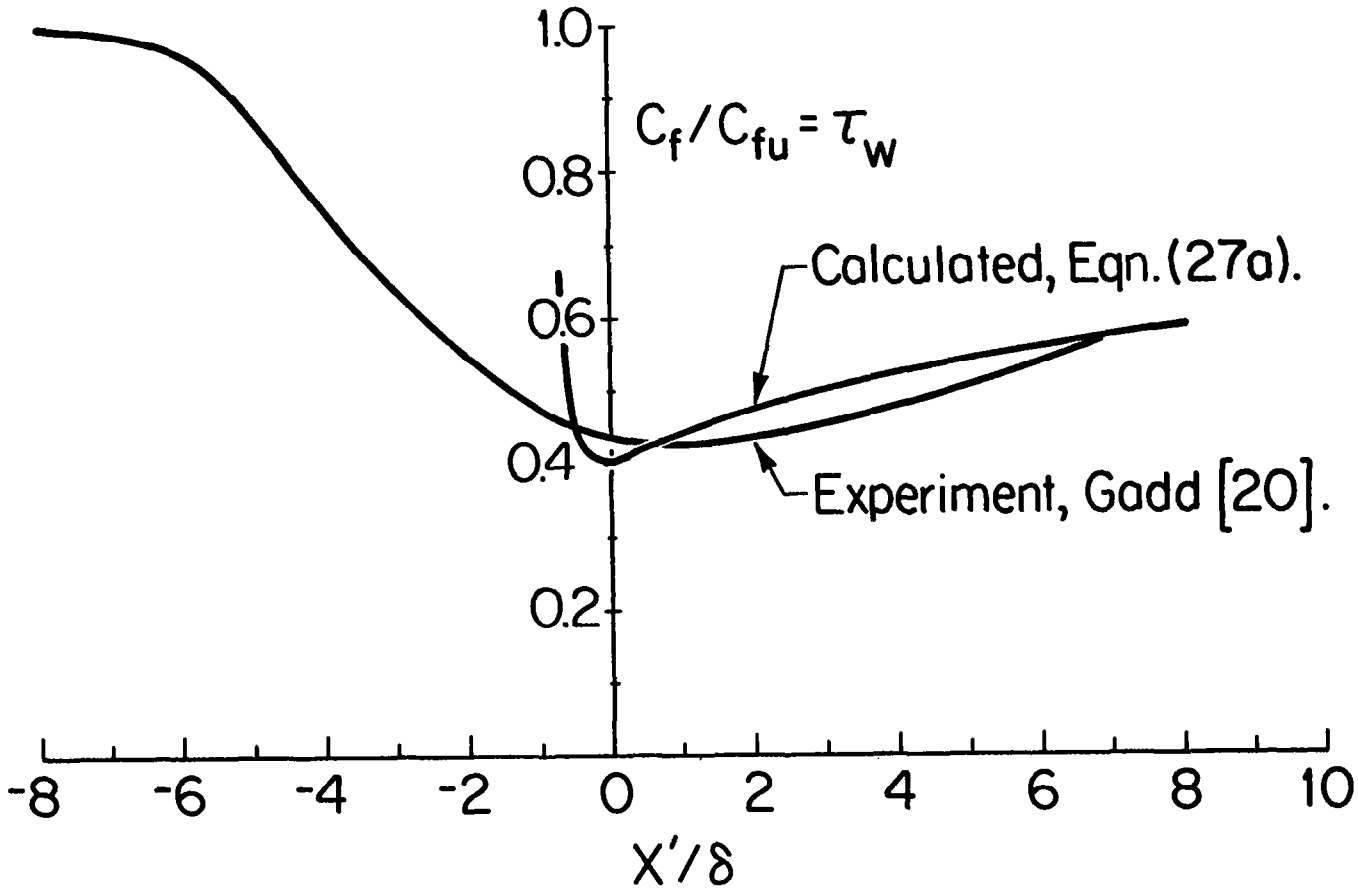

Figure 2. Comparison of calculated (eqn. (27a)) and experimental (ref. 20) values of c_f/c_{fu} vs X'/δ. Experimental conditions; Me = 1.15, $Re_{\overline{\delta}} = 7 \times 10^6$, wall temperature = 15°C (59°F), $\overline{P}_{te}$ = 137.9kP$_a$ gauge (20 psig), $\overline{\delta}$ = 0.305 cm (0.12 in.). Corresponding calculated parameters; $\varepsilon = 0.120$, $u_\tau = 0.03968$, $\delta = 0.01634$, $\Pi = 0.312$, $K = 0$. $X'/\delta = 0$ at $P_w/P_{te} = 0.528$ from eqn. (7a).

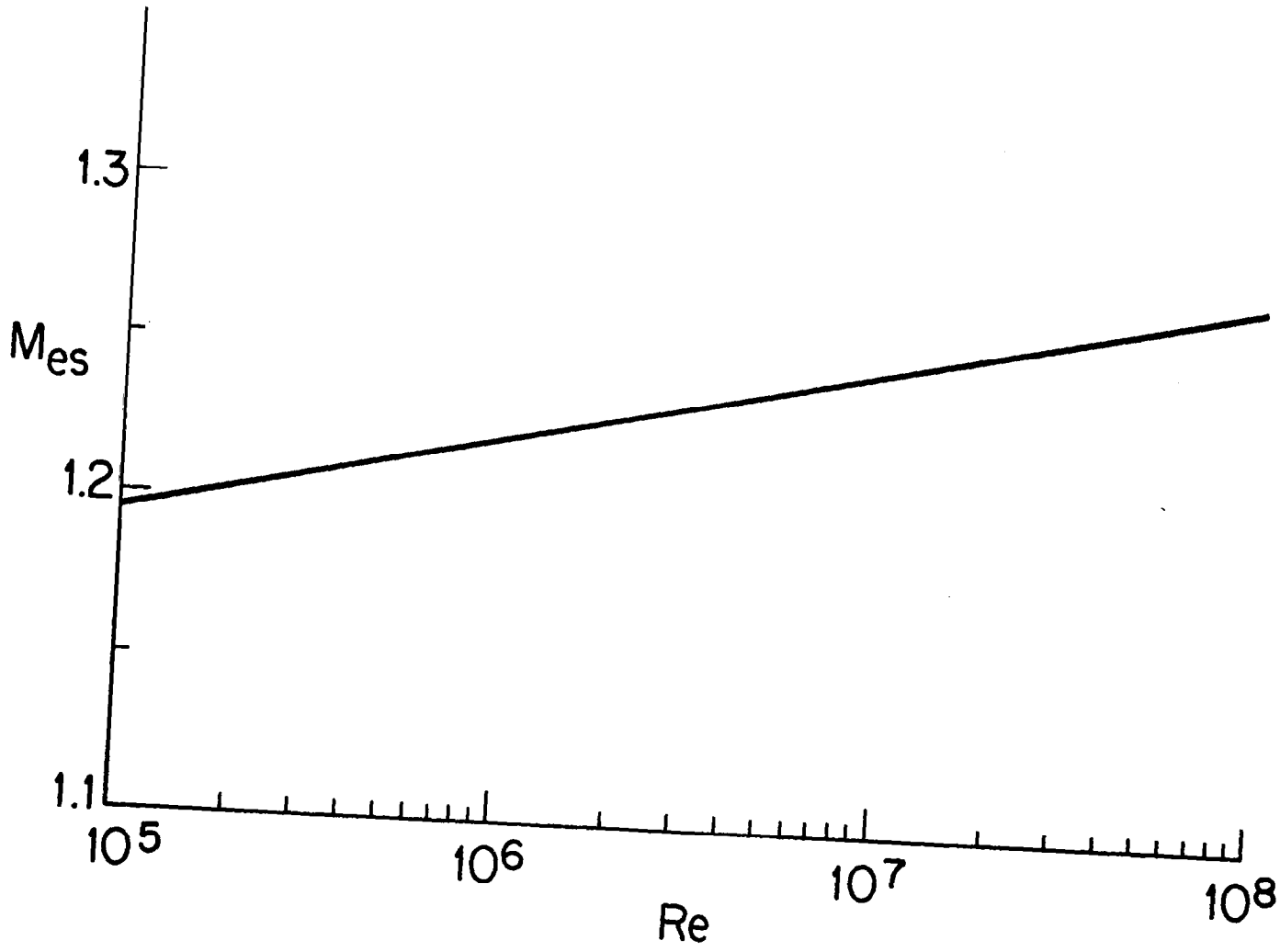

Figure 3. M_{es} (Mach number at incipient separation) vs Re for flow over a flat plate, calculated using eqn. (27a) with $(\tau_w)_{min} = 0$, $\Pi = 0.5$, $K = 0$.

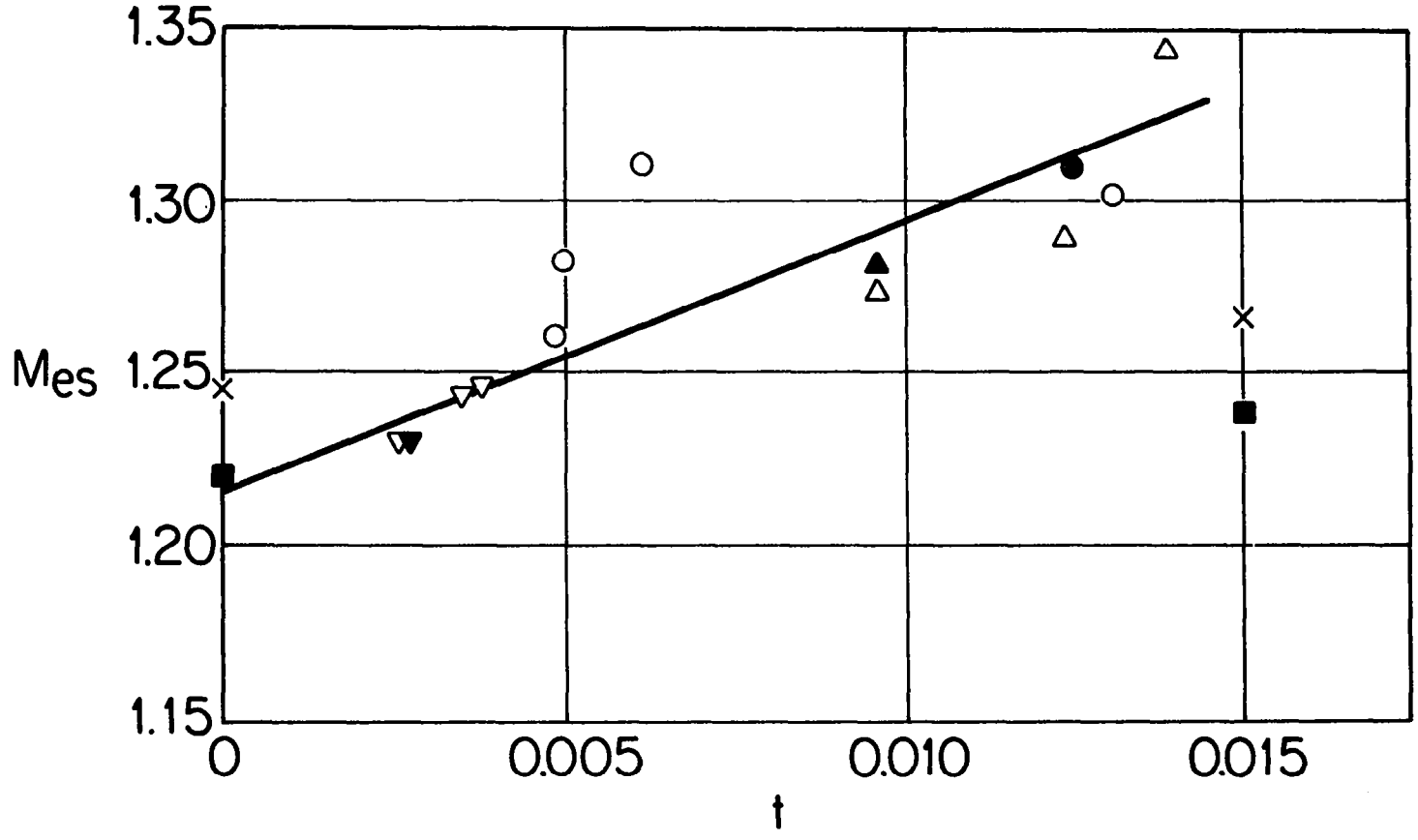

Figure 4. Effect of curvature parameter, t, on Mach number for incipient separation, M_{es}, from reference [20]. Triangles and circles correspond to different airfoils. Present calculations shown as follows: at t = 0, ■ - Re = 10^6, Π = 0.5, K = 0; x - Re = 10^7, Π = 0.5, K = 0. At t = 0.015, ■ - Re = 10^6, Π = 0, K = 0.21; x - Re = 10^7, Π = 0, K = 0.28.

INTERACTION BETWEEN A NORMAL SHOCK WAVE AND A TURBULENT BOUNDARY LAYER AT HIGH TRANSONIC SPEEDS

Part III - Simplified Formulas for the Prediction of Surface Pressures and Skin Friction

A. F. Messiter and T. C. Adamson, Jr.

1. Introduction

In Parts I and II an asymptotic description of the interaction between a fully turbulent boundary layer and a weak normal shock wave is derived in detail for a particular limiting case. Here in Part III simple approximate numerical calculations of the corresponding wall pressure and skin friction distributions are described.

2. Undisturbed Boundary Layer

The interaction is characterized by two small parameters, a nondimensional friction velocity u_τ and a nondimensional shock-wave strength ϵ. If U_e is the undisturbed external-flow velocity immediately outside the boundary layer and ahead of the shock wave, made nondimensional with the critical sound speed, ϵ is defined by

$$U_e = 1 + \epsilon \tag{1}$$

If M_e is the corresponding external-flow Mach number,

$$(1 + \epsilon)^2 = \frac{\frac{1}{2}(\gamma+1)M_e^2}{1 + \frac{\gamma-1}{2}M_e^2} \tag{2}$$

The friction velocity is likewise made nondimensional with the critical sound speed, and is defined in terms of the skin-friction coefficient c_f just ahead of the interaction by

$$u_\tau^2 = \frac{1}{2}U_e^2 c_f \tag{3}$$

For simplicity an adiabatic wall is assumed and the total enthalpy is taken to be uniform. Thus the ratio of the wall temperature to the temperature in the external flow is

$$\frac{T_w}{T_e} = 1 + \frac{\gamma-1}{2} M_e^2 \tag{4}$$

where γ is the ratio of specific heats, taken to be constant. For numerical calculations, the viscosity coefficient is represented by a power law:

$$\frac{\mu_w}{\mu_e} = \left(\frac{T_w}{T_e}\right)^n \tag{5}$$

The Reynolds number Re is based on external-flow quantities just ahead of the shock wave and on the boundary-layer length L, the distance from the leading edge to the shock wave.

The undisturbed mean-velocity profile U_u used in Parts I and II is given as a transformed incompressible profile by

$$\Gamma \sin^{-1}(\Gamma^{-1} U_u) = U_i(\epsilon) + (T_w/T_e)^{1/2} u_\tau u_{01}(y) \tag{6}$$

where

$$U_i(\epsilon) = \Gamma \sin^{-1}(\Gamma^{-1} U_e), \qquad \Gamma = \left(\frac{\gamma+1}{\gamma-1}\right)^{1/2} \tag{7}$$

Also, $y = Y/\delta$, where Y is the coordinate normal to the wall and δ is the boundary-layer thickness, both made nondimensional with the boundary-layer length L. For some of the derivations the

function $u_{01}(y)$ is represented in Coles' form

$$u_{01}(y) = \kappa^{-1} \ln y - \kappa^{-1} \Pi \, (1 + \cos \pi \, y) \tag{8}$$

where $\kappa \approx 0.41$ is the von Kármán constant and Π is a profile parameter. For very large Reynolds numbers and for zero pressure gradient, $\Pi \approx 0.5$ or a little larger; for a favorable pressure gradient, as appears over most of an airfoil surface, the value is smaller. An equation defining the nondimensional distance $Y = \delta_*$ from the wall to the sonic line in the undisturbed boundary layer is found by setting $U_u = 1$ in Eqn. (6):

$$u_\tau \kappa^{-1} \ln(\delta/\delta_*) = (T_e/T_w)^{1/2} [U_i(\epsilon) - U_i(0)] - u_\tau \kappa^{-1} \Pi [1 + \cos(\pi \, \delta_*/\delta)] \tag{9}$$

where $U_i(0) = \Gamma \sin^{-1}(\Gamma^{-1})$. If $\epsilon << 1$, the first term on the right-hand side becomes $(T_e/T_w)^{1/2} [\, U_i(\epsilon) - U_i(0)] \sim \epsilon[1 - (\gamma-1)\epsilon/4 \ldots]$; if $u_\tau << \epsilon$, then $\delta_* << \delta$.

In the calculation procedures shown below, the parameters needed are M_e, Re, δ, u_τ, Π, and δ_*; as already noted, δ and δ_* are dimensionless. Values for these quantities might be obtained in a number of different ways. If the first three were given, the last three can be calculated, as shown below; instead, all six quantities might be available from a numerical boundary-layer solution; or perhaps the nondimensional displacement

thickness δ^* or momentum thickness θ might be among the given quantities. If needed, the definitions of δ^* and θ give, for small u_τ/U_e,

$$\frac{\delta^*}{\delta} \sim \frac{1+\Pi}{\kappa}\left(2\frac{T_w}{T_e}-1\right)\frac{u_\tau}{U_e} - \frac{2+3.18\Pi+1.5\Pi^2}{\kappa^2}\left(\frac{T_w}{T_e}-1\right)\left(3\frac{T_w}{T_e}-\frac{1}{2}\right)\frac{u_\tau^2}{U_e^2} \tag{10}$$

$$\frac{\theta}{\delta} \sim \frac{1+\Pi}{\kappa}\frac{u_\tau}{U_e} - \frac{2+3.18\Pi+1.5\Pi^2}{2\kappa^2}\left(3\frac{T_w}{T_e}-1\right)\frac{u_\tau^2}{U_e^2} \tag{11}$$

For illustration, the parameters M_e, Re, and δ will be regarded as given; then Eqn. (9) relates δ_* to the other quantities, and two additional relations can be derived. As described in Part I, asymptotic matching of Eqn. (6) with a wall-layer solution gives

$$u_\tau \kappa^{-1} \ln(\delta/\tilde{\delta}) = (T_e/T_w)^{1/2} U_i(\epsilon) - u_\tau(2\Pi\kappa^{-1} + c) \tag{12}$$

where $\tilde{\delta}$ is the nondimensional wall-layer thickness

$$\tilde{\delta} = \frac{\mu_w}{\mu_e}\left(\frac{T_w}{T_e}\right)^{1/2}\frac{U_e}{u_\tau}\frac{1}{Re} \tag{13}$$

and $c \approx 5.0$ is a constant appearing in the wall-layer solution. The momentum-integral equation gives

$$\frac{1+\Pi}{\kappa}\,\delta = \frac{u_\tau}{U_e}$$

$$+\frac{2}{\kappa}\left\{\frac{U_e}{U_i}\left(\frac{T_w}{T_e}\right)^{1/2} + \left(3\,\frac{T_w}{T_e} - 1\right)\frac{2 + 3.18\Pi + 1.5\Pi^2}{4(1+\Pi)}\right\}\frac{u_\tau^2}{U_e^2} \tag{14}$$

Equations (12) and (14) can be solved simultaneously for u_τ and Π. In an iteration, perhaps an assumed value of Π (say 0.5) should be substituted into both right-hand sides; Equation (12) would then be solved for u_τ, and that result would be substituted into Eqn. (14) to give a new value of Π; the new Π would again be substituted into both right-hand sides, etc. It can be seen from these equations that, since u_τ is small, the choice of definition for δ does not have a strong effect on the solutions for u_τ and for the product $(1+\Pi)\delta$; also, the largest term in the pressure given below is proportional to $u_\tau(1+\Pi)\delta$.

3. Pressure Distribution

The solutions of Part I are derived for values of u_τ and ϵ such that $u_\tau \ll \epsilon \ll 1$. The coordinate X, nondimensional with L, is measured along the wall, with origin taken here to be at the intersection of the shock wave and the edge of the boundary layer. The shock-wave shape is $X = X_s(Y)$, where $|X_s(Y)|$ is small but

nonzero because of the interaction. The solutions are written in terms of coordinates x and x^* defined by

$$x = \frac{X}{b_o \delta} = \frac{X}{\Delta} \tag{15}$$

$$x^* = \frac{(\kappa\, T_e^{1/2})^{1/2}}{(\gamma+1)^{1/2} u_\tau^{1/2}} \frac{X - X_s(0)}{\delta_*} = \frac{X - X_s(0)}{\Delta_*} \tag{16}$$

where $b_o^2 = 1 - M_o^2$ and M_o is the Mach number behind a normal shock wave with upstream Mach number M_e. It follows that

$$b_o^2 = \frac{U_e^2 - 1}{U_e^2 - \frac{\gamma-1}{\gamma+1}} \tag{17}$$

and for $\epsilon \ll 1$, $b_o^2 = (\gamma+1)\ \epsilon \{1 - \frac{1}{2}(2\gamma+1)\epsilon + \ldots\}$. The value of $X_s(0)$ is found approximately from the results of Part I as

$$X_s(0) = -\frac{2 u_\tau b_o \delta}{\pi \kappa\ \epsilon} [1 + (\gamma - \tfrac{1}{2})\epsilon + \ldots] (2 + 1.59\Pi) \tag{18}$$

The pressure P is nondimensional with the critical value in the external flow; P_e and P_f refer to values upstream and downstream of a normal shock wave at Mach number M_e; P_t is the stagnation pressure in the undisturbed external flow; and P_w is the wall pressure. The solution for $x = O(1)$ is expressed in terms of source distributions and is approximated downstream, as $x \to \infty$, by $P_w = P_f + (\text{const.})/x$. The first term in the constant

factor is proportional to the increase in boundary-layer displacement thickness caused by the shock wave, as also found by Melnik and Grossman [1, 2] . This first term, representing the effect of a source at the origin, is found to approximate the effect of the distributed sources quite accurately for $x \gtrsim 2$. An expression for the smaller second term is found by using an approximation for the shock-wave shape to evaluate one of the integrals derived in Part I; the function of Π appearing in this second-order source strength is then approximated by a linear function for $0 \lesssim \Pi \lesssim 0.5$. The solution for $x^* = O(1)$ is needed only in a region which is extremely small if $u_\tau << \epsilon$ and would require solution of the transonic small-disturbance equations. Upstream, as $x^* \to -\infty$, these equations are approximated by linearization about the undisturbed profile, and the solution for $x^* \to -\infty$ is found to have the form $P_w/P_t \sim P_e/P_t + u_\tau \exp\{k(x^* - x_o^*)\}$, where $k \approx 0.59$ and x_o^* is as yet unknown.

The description given in the preceding paragraph would suffice for the idealized case of a flat plate in a uniform flow, where the pressure approaches constant values upstream and downstream of the interaction. For flow past an airfoil the boundary-layer effect can be expressed instead in terms of the pressure difference from a potential-theory pressure which continues to vary as the distance

from the shock wave increases. Upstream, for $X < X_u$, the exponential solution is added to a potential-flow solution $P_w = P_u(X)$. Downstream, for $X > X_d$, the source solution is added to a potential-flow solution $P_w = P_d(X)$. Close to the shock wave, for $X_u < X < X_d$, P_w is approximated by a straight line drawn tangent to these upstream and downstream representations. The tangency conditions are sufficient to determine the equation of the straight line and the values for X_u and X_d.

The functions $P_u(X)$ and $P_d(X)$ include the effects of nonuniform external flow associated with nonzero values of $\partial P/\partial X$ and $\partial P/\partial Y$ ahead of the shock wave. If $P_d(X)$ were known very accurately, the singular behavior $dP_d/dX = O(K \ln X)$, where K is the local surface curvature, would appear for $X \to 0$, as explained in Part I. However, the potential-flow pressure distribution is presumably found numerically, with the shock wave spread over a few mesh points, so that the singularity is obscured. The values of X_u and X_d are expected to lie outside the region of rapid pressure rise corresponding to the shock wave; if this is not true, some simple extrapolation of $P_u(X)$ and/or $P_d(X)$ should be used so that the smearing of the shock wave resulting from the numerical calculation does not influence the pressures calculated here. A specific location must be estimated for the shock wave, so that

the origin for x can be defined.

Three representations for the wall pressure are therefore proposed, one for each of three intervals, as follows:

$$X < X_u: \quad \frac{P_w}{P_t} = \frac{P_u(X)}{P_t} \left\{ 1 + u_\tau e^{k(x^* - x_o^*)} \right\} \tag{19}$$

$$X_u < X < X_d: \quad \frac{P_w}{P_t} = \frac{P_d(X_d)}{P_t} + \alpha x + \beta \tag{20}$$

$$X > X_d: \quad \frac{P_w}{P_t} = \frac{P_d(X)}{P_t} - \frac{1}{P_t} \frac{\gamma m u_\tau}{2\pi x} \tag{21}$$

where $P_t = \{(\gamma+1)/2\}^{\gamma/(\gamma-1)} = 1.893$ for $\gamma = 1.4$. The constants X_u, X_d, α, and β are determined below from the requirements that P_w and dP_w/dX be continuous. As already noted, $k \approx 0.59$. A value $x_o^* = -14$ was proposed in Part I for agreement with a particular experimental pressure distribution. Here Eqn. (19) is given in a slightly modified form, and the choice made is $x_o^* = -10$, partly to improve agreement with a second set of data and partly to avoid any implication that the value is accurate to two significant figures. Finally,

$$m = 8 \frac{1 + \Pi}{\kappa} \{1 + (\gamma-1)\epsilon + \ldots\} + 120(1 + 6\Pi)u_\tau \tag{22}$$

where the first term is the integrated first-order source strength given in Part I, and some simplifying approximations have been

introduced in the second term, as explained above.

The continuity requirements for P_w and dP_w/dX then lead to the following system of equations to be solved for X_u, X_d, α and β:

$$\frac{P_d(X_d) - P_u(X_u)}{P_t} x_d = \frac{\gamma m u_\tau}{\pi P_t}\left(1 - \frac{x_u}{2x_d}\right) + x_d(x_d - x_u)\frac{P'_d(X_d)}{P_t}\Delta$$

$$+ \frac{P_u(X_u)}{P_t} x_d u_\tau \exp\{k(x_u^* - x_o^*)\} \qquad (23)$$

$$\left\{\frac{P_u(X_u)}{P_t} k \frac{\Delta}{\Delta_*} + \frac{P'_u(X_u)}{P_t}\Delta\right\} u_\tau \exp\{k(x_u^* - x_o^*)\} = \frac{\gamma m u_\tau}{2\pi x_d^2 P_t}$$

$$+ \frac{P'_d(X_d) - P'_u(X_u)}{P_t}\Delta \qquad (24)$$

$$\alpha = \frac{\gamma m u_\tau}{2\pi x_d^2 P_t} + \frac{P'_d(X_d)\Delta}{P_t} \qquad (25)$$

$$\beta = -\frac{\gamma m u_\tau}{\pi x_d P_t} - \frac{x_d P'_d(X_d)\Delta}{P_t} \qquad (26)$$

where

$$x_u = \frac{X_u}{\Delta} = \frac{\Delta_* x_u^* + X_s(0)}{\Delta} \qquad (27)$$

$$x_d = \frac{X_d}{\Delta} \qquad (28)$$

Equations (23) and (24) are to be solved simultaneously for x_u and x_d. If $u_\tau << \epsilon$, then $\Delta_* << \Delta$, the exponential function is numerically small, and $|x_u| << x_d$. Also $P_u(X_u) \approx P_u(0)$ and $P_d(X_d) \approx P_d(0)$, the values found at X = 0 by extrapolation, and terms containing $P'_u(X_u)$ or $P'_d(X_d)$ are numerically small. These estimates can be used to give a first guess for x_d, and the equations can then be solved iteratively in essentially the form given.

The constants found from Eqns. (23) - (28) are to be substituted into Eqns. (19) - (21) to give the wall pressure as a simple function of distance and a somewhat more complicated but known function of the parameters. To indicate the level of accuracy which might be expected, some of the curves from Figs. 3 and 5 of Part I are replotted here, with x_o^* now set equal to -10. A comparison with experimental pressures from Ref. [3] is shown in Fig. 1 for $M_e = 1.322$, $Re = 9.6 \bullet 10^5$, $\delta = 0.021$, $u_\tau = 0.051$, $\Pi = 0.28$, and $\delta_*/\delta = 0.26$. Effects of nonuniform external flow, resulting from tunnel area change and longitudinal wall curvature, have been estimated and included in the predicted pressure. For a circular pipe, a comparison with experimental results from Ref. [4] and a numerical solution from Ref. [2] is shown in Fig. 2, for $M_e = 1.12$,

$Re = 6 \times 10^6$, $\delta = 0.02$, $u_\tau = 0.04$, $\Pi = 0.1$ and $\delta_*/\delta = 0.45$. Again the effects of a nonuniform external flow, in this case resulting from a finite pipe radius and a small area change, are included. For these comparisons a value for δ_* or for δ_*/δ was regarded as given and the value of Π was calculated using the approximate form of Eqn. (9), with δ_*/δ taken to be small; use of the complete equation would change the theoretical curves slightly.

The representation for the wall pressure given by Eqns. (19) - (21) is an approximation to the asymptotic solution derived in the limit as $u_\tau \to 0$, $\epsilon \to 0$, and $u_\tau/\epsilon \to 0$. The scaling is then clearly correct if u_τ/ϵ is very small and can be shown to remain correct if $u_\tau/\epsilon = O(1)$. The complete problem formulation for $u_\tau = O(\epsilon)$ was given by Melnik and Grossman [1, 2], in terms of the nonlinear transonic small-disturbance equations with prescribed vorticity, subject to suitable boundary conditions. For a given value of Π a one-parameter (essentially u_τ/ϵ) family of numerical solutions can be obtained; in their calculations $\Pi = 0.5$. Their results likewise have exponential decay upstream and source-like behavior downstream. Values for the constants k, m, and x_o^* could in principle be inferred from a sequence of numerical solutions as $u_\tau/\epsilon \to 0$; however, the value of m for a given Π would differ somewhat from that given above because second-order terms included here do not

correspond exactly to terms in the solutions of Refs. [1] and [2] which become of second order as $u_\tau/\epsilon \to 0$. A value of x_o^* obtained from numerical solutions would differ from the value $x_o^* = -10$ inferred from the two measured pressure distributions shown in Figs. 1 and 2.

The present results are quite simple in form and give good accuracy for the cases shown in Figs. 1 and 2. The numerical solutions of Refs. [1] and [2], which give a correct approximation to the pressure for small values of u_τ and ϵ and for $\epsilon/u_\tau = O(1)$, require a considerably greater amount of computation and depend on two parameters. It would therefore seem that the present results might be considered adequate for a practical airfoil calculation.

Any approximate description of the interaction which is to be considered reliable should be based on a correct representation of the undisturbed mean-velocity profile. The profile is characterized by two very different length scales, a boundary-layer thickness and a much smaller viscous length, and so is represented in terms of the law of the wake and the law of the wall, described by Coles [5] for incompressible flow and extended for compressible flow by Maise and McDonald [6]. Both the present work and that of Melnik and Grossman are based on this two-layer structure for the undisturbed profile. The derivations of Refs. [7] and [8], on the other

hand, do not properly represent the undisturbed profile and introduce approximations into the equations of motion in a rather arbitrary way. In spite of these supposedly simplifying assumptions, the derivations remain complicated and do not show the dependence on parameters analytically.

The present results, therefore, (a) are expressed by simple functions of distance with dependence on parameters shown explicitly; (b) are based on a systematic approximation to the equations of motion; and (c) for the cases shown in Figs. 1 and 2, reproduce numerical and experimental results quite well. Furthermore, by use of results given in Parts I and II the pressure distribution away from the wall and the shear stress at the wall can also be calculated. Several comments should be made, however, concerning values of constants and expected accuracy for P_w:

(1) The tentative value $x_o^* = -10$ is a rough estimate based on a comparison with two measured pressure distributions, and perhaps should be improved.

(2) Additional uncertainties appear in both theory and experiment. The shock-wave position is unsteady because of turbulent fluctuations in the boundary layer, and the maximum measured dP_w/dX is therefore at least slightly reduced. If even a very thin separation bubble is present, the beginning of the pressure rise will be

moved somewhat upstream. In the theory, some simplifying approximations have been introduced here in the expressions derived in Part I for $X_s(0)$ and for the second term in m. Moreover, omitted terms of still higher order than retained in Part I might be numerically important.

(3) The origin x = 0 has been placed at the intersection of the shock wave with the edge of the boundary layer; the position estimated from numerical potential-flow solutions alone is not sufficiently accurate. Perturbations in the external flow resulting from the local boundary-layer displacement effect must therefore be calculated, so that x can be measured from the perturbed shock-wave position. For the simplest correction method, P_w obtained for the undisturbed shock wave can be used in the boundary-layer equations for calculation of the displacement thickness as a function of X in the interaction region. Calculation of the potential flow over the new equivalent body then gives the perturbed shock-wave shape, and the origin for P_w can then simply be shifted appropriately. In this calculation, the neglect of P_Y is not justified; however, the error arises primarily for $X_u < X < X_d$, where the interpolation formula for P_w has been used. In a sense, then, this additional approximation can be regarded instead as a kind of interpolation for the displacement thickness, and probably introduces very little additional error.

(4) The theory was derived for unseparated flows with $u_\tau << \epsilon << 1$, but the approximate version, with the straight-line interpolation, is being proposed for use in a broader range. For Fig. 1, as noted in Part II, it is believed that a very thin separation bubble was present in the experiment. For Fig. 2, the Mach number is low enough that $u_\tau/\epsilon \approx 0.4$, which is certainly not very small. More comparisons with experimental data are needed to provide a better guide to the parameter ranges for which the approximation might remain reasonable.

4. Skin Friction

Simple equations for the shear stress in the interaction region may be derived also, when the approximate forms for the pressure, given in Eqns. (19) and (21), are used in the equation for τ_w. That is, in Part II, it was shown that τ_w could be written in terms of the perturbation in pressure at the wall, $P_1(x) = -\gamma u_1(x)$, in the major (outer) part of the interaction region, It is easily shown [9], that the same holds true in the initial part of the interaction region where upstream influence first causes changes from the undisturbed surface pressure and skin friction. Thus, from Ref. [9], it is shown that in this (inner) region,

$$\tau_w = 1 + u_\tau \frac{a_1}{2} \frac{P_1^*(x^*)}{\gamma} + \ldots \tag{29}$$

and so, using Eqn. (19) for $P_1^*(x^*)$, for $X < X_u$,

$$\tau_w = 1 + \frac{u_\tau a_1}{2\gamma} e^{k(x^* - x_o^*)} + \ldots \tag{30}$$

Likewise, if Eqn. (21) is used for the pressure perturbation, $P_1(x) = -\gamma u_1(x)$, in equation (27a) of Part II, one can show that, for $X > X_d$

$$\tau_w = \tau_{wd} + u_\tau \frac{A}{x} + \epsilon u_\tau (-B + C \ln x) \tag{31a}$$

$$A = -\frac{a_1}{4\pi} \frac{m}{(1+(\gamma-1)\epsilon)} \left\{1 - \frac{\epsilon}{2}\left[1 - 3\gamma - \frac{3a_1}{2} + \frac{4\gamma}{a_1}(\gamma + \frac{1}{2})\right]\right\} \tag{31b}$$

$$B = -\kappa^{-1}\ln\left(\frac{\hat{\delta}}{\delta}\right)(2\gamma-a_1)\left(\gamma+\frac{1}{2}-\frac{a_1}{4}\right) + \kappa^{-1}\left[2\Pi\,(2\gamma-a_1)\left(\gamma+\frac{1}{2}-\frac{a_1}{4}\right)\right.$$

$$\left. + \left(2\gamma+1-\frac{a_1}{2}\right)\left(\gamma-\frac{a_1}{2}\right)(\gamma_e - \ln 2\kappa)\right] \qquad (31c)$$

$$C = \kappa^{-1}\left(2\gamma+1-\frac{a_1}{2}\right)\left(\gamma-\frac{a_1}{2}\right)$$

$$a_1 = -4\sqrt{\frac{\gamma-1}{2}}\left(\sin^{-1}\frac{1}{\Gamma}\right)^{-1} + 2\gamma \qquad (31d)$$

In Eqn. (31c) $\gamma_e = 0.57721$ is Euler's constant and $\kappa = 0.41$ is the Kármán constant. In Eqn. (31a), τ_{wd} represents the wall shear stress calculated using the pressure downstream of the shock wave. For flow over a flat plate, τ_{wd} is given by Eqn. (32) of Part II; for $\epsilon \ll 1$, $\tau_{wd} = 1 + a_1\epsilon + a_1(a_1-1)\epsilon^2/2 + \ldots$ as in Eqn. (27a). Finally, $\tau_w = c_f/c_{fu}$ where c_f is the skin friction and the subscript u refers to conditions upstream of the interaction.

Equations (30) and (31a) are simple relations for c_f/c_{fu} upstream of X_u and downstream of X_d. In the intermediate region, just as was done for the surface pressure, we use a straight line tangent to the solution given by Eqn. (30) at X_u and to the solution given by Eqn. (31a) at X_d. The values for X_u and X_d found here are clearly not the same as those found for the surface pressure distribution. In addition, c_{fu} and c_{fd}, the skin friction upstream and downstream of the interaction respectively, are considered

to be known functions of X. That is, the present calculations may be considered to be a correction to the c_f distribution found using typical boundary layer methods, this distribution being in error within the interaction region. Because c_{fu} and c_{fd} would include the effects of wall curvature, terms involving these effects are not included here. The proposed equations to be used, then, are

$$X < X_u \qquad c_f = c_{fu}(X)\left[1 + u_\tau \frac{a_1}{2\gamma} e^{k(x^* - x_o^*)} + \ldots\right] \tag{32a}$$

$$X_u < X < X_d \qquad c_f = c_{fd}(X_d) + \alpha_c x + \beta_c \tag{32b}$$

$$X > X_d \qquad c_f = c_{fd}(X) + c_{fu}(X_u)\left[u_\tau \frac{A}{x} + \epsilon\, u_\tau(-B + C \ln x)\right] \tag{32c}$$

where

$$x = \frac{X}{\Delta} = \frac{\Delta_* X^* + X_s(0)}{\Delta} \tag{33}$$

It may be noted that as x becomes very large, the term $-B + C \ln x$ does not approach zero. This term evidently indicates that relaxation to a final value of c_f takes place on a scale large compared to a boundary layer thickness. Because B is a large number $-B + C \ln x$ goes through zero for x large (e.g., $x \approx 200$). Moreover, since ln x does not vary rapidly with large x, the contribution of this term is not significant for a considerable range of values of x about the point at which it equals zero. Hence after the term $-B + C \ln x$ has gone to zero, it should be dropped from the

expression for c_f.

The equations necessary to find X_u, X_d, α_c, and β_c are obtained by equating the relevant expressions for c_f and $d\,c_f/dX$ at X_u and X_d. They may be written as follows:

$$c_{fu}(X_u) - c_{fd}(X_d) = \Delta x_u\, c'_{fd}(X_u) - \Delta x_d\, c'_{fd}(X_d) + u_\tau\, c_{fu}(X_u)\left[\frac{2A}{x_d} - \epsilon(B + C(1 - \ln x_d))\right] - u_\tau\left\{\Delta\ c'_{fu}(X_u) + \frac{k\Delta}{\Delta_*}\ c_{fu}(X_u)\right\}^{-1} \cdot \left\{\frac{\Delta}{u_\tau}(c'_{fu}(X_d) - c'_{fu}(X_u)) + c_{fu}(X_u)\left(-\frac{A}{x_d^2} + \frac{\epsilon C}{x_d}\right)\right\} \cdot \left\{c_{fu}(X_u)\left(1 - k\,x_u\,\frac{\Delta}{\Delta_*}\right) - x_u \Delta\, c'_{fu}(X)\right\} \qquad (34a)$$

$$e^{k(x_u^* - x_o^*)} = \frac{2\gamma}{a_1}\left[\Delta\, c'_{fu}(X_u) + k\,\frac{\Delta}{\Delta_*}\ c_{fu}(X_u)\right]^{-1} \cdot \left\{\frac{\Delta}{u_\tau}\left[c'_{fu}(X_d) - c'_{fu}(X_u)\right] + c_{fu}(X_u)\left[-\frac{A}{x_d^2} + \frac{\epsilon C}{x_d}\right]\right\} \qquad (34b)$$

$$\alpha_c = \Delta\, c'_{fu}(X_d) + c_{fu}(X_u)\left\{-\frac{u_\tau A}{x_d^2} + \epsilon\, u_\tau\,\frac{C}{x_d}\right\} \qquad (34c)$$

$$\beta_c = -\Delta x_d\, c'_{fu}(X_d) + u_\tau\, c_{fu}(X_u)\left\{\frac{2A}{x_d} - \epsilon(B + C(1 - \ln x_d))\right\} \qquad (34d)$$

where

$$c_f' = d\, c_f/dX.$$

An illustration of the results obtained using the present simplified equations is shown in figure (3) where the experimental results are those of Gadd [4]. The numerical values of the parameters are those given in figure 2, Part II. In addition, $x_s = 1.54$, $x_d \cong 1.37$, $x_u = -6.10$, and $\tau_{wd} = c_{fd}/c_{fu} = 0.85$ and $x_o^* = -10$. If the calculated results in figure (3) and figure (2) of Part II are compared, one can see that the effect of using the approximate form for $P_1(x)$ is to change the location and value of $(\tau_w)_{min} = (c_f/c_{fu})_{min}$ slightly. Comparison of calculated and experimental values in figure (3) shows that the upstream influence is underpredicted for $x_o^* = -10$ as in the surface pressure calculations. However, unsteadiness in the shock wave position, with oscillations of relatively small amplitude, could easily account for the difference between calculated and experimental values.

References

[1] R. E. Melnik and B. Grossman, Analysis of the Interaction of a Weak Normal Shock Wave with a Turbulent Boundary Layer. AIAA Paper No. 74-598 (1974).

[2] R. E. Melnik and B. Grossman, Further Developments in an Analysis of the Interaction of a Weak Normal Shock Wave with a Turbulent Boundary Layer. Symposium Transsonicum II, K. Oswatitsch and D. Rues, eds., Springer-Verlag (1976), pp. 262-272; Interactions of Normal Shock Waves with Turbulent Boundary Layers at Transonic Speeds. Transonic Flow Problems in Turbomachinery, T. C. Adamson, Jr., and M. F. Platzer, eds., Hemisphere Publ. Co. (1977), pp. 415-433.

[3] J. Ackeret, F. Feldmann, and N. Rott, Untersuchungen an Verdichtungsstössen und Grenzschichten in schnell bewegten Gasen. Mitteilungen aus dem Inst. für Aerodyn., ETH Zürich, Nr. 10 (1946). Translated as NACA TM 1113 (1947).

[4] G. E. Gadd, Interactions between Normal Shock Waves and Turbulent Boundary Layers. A.R.C. 22559, R. and M. 3262 (1961).

[5] D. E. Coles, The Law of the Wake in the Turbulent Boundary Layer. J. Fluid Mech. 1, 191-226 (1956).

[6] G. Maise and H. McDonald, Mixing Length and Kinematic Eddy Viscosity in a Compressible Boundary Layer. AIAA J. 6, 73-80 (1968).

[7] R. Bohning and J. Zierep, Der senkrechte Verdichtungsstoss an der gekrümmten Wand unter Berücksichtigung der Reibung, Z. Angew. Math. Phys. 27, 225-240 (1976).

[8] G. R. Inger and W. H. Mason, Analytical Theory of Transonic Normal Shock-Turbulent Boundary-Layer Interactions, AIAA J. 14, 1266-1272 (1976).

[9] M. S. Liou, Asymptotic Analysis of Interaction between a Normal Shock Wave and a Turbulent Boundary Layer in Transonic Flow, Ph. D. Dissertation, The University of Michigan, Ann Arbor, Michigan (1977).

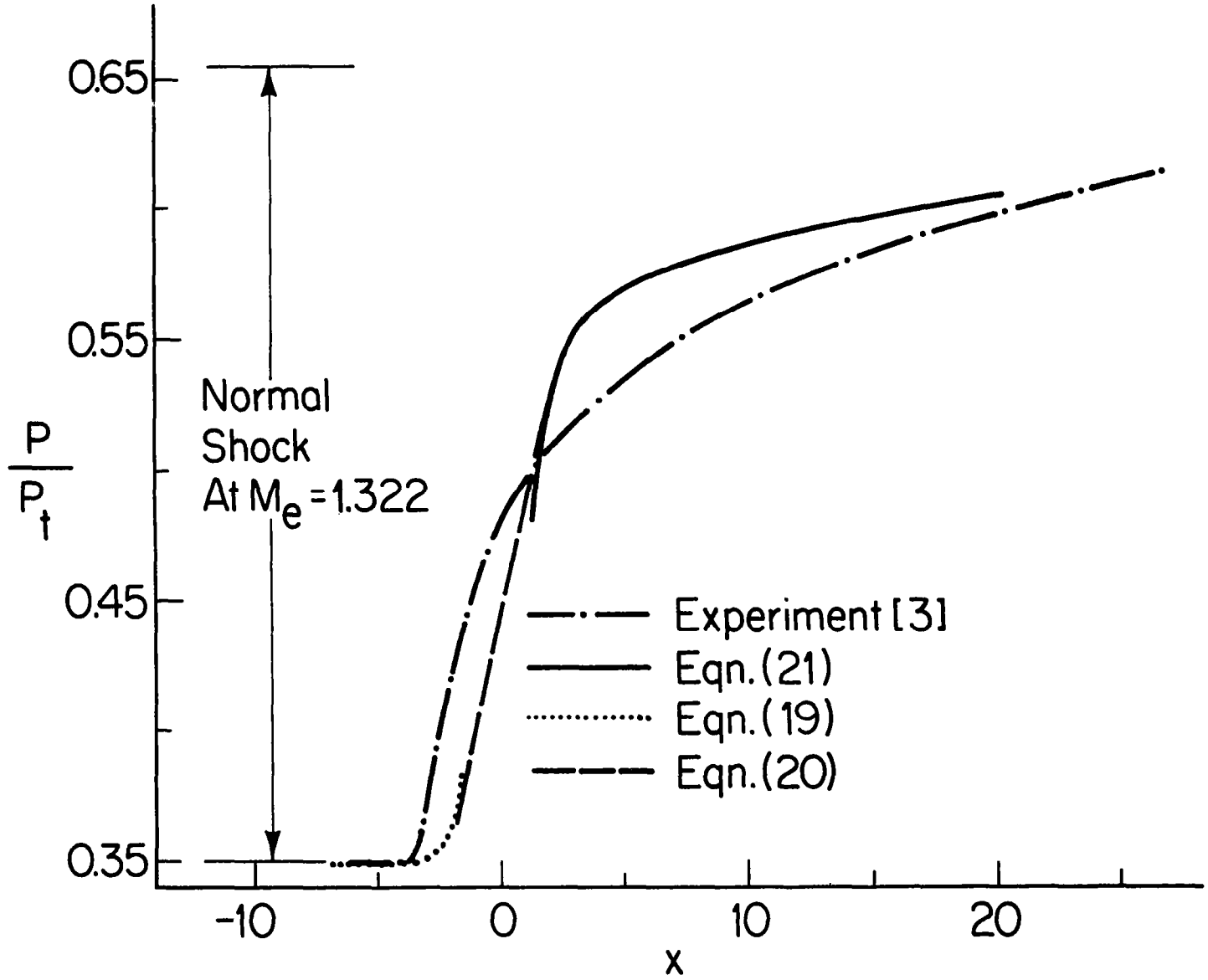

Figure 1. Pressure at wall with longitudinal curvature: $M_e = 1.322$, $Re = 9.6 \times 10^5$; $P_d(X)$ is calculated from theory of Part I, with curvature effect ($K \approx 0.2$) included.

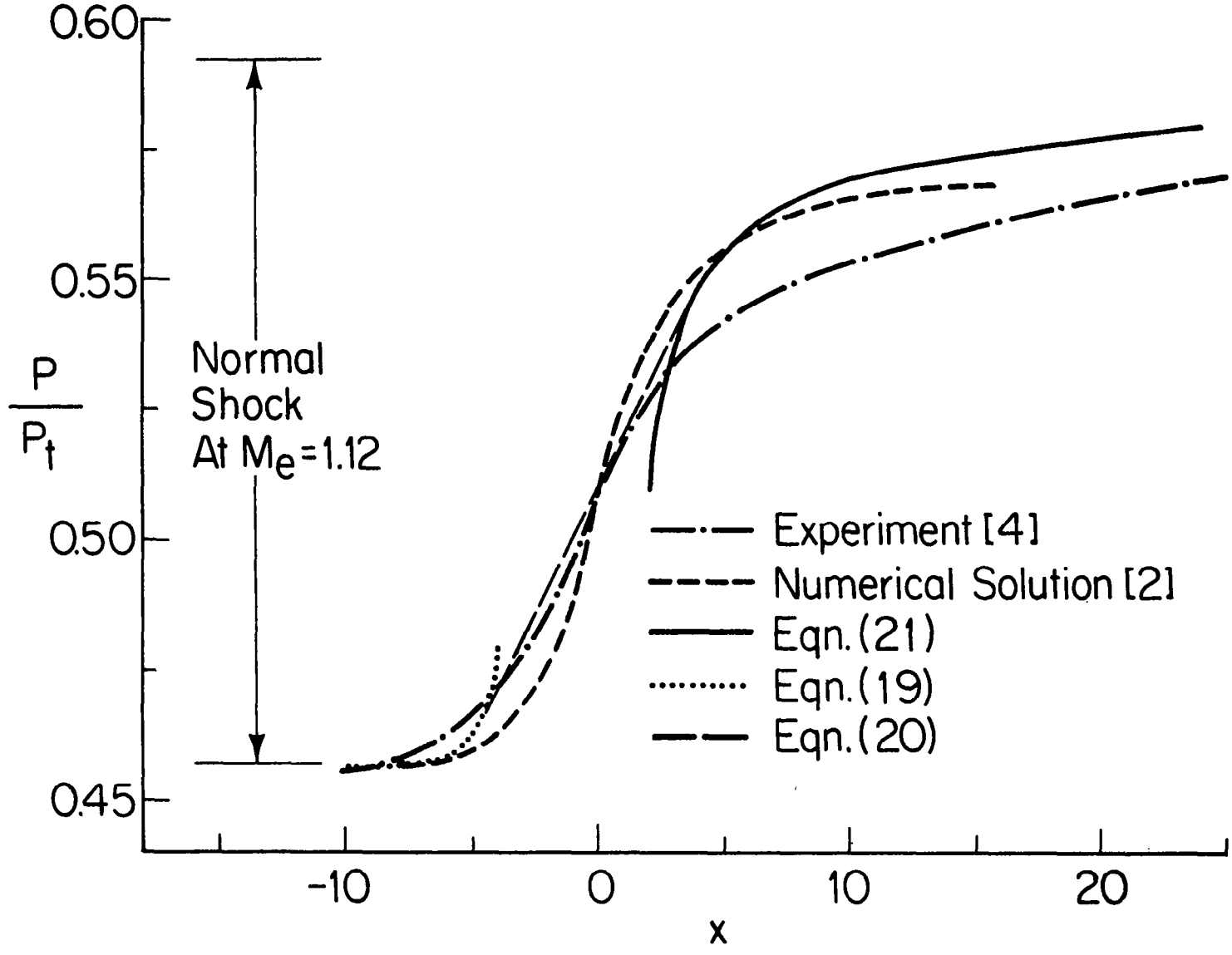

[1]Figure 2. Pressure at wall of circular pipe: $M_e = 1.12$, $Re \approx 6 \times 10^6$; $P_d(X)$ is calculated from theory of Part I, with effect of finite pipe radius ($\delta/R \approx 0.055$) included.

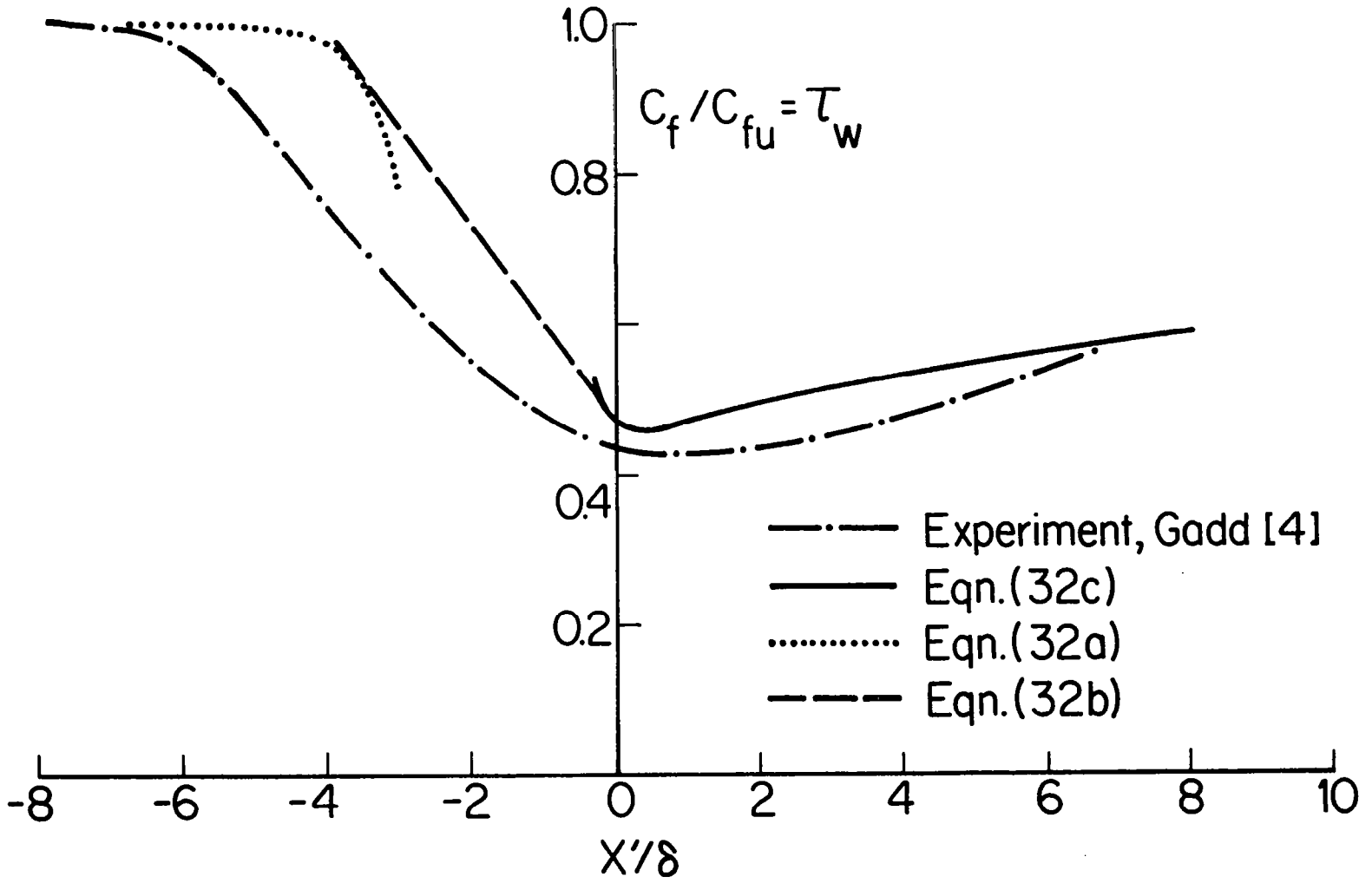

Figure 3. Comparison of calculated and experimental values of c_f/c_{fu} vs X'/δ, where $X'/\delta = 0$ at $P_w/P_{te} = 0.528$. Parameters as in Figure 2, Part II.